

UNIVERSITY OF CALIFORNIA, SAN DIEGO

Epidermal Innervation and Thermal Nociception in Rodent Models of Diabetic
Neuropathy

A dissertation submitted in partial satisfaction of the requirements for the degree
of Doctor of Philosophy

in

Molecular Pathology

by

Kristina Beiswenger

Committee in charge:

Nigel A. Calcutt, Chair
Martin Marsala
Andrew P. Mizisin
Henry C. Powell
G. Diane Shelton

2008

Copyright
Kristina Beiswenger, 2008
All rights reserved.

The dissertation of Kristina Beiswenger is approved and it is acceptable in quality and form for publication on microfilm:

Chair

Table of Contents

Signature Page.....	iii
Table of Contents.....	iv
List of Figures.....	vi
List of Tables.....	viii
Acknowledgments.....	ix
Curriculum Vita.....	x
Abstract of the Dissertation.....	xi
1 <u>Introduction</u>	
1.1 Diabetes mellitus.....	1
1.2 Animal models of diabetes.....	4
1.3 Pathogenic mechanisms.....	6
1.4 Characteristics of skin.....	14
1.5 Epidermal nerve fiber quantification.....	17
<u>Specific Aims</u>	30
2 <u>Methods</u>	
2.1 Rodent models of diabetes.....	31
2.2 Behavioral assessment.....	32
2.3 Rodent physiology.....	33
2.4 Immunohistochemical assessment of skin biopsy.....	34
2.5 ELISA assays.....	37
2.6 Measurement of protein oxidation.....	38
3 <u>Assessment of Epidermal Innervation in Rodent Models of Diabetes</u>	
3.1 Introduction.....	39
3.2 Methods.....	41
3.3 Results.....	43
3.4 Discussion.....	55
4 <u>The Relationship Between Thermal Hypoalgesia and Epidermal Nerve Fiber Loss</u>	
4.1 Introduction.....	62
4.2 Methods.....	64
4.3 Results.....	65
4.4 Discussion.....	71
5 <u>The Pathogenesis of Diabetic Neuropathy</u>	
5.1 Introduction.....	78
5.2 Methods.....	82
5.3 Results.....	83
5.4 Discussion.....	92

6	<u>Insulin as a Neurotrophic Factor</u>	
	5.1 Introduction.....	96
	5.2 Methods.....	98
	5.3 Results.....	101
	5.4 Discussion.....	117
7	<u>Discussion</u>	
	7.1 Summary of results.....	124
	7.2 Clinical and experimental relevance of epidermal nerve fiber assessment.....	127
	7.3 The dissociation of thermal nociception and epidermal innervation: clinical implications.....	128
	7.4 The utility of mouse models in the study of epidermal nerve fiber loss.....	132
	7.5 Implications of epidermal thinning.....	136
	7.6 Mechanisms of thermal hypoalgesia and epidermal nerve fiber loss.....	138
	7.7 Final conclusions.....	142
	<u>References</u>	143

List of Figures

<u>Chapter 2</u>		
Figure 2.1	A representative micrograph of PGP9.5-immunostained skin.....	36
 <u>Chapter 3</u>		
Figure 3.1	A comparison of PGP9.5 and HMW Tau immunoreactivity.....	44
Figure 3.2	Micrographs of PGP9.5-immunostained skin from control and diabetic rats.....	46
Figure 3.3	Immunoreactive profile densities of control and STZ-diabetic rats.....	47
Figure 3.4	Micrographs of PGP9.5-immunostained skin from control and diabetic mice.....	48
Figure 3.5	Immunoreactive profile densities of control and diabetic mice.....	49
Figure 3.6	A comparison of immunoreactive profile densities of control and diabetic rats on 2 separate diets.....	51
Figure 3.7	Levels of oxidized proteins.....	53
Figure 3.8	Epidermal thicknesses of control and diabetic rats and mice.....	54
Figure 3.9	Epidermal nuclear density in control and diabetic mice....	55
 <u>Chapter 4</u>		
Figure 4.1	Withdrawal latency and blood flow.....	66
Figure 4.2	The impact of 2 weeks of diabetes.....	67
Figure 4.3	The impact of 4 weeks of diabetes.....	69
Figure 4.4	A reanalysis of immunoreactive profile density in control and diabetic Swiss Webster mice.....	70
 <u>Chapter 5</u>		
Figure 5.1	MNCVs – IDD 676 and Neotrofin treatment study.....	84
Figure 5.2	Thermal withdrawal latencies – IDD 676 and Neotrofin treatment study.....	85
Figure 5.3	Immunoreactive profile densities – IDD 676 and Neotrofin treatment study.....	85
Figure 5.4	Epidermal thickness – IDD 676 and Neotrofin treatment study.....	86
Figure 5.5	Thermal withdrawal latencies – CNTF and TX14(A) treatment study.....	87
Figure 5.6	Immunoreactive profile densities – CNTF and TX14(A) treatment study.....	88
Figure 5.7	Epidermal thickness – CNTF and TX14(A) treatment study.....	88
Figure 5.8	MNCVs – Reversal study.....	89

Figure 5.9	Thermal withdrawal latencies – Reversal study.....	90
Figure 5.10	Immunoreactive profile densities – Reversal study.....	90
Figure 5.11	Epidermal thickness – Reversal study.....	91
 <u>Chapter 6</u>		
Figure 6.1	Blood glucose levels of db/db mice.....	102
Figure 6.2	Insulin levels of db/db mice.....	103
Figure 6.3	MNCVs of db/db mice.....	103
Figure 6.4	Thermal withdrawal latencies of db/db and STZ-diabetic C57Bl/6 mice.....	104
Figure 6.5	Immunoreactive profile densities of db/db and STZ-diabetic C57Bl/6 mice.....	104
Figure 6.6	MNCVs – 4 week insulin pellet study.....	106
Figure 6.7	Thermal withdrawal latencies – 4 week insulin pellet study.....	107
Figure 6.8	Immunoreactive profile densities – 4 week insulin pellet study.....	108
Figure 6.9	Epidermal thickness – 4 week insulin pellet study.....	108
Figure 6.10	MNCVs – 8 week insulin pellet study.....	111
Figure 6.11	Thermal withdrawal latencies – 8 week insulin pellet study.....	111
Figure 6.12	Immunoreactive profile densities – 8 week insulin pellet study.....	112
Figure 6.13	Epidermal thickness – 8 week insulin pellet study.....	112
Figure 6.14	Blood glucose levels of STZ-injected mice.....	113
Figure 6.15	Thermal withdrawal latencies of STZ-injected mice.....	114
Figure 6.16	Immunoreactive profile densities of STZ-injected mice.....	114
Figure 6.17	Epidermal thickness of STZ-injected mice.....	115
Figure 6.18	Thermal withdrawal latencies of insulin-injected mice.....	116
Figure 6.19	Immunoreactive profile densities of insulin-injected mice...	116
Figure 6.20	Epidermal thickness of insulin-injected mice.....	117
Figure 6.21	GAP-43-immunoreactive profile densities of insulin-injected mice.....	117
 <u>Chapter 7</u>		
Figure 7.1	A plot of IENF density vs. insulin levels.....	134
Figure 7.2	A schematic summarizing major findings.....	139

List of Tables

Chapter 3

Table 3.1	Strain, gender, duration of diabetes, final body weight and final blood glucose levels of rats and mice.....	45
Table 3.2	Final body weight and blood glucose levels for rats on 2 separate diets.....	51
Table 3.3	A comparison of Harland Teklad diets 8604 and 7001..	52

Chapter 4

Table 4.1	Final body weight and blood glucose levels after 2 weeks of diabetes.....	66
Table 4.2	SP and GAP-43 immunoreactivity after 2 weeks of diabetes.....	68

Chapter 5

Table 5.1	Final body weight and blood glucose levels – IDD 676 and Neotrofin treatment study.....	84
Table 5.2	Final body weight and blood glucose levels – CNTF and TX14(A) treatment study.....	87
Table 5.3	Final body weight and blood glucose levels – Reversal study.....	91

Chapter 6

Table 6.1	Final body weight and blood glucose levels – 4 week insulin pellet study.....	105
Table 6.2	Final body weight and blood glucose levels – 8 week insulin pellet study.....	110

Chapter 7

Table 7.1	Comparison of IENF density assessments.....	129
Table 7.2	Body weights from previous studies.....	133

Acknowledgements

I would like to acknowledge the colleagues that contributed to the data in this manuscript. Protein oxidation data was provided by Dr. Joice Cunha. Sciatic nerve substance P levels were measured by Marleen Kawahara, and the thermal withdrawal latencies of the C57Bl/6 mice were provided by Dr. Khara Ramos.

Data from chapter 3 was published in part in Beiswenger KK, Calcutt NA, Mizisin AP (2008) Epidermal nerve fiber quantification in the assessment of diabetic neuropathy. *Acta Histochem.* Mar 31; [Epub ahead of print]. The dissertation author was the primary author of this publication.

Data from chapter 4 was published in part in Beiswenger KK, Calcutt NA, Mizisin AP (2008) Dissociation of thermal nociception and epidermal innervation in streptozotocin-diabetic mice. *Neurosci Lett.* Jul 3; [Epub ahead of print]. The dissertation author was the primary author of this publication.

Curriculum Vita

Education:

University of California, San Diego
Ph.D. in Molecular Pathology, 2008

University of Chicago
B.A. in Biology, 2002

Publications:

Beiswenger KK, Calcutt NA, Mizisin AP (2008) The dissociation of thermal nociception and epidermal innervation in streptozotocin-diabetic mice. *Neurosci Lett* In Press.

Beiswenger KK, Calcutt NA, Mizisin AP (2008) Epidermal nerve fiber quantification in the assessment of diabetic neuropathy. *Acta Histochem* In Press.

Jolivalt CG, Lee CA, Beiswenger KK, Smith JL, Orlov M, Torrance MA, Masliah E (2008) Defective insulin signaling pathway and increased GSK-3 activity in the brain of diabetic mice: parallels with Alzheimer's disease and correction by insulin. *J Neurosci Res* In Press.

Robinson FL, Niesman IR, Beiswenger KK, Dixon JE (2008) Loss of the inactive myotubularin-related phosphatase Mtmr13 leads to a Charcot-Marie-Tooth 4B2-like peripheral neuropathy in mice. *Proc Natl Acad Sci USA* In Press.

Hara M, Alcoser S, Qadir A, Beiswenger KK, Cox N, Ehrmann D (2002) Insulin resistance is attenuated in women with polycystic ovary syndrome with the Pro12Ala polymorphism in the PPARgamma gene. *J Clin Endocrinol Metab* 87(2):772-5.

Abstracts:

Beiswenger KK, Calcutt NA, Mizisin AP (2007) The time course of structural and functional changes in epidermal nerves of a mouse model of type 1 diabetes. 2007 meeting of the Peripheral Nerve Society.

Beiswenger KK, Mizisin AP, Ramos KM, Calcutt NA (2005) Epidermal nerve fiber loss in mouse models of type 1 diabetes. 15th annual meeting of the diabetic neuropathy study group of the EASD.

Awards Received:

Recipient of a travel fellowship to the 2007 meeting of the Peripheral Nerve Society

ABSTRACT OF THE DISSERTATION

Epidermal Innervation and Thermal Nociception in Rodent Models of Diabetic Neuropathy

by

Kristina Beiswenger

Doctor of Philosophy in Molecular Pathology
University of California, San Diego, 2008
Professor Nigel A. Calcutt, Chair

The assessment of epidermal innervation is emerging as a valuable means of diagnosing and staging clinical diabetic neuropathy. In order to address whether or not rodent models of diabetes develop a similar loss of cutaneous innervation, we quantified epidermal nerve fiber density in various strains of diabetic rats and mice. After confirming that each of these strains developed epidermal nerve fiber loss, as well as epidermal thinning, we examined the relationship between changes in epidermal nerve fiber density and changes in heat sensitivity. After 2 weeks of diabetes, Swiss Webster mice developed significant thermal hypoalgesia. However, a significant reduction in epidermal innervation did not develop until after 4 weeks of diabetes, indicating that loss of heat sensitivity precedes a detectable reduction in epidermal innervation.

Next we attempted to examine the mechanisms of thermal hypoalgesia by examining the effects of an aldose reductase inhibitor and exogenous neurotrophic support in type 1 diabetic Swiss Webster mice. The aldose reductase inhibitor IDD 676 and the NGF-enhancing compound Neotrofin partially ameliorated motor nerve conduction velocity slowing, but were unable to prevent thermal hypoalgesia. CNTF and the prosaposin-like peptide TX14(A) prevented the development of thermal hypoalgesia, but none of these compounds were able to reverse established deficits.

Next we examined the neurotrophic properties of insulin by comparing the severity of neuropathy in type 1 and type 2 diabetic mouse models. Both models developed thermal hypoalgesia and IENF deficits, indicating that insulin does not protect against the development of these deficits. To further explore insulin's neurotrophic properties, we examined the effects of insulin supplementation in a type 1 diabetic mouse model. Low doses of insulin prevented epidermal thinning after 4 weeks of diabetes and high doses of insulin prevented thermal hypoalgesia after 4 and 8 weeks of diabetes, indicating neurotrophic effects of insulin. Together, these results demonstrate that rodent models develop the epidermal nerve fiber loss observed in humans with diabetes. However, a loss of thermal sensitivity precedes reductions in epidermal innervation. Loss of neurotrophic support may be involved in the development of these deficits.

1 – INTRODUCTION

1.1 Diabetes Mellitus

Although the worldwide prevalence of diabetes mellitus is estimated at 124 million and the incidence is increasing, certain facets of this disease remain poorly understood. Diabetes mellitus affects multiple organ systems, including the cardiovascular, renal and nervous systems. According to the National Diabetes Information Clearinghouse, diabetes-induced peripheral neuropathy, which often results in foot ulcerations, is the leading cause of non-traumatic lower limb amputations in the United States. A better understanding of how peripheral nerves, particularly those innervating the skin, are affected by diabetes mellitus could lead to the development of treatments that could prevent or reverse peripheral neuropathy. The goal of this dissertation was to first examine diabetes-induced changes in the innervation of the skin of rodent models, and then to explore the pathogenesis of loss of thermal sensation and loss of epidermal innervation.

1.1.1 Classifications of diabetes

According to the CDC, diabetes mellitus afflicts more than 20 million people in the United States alone. The number of people with diabetes mellitus has more than doubled in the last twenty years and is expected to double again in the next fifty years. Responsible for more than 200,000 deaths a year, diabetes mellitus is the sixth leading cause of death in the United States and

costs roughly \$132 billion a year in both direct medical costs and loss of productivity. The term diabetes mellitus encompasses a group of disorders sharing the common feature of hyperglycemia. The majority of cases are classified as either type 1 or type 2.

Type 1 diabetes, also known as juvenile or insulin-dependent diabetes, is caused by the autoimmune destruction of the insulin-producing beta cells of the pancreatic islets. It is most often diagnosed during childhood. Type 2 diabetes, also referred to as adult-onset or non-insulin-dependent diabetes, is characterized by insulin resistance. Type 2 diabetes can develop at any age and is often linked to obesity. Gestational diabetes, caused by pregnancy hormones and shortages of insulin, develops during the later stages of pregnancy.

Although it usually recedes after pregnancy, women who develop gestational diabetes experience an increased risk of developing type 2 diabetes later in life. Another category of diabetes, referred to as maturity-onset diabetes of the young (MODY), is caused by genetic defects in beta cell function, including mutations in glucokinase, insulin promoter factor and hepatocyte nuclear factors. Other genetic defects, diseases of the exocrine pancreas and endocrinopathies can also cause diabetes mellitus.

Complications associated with diabetes include blindness due to retinopathy, cataracts or glaucoma. The cardiovascular system is also affected, causing hypertension and atherosclerosis, which can result in heart attack and stroke. Diabetes also causes nephropathy and is the leading cause of kidney

failure. Neuropathies of a sensory, motor and autonomic origin also develop in patients with diabetes.

1.1.2 Types of diabetic neuropathy

Diabetic neuropathy has been reported to develop in nearly 50% of diabetic patients (Pirart et al., 1978). Although there is no universally accepted classification system, Thomas (1997) proposed a system based on distribution and type of nerve affected that classifies diabetic neuropathies as either focal or generalized. Focal neuropathies, which affect single or multiple isolated nerves, include cranial neuropathies, thoracolumbar radiculoneuropathy and proximal diabetic neuropathy. Cranial neuropathies most commonly affect the nerves innervating the external ocular muscles and often result in pain. Thoracolumbar radiculoneuropathy can result in pain, sensory loss or weakness, and both unilaterally and bilaterally affects the spinal nerves and nerve roots. Proximal diabetic neuropathy, also referred to as diabetic amyotrophy, presents in both unilateral and bilateral distributions and can result in pain, sensory loss and muscle weakness.

Generalized neuropathies include acute painful sensory neuropathy, acute motor neuropathy, autonomic neuropathy and distal symmetric sensorimotor polyneuropathy. Acute painful sensory neuropathy is characterized by burning pain in the lower and sometimes upper limbs. Acute motor neuropathy, although less common than other types of diabetic neuropathy, can result in facial weakness. Autonomic neuropathy affects the nerves that control involuntary actions of the body and is the cause of gastroparesis, postural hypotension,

bladder dysfunction and erectile dysfunction. Distal symmetric sensorimotor polyneuropathy is the most common form and affects both sensory and motor nerves, including myelinated $A\alpha$, $A\beta$ and $A\delta$ fibers, which are involved in limb proprioception, vibration and pressure sensation, and mechanical sensation, respectively. Unmyelinated C-fibers, which are involved in thermal and mechanical burning pain, are also affected. The effects of distal symmetric sensorimotor polyneuropathy include altered perception of thermal, tactile, and vibratory stimuli and can range from hyperalgesia and allodynia to hypoalgesia. Many patients experience a complete loss of sensation in hands and feet, which can increase the risk of trauma and infection, ultimately leading to amputation. Dysfunction of the small cutaneous nerve fibers that respond to thermal stimuli is most commonly reported by patients and diagnosed by clinicians.

1.2 Animal Models of Diabetes

1.2.1 Rodent models

In rodent models, diabetes can be either chemically-induced, genetic or diet-induced. Chemical induction of diabetes involves the injection of a toxin, usually streptozotocin (STZ), that selectively targets and destroys the insulin-producing beta cells. Within several days, the rodents become hyperglycemic. In most injected rodents, the hyperglycemia persists, often exceeding 33mmol/l. The STZ-diabetic rodent model was used in the majority of the experiments described in this dissertation, and the structural and behavioral defects that develop in these animals will be discussed in the next section.

Genetically diabetic rodents are bred to develop hyperglycemia through either impaired insulin secretion or insulin resistance. Rat strains include the BB Wistar model of type 1 diabetes and the Zucker Diabetic Fatty model of type 2 diabetes. Non-obese diabetic (NOD) mice develop type 1 diabetes, while the db/db and ob/ob strains of mice develop type 2 diabetes. These models generally have a longer life-span, but timing of the onset of diabetes can be variable.

Diet-induced models involve feeding rodents either a high-fat or galactose-rich diet. When rodents are fed a diet sufficiently high in fat, they become obese and eventually develop type 2 diabetes. Galactose-fed rodents have normal insulin levels, but experience increased flux through the first stage of the polyol pathway. This model allows the role of aldose reductase in the development of diabetes-induced complications to be separated from the role of insulin deficiency.

1.2.2 Neuropathy in diabetic rodents

Rodent models replicate many, but not all, of the structural and functional defects that develop in humans with diabetes. STZ-diabetic rats develop tactile allodynia (Calcutt et al., 1996), as well as thermal hyperalgesia that ultimately progresses to thermal hypoalgesia (Calcutt et al., 2004). An exaggerated response to the chemogenic stimuli formalin has also been reported in the STZ-diabetic rat model (Calcutt et al., 1994b; Calcutt et al., 1995). Both tactile allodynia and mechanical hypoalgesia have been reported in STZ-diabetic mouse models (Christianson et al., 2007; Drel et al., 2007). STZ-diabetic mice

can also exhibit either thermal hyperalgesia or thermal hypoalgesia (Levine et al., 1982; Gabra and Sirois, 2002, Gabra and Sirois, 2003; Chattopadhyay et al., 2007; Drel et al., 2007). Differences in strain may be accountable for some of this variability (Sullivan et al., 2008). Unlike the rat model, STZ-diabetic mice exhibit reduced pain behavior in response to formalin (Christian et al., 2003b; Johnson et al., 2007). However, both rat and mouse models of STZ-induced diabetes exhibit nerve conduction velocity slowing (Eliasson, 1964; Tomlinson et al., 1982; Mayer and Tomlinson 1983; Obrosova et al., 2005).

In addition to behavioral changes, diabetic rats and mice exhibit shrinkage of both dorsal root ganglia (DRG) neurons (Jiang and Jakobsen, 2004) and myelinated fiber axons (Jakobsen, 1976; Sima and Robertson, 1979).

Degeneration of Schwann cells (Sima and Robertson, 1979; Kalichman et al., 1998) and loss of the paranodal axo-glial junction (Sima et al., 1986) also occur.

The loss of epidermal innervation that develops in rat and mouse models of diabetes (Bianchi et al., 2004; Christianson et al., 2003) will be discussed in detail later in this chapter. Unfortunately, unlike humans with diabetic neuropathy, rodent models do not develop axonal degeneration and myelinated fiber loss (Thomas and Lascelles, 1966).

1.3 Pathogenic Mechanisms

1.3.1 Potential mechanisms

The direct cause of diabetic neuropathy is unknown, but several biochemical pathways are thought to contribute. The metabolic changes induced by hyperglycemia contribute to diabetic neuropathy through defects in the polyol

pathway, activation of protein kinase C, activation of the hexosamine pathway, the generation of advanced glycosylation endproducts (AGEs) and an increased susceptibility to oxidative stress. However, the presence of diabetic neuropathy in patients receiving insulin therapy and maintaining normal glycemic levels suggests that non-metabolic factors may also contribute to diabetic neuropathy. Loss of neurotrophic support is also thought to play a role in the development of diabetic neuropathy.

1.3.2 The polyol pathway

The polyol pathway involves the reduction of glucose to sorbitol by aldose reductase and the consequent oxidation of NADPH to NADP⁺. The sorbitol is then oxidized to fructose by sorbitol dehydrogenase with the reduction of NAD⁺ to NADH. Chronic hyperglycemia can result in a buildup of the organic osmolyte sorbitol, which results in cellular swelling and a decrease in myo-inositol levels (Gillon et al., 1983). The decrease in myo-inositol may ultimately lead to a disruption of the sodium, potassium-ATPase (Greene and Lattimer, 1983). However, the disruption of the sodium, potassium-ATPase has also been attributed to the activation of PKC (Xia et al., 1995), and will be discussed later. The accumulation of sorbitol also results in a reduction of the levels of taurine, which is an antioxidant and promoter of nerve regeneration (Obrosova et al., 2001; Pop-Busui et al., 2001).

Yet another consequence of increased polyol pathway activation is the depletion of NADPH, which is also involved in the glutathione (GSH) cycle and nitric oxide synthesis (Lee and Chung, 1999). NADPH depletion results in a

decrease in both nitric oxide levels and the conversion of GSSG to GSH, which can contribute to oxidative stress. In a study examining the effects of STZ-induced diabetes on transgenic mice lacking aldose reductase, the transgenic mice were protected against both the depletion of GSH and the nerve conduction velocity slowing that was observed in the STZ-diabetic wild type mice (Chung et al., 2003)

In rat models of diabetes, inhibitors of aldose reductase have been shown to improve nerve conduction velocity (Tomlinson et al., 1982; Yue et al., 1982; Mayer and Tomlinson, 1983; Cotter et al., 1998; Obrosova et al., 2002) and axonal transport (Tomlinson et al., 1982; Mayer and Tomlinson et al., 1983), prevent reductions in nerve blood flow (Calcutt et al., 1994; Cotter et al., 1998; Kuzomoto et al., 2006), and prevent both transient thermal hyperalgesia and the development of thermal hypoalgesia (Calcutt et al., 2004). Aldose reductase inhibition also increases neurotrophic activity (Mizisin et al., 1997; Ohi et al., 1998) and prevents reductions in GSH in diabetic rats (Obrosova et al., 2002; Kuzomoto et al., 2006). Although diabetic mice do not accumulate sorbitol, there is a flux of glucose through the polyol pathway (Calcutt et al., 1988) and aldose reductase inhibition has been shown to improve nerve conduction velocity (Miwa et al., 1989; Drel et al., 2006), alleviate thermal hypoalgesia and prevent the loss of epidermal innervation (Drel et al., 2006). In clinical trials roughly 60% of patients showed some improvement in peripheral neuropathy (Pfeifer et al., 1997). However, many large-scale clinical trials have been plagued by safety concerns and poor trial design. Problems with variability of endpoints, as well as

inadequate length and quality control, may have masked potentially beneficial effects of aldose reductase inhibitors.

1.3.3 Activation of PKC

Increased flux through of the polyol pathway also increases the cytosolic NADH/NAD⁺ ratio (Ramasamy et al., 1997), which results in inhibition of GAPDH. The inhibition of GAPDH elevates triose phosphate levels and the triose phosphate lipid second messenger DAG, which activates the β and δ isoforms of protein kinase C (PKC). PKC overactivity can damage blood vessels by altering expression of eNOS, endothelin-1, VEGF, collagen, fibronectin, TGF- β , and plasminogen activator inhibitor-1 (for review see Brownlee 2001, and references therein). The decrease in eNOS expression and increase in endothelin-1 expression cause blood-flow abnormalities, while increases in VEGF expression can result in changes in vascular permeability and angiogenesis. Increases in TGF- β and subsequent increases in collagen and fibronectin, as well as increases in plasminogen activator inhibitor-1 expression, can result in the occlusion of capillaries and other vessels. The activation of PKC also increases cytosolic phospholipase A2 activity, which leads to an increase in the production of the sodium, potassium-ATPase inhibitors arachidonate and PGE2 (Xia et al., 1995).

1.3.4 The hexosamine pathway

The inhibition of GAPDH also results in increased activity of the hexosamine pathway. In the hexosamine pathway, the glycolytic intermediate fructose-6-phosphate is diverted from the glycolytic pathway and instead converted to

glucosamine-6-phosphate by the enzyme glutamine:fructose-6-phosphate amidotransferase (GFAT). Glucosamine-6-phosphate is then glycosylated by the addition of N-acetylglucosamine (GlcNAc) to serine and threonine, with the enzyme O-GlcNAc transferase (OGT) catalyzing the reaction. Increased activity of this pathway results in increased production of PAI-1 and TGF- β 1 (Sharma and McGowan, 2000; Carr, 2001), which are responsible for damage to the kidneys and vascular system. Hyperglycemia induced activation of the hexosamine pathway may also disrupt protein function by O-acetylglucosaminylation (For review see Brownlee 2001, and references therein).

1.3.5 Non-enzymatic glycosylation

Chronic hyperglycemia results in non-enzymatic glycosylation or glycation of proteins, which can ultimately result in the irreversible formation of advanced glycosylation end products (AGEs) (Vlassara et al., 1981). These AGEs are thought to contribute to diabetic neuropathy by accumulating on myelin and activating macrophages, resulting in demyelination (Vlassara et al., 1985). AGEs are also involved in the covalent entrapment of plasma proteins in the extracellular matrix, the cross-linking of basement membrane proteins and alterations in axonal transport by disruption of actin and tubulin (Vlassara et al., 1981). AGEs interfere with the action of nitric oxide and are a source of oxidative stress through the activation of receptors for AGEs (RAGE) and subsequent production of reactive oxygen species (ROS) (for review see Vincent et al., 2004 and references therein). Increased levels of RAGE mRNA and protein have recently been reported in the epidermal axons, sural axons and Schwann cells of

STZ-diabetic mice. Mice lacking RAGE were protected against the development of neuropathy (Toth et al., 2008).

1.3.6 Oxidative stress

The activation of the polyol pathway, the activation of PKC, the activation of the hexosamine pathway and non-enzymatic glycation may be linked by their capacity to generate oxidative stress. In experimental diabetes, several of the antioxidant defenses of peripheral nerves are lowered, including cupric superoxide dismutase (Low and Nickander, 1991), GSH (Nickander et al., 1994), GSH peroxidase (Hermenegildo et al., 1993) and ascorbic acid (Jennings et al., 1997). Lipids, proteins and nucleic acids become oxidized and nitrosylated when these antioxidants are unable to remove free radicals. These altered molecules are unable to perform their required functions and are ultimately targeted for degradation. This process affects cellular activity (Vincent and references therein, 2004).

Multiple studies have demonstrated the ability of various antioxidants to improve diabetes-induced motor and sensory nerve conduction deficits (Cameron et al., 1993; Cameron et al., 1994; Sagara et al., 1996; Cotter and Cameron, 1995; Cameron and Cotter, 1996; Sharma and Sayyed, 2006; Saini et al., 2007), correct changes in thermal sensitivity (Ueno et al., 2002; Sharma and Sayyed, 2006; Saini et al., 2007) and increase endoneurial blood flow (Cameron et al., 1994; Cotter and Cameron, 1995; Sharma and Sayyed, 2006) in rodent models. In clinical trials, various antioxidants have been able to decrease lipid peroxidation (Lubec et al., 1997; Butler et al., 2000), improve blood flow (Butler

et al., 2000) and reduce symptoms of neuropathy (Ziegler et al., 1995) in patients with diabetes. However, at present no definitive proof of the efficacy of antioxidants in preventing or ameliorating diabetic neuropathy has been accepted by the FDA.

1.3.7 Loss of neurotrophic support

Neurotrophic factors are vital to the development and maintenance of nerve fibers and abnormalities in their expression have been detected in both human patients and rodent models of diabetes. Reduced levels of NGF have been observed in skin biopsies from human patients with diabetes (Anand et al., 1996). Reductions in NGF have also been reported in sciatic nerves and superior cervical ganglia of STZ-diabetic rats (Hellweg and Hartung, 1990). Reductions in NGF mRNA have been observed in muscle and foot skin from STZ-diabetic rats (Ferryhough et al., 1994). Decreased levels of the neuropeptides substance P (SP) and calcitonin gene-related peptide (CGRP) in the sciatic nerve were also observed in these animals. Retrograde axonal transport of NGF is also reduced in STZ-diabetic rats (Hellweg et al., 1994). In STZ-diabetic mice, reductions in both serum NGF levels and submaxillary gland NGF content have been observed. However, NGF content in the sciatic nerve was not significantly decreased in these diabetic mice (Ordonez et al., 1994).

Treatments with NGF have been shown to alleviate symptoms of neuropathy in diabetic animals. In STZ-diabetic rats, NGF treatment was able to prevent both the development of thermal hypoalgesia and the depletion of SP and CGRP (Apfel et al., 1994; Diemel et al., 1994). In STZ-diabetic mice, NGF

treatments stimulated axonal branching in the skin, but were unable to restore innervation (Christianson et al., 2003). In a phase II clinical trial, improvements in small fiber function were observed after 6 months of treatment with rhNGF (Freeman, 1999). However, a phase III clinical trial failed to confirm these findings (Apfel et al., 2000). The NGF treatments administered in these clinical trials also resulted in hyperalgesia at the site of injection (Apfel et al., 2000).

Ciliary Neurotrophic Factor (CNTF), which is produced by Schwann cells, serves as a neurotrophic factor for both sensory and motor neurons. CNTF-like activity was found to be reduced in the sciatic nerves of STZ-diabetic and galactose fed rats (Calcutt et al., 1992). Treatments with CNTF have been shown to prevent the development of thermal hypoalgesia (Calcutt et al., 2004), improve nerve conduction velocity and promote regeneration after nerve crush injury in STZ-diabetic rats (Mizisin et al., 2004).

The mRNA of prosaposin, a peptide involved in differentiation and prevention of cell death in a variety of nerve cell types (Hiraiwa et al., 1996), is elevated in the peripheral nerve of STZ-diabetic rats (Calcutt et al., 1999). TX14(A), a prosaposin-derived peptide, has been shown to preserve both axonal caliber and sodium, potassium-ATPase activity, attenuate reductions in SP levels and prevent the development of thermal hypoalgesia in STZ-diabetic rats (Calcutt et al., 1999). The peptide prevents both formalin hyperalgesia and SP-induced thermal hyperalgesia in STZ-diabetic rats and alleviates tactile allodynia (Calcutt et al., 2000; Jolivald et al., 2006). TX14(A) also both prevents and reverses nerve conduction velocity slowing (Calcutt et al., 1999; Mizisin et al., 2001).

Altered expression of neurotrophin-3 (NT-3) (Fernyhough et al., 1995; Fernyhough et al., 1998; Ihara et al., 1996), neurotrophin-4 (NT-4), BDNF (Rodriguez-Pena et al., 1995; Mizisin et al., 1999), IGF-1 (Wuarin et al., 1994), and GDNF (Christianson et al., 2003) has also been detected in skin, muscle, nerve and other organs in experimental diabetes. Administration of exogenous IGF-II (Zuang et al., 1997), NT-3 (Mizisin et al., 1998), and GDNF (Akinna et al., 2001) all demonstrated efficacy in the treatment of diabetic neuropathy. However, to date, none of these therapies have been approved for clinical use.

1.4 Characteristics of Skin

1.4.1 Skin structure

The integumentary system is composed of the epidermis and dermis. The epidermis consists of 4 to 5 layers, including the stratum corneum, the stratum lucidum, the stratum granulosum, the stratum spinosum and the stratum basale. The stratum corneum, the outermost layer, is composed of anucleate keratinized cells. In thick skin, the stratum lucidum is found beneath the stratum corneum. In hematoxylin-stained sections of both thick and thin skin, the stratum granulosum is prominent due to intensely basophilic keratohyalin granules and sits above the stratum spinosum. The stratum spinosum, which is several layers thick, exhibits spiny cytoplasmic processes that are connected to adjacent cells by desmosomes. The stratum basale, the lowermost layer, rests on a basal lamina immediately above the dermis and contains the stem cells from which new keratinocytes arise.

The epidermis is composed primarily of keratinocytes, but also contains melanocytes, Langerhans cells and Merkel's cells. Keratinocytes are epithelial cells that produce various keratins, which are the major structural proteins of the epidermis. By dividing, differentiating, dying and eventually exfoliating, keratinocytes promote the continual turnover of the epidermis.

Melanocytes are derived from neural crest tissue and generate the melanin pigment that gives skin its color. Long dendritic processes emanate from each melanocyte and make contact with keratinocytes, forming a dermal-melanin unit. Melanosomes, containing melanin pigment, are transferred to neighboring keratinocytes through a process called pigment donation. Variations in the rate of melanin synthesis and degradation, rather than melanocyte number, are responsible for differences in skin color.

Langerhans cells are found within stratum spinosum where they present antigens that enter through the skin. These dendritic cells are immunoreactive to antibodies against the pan-neuronal marker protein gene product 9.5 (PGP9.5). In PGP9.5-immunostained skin sections, Langerhans cell processes can be mistaken for epidermal nerve fibers, which results in complications that will be discussed in another chapter.

Merkel's cells, found in the stratum basale, contain dense-core vesicles, form desmosomal attachments with neighboring keratinocytes and are also associated with the terminals of myelinated nerve fibers. Together, the Merkel's cell and associated nerve ending are thought to be involved in mechanical sensation. The innervation of the skin will be further discussed in section 1.4.2.

The dermis is divided into papillary and reticular layers. The papillary layer consists of loose connective tissue, containing both type I and type III collagen, in addition to irregularly arranged elastic fibers. Portions of the papillary dermis, referred to as dermal papillae, project into the epidermis, which allows for a more extensive dermal-epidermal interface. The deeper reticular layer is composed primarily of elastic fibers and thick bundles of type I collagen.

The skin also contains several specialized structures, including hair follicles, nails, sebaceous glands and sweat glands. Hair follicles are only found in thin skin and extend into the dermis and hypodermis. Nails are made of hard keratin and form protective coverings over the epidermis on fingers and toes. Sebaceous glands are often associated with hair follicles and secrete sebum, which lubricates the skin and may have antimicrobial properties. Sweat glands can be classified as either eccrine or apocrine. Eccrine sweat glands cover most of the body and secrete a watery solution that evaporates to cool the blood and lower body temperature. Apocrine sweat glands are found in the axillary, pubic and anal regions. These glands produce produce a fluid that can develop a distinctive odor due to subsequent bacterial degradation.

1.4.2 Innervation

The innervation of the skin consists of low-threshold mechanoreceptors, thermoreceptors and nociceptors, along with their myelinated and unmyelinated axons (for review see Birder and Perl, 1994). The dermis contains low-threshold mechanoreceptors, which are myelinated $A\delta$ or $A\alpha\beta$ fibers with specialized terminals. The terminals are generally associated with hair-follicle receptors

involved in tactile sensation, Meisser's corpuscles involved in touch velocity and low-frequency vibration, Pacinian corpuscles involved in touch acceleration and high-frequency vibration or Ruffini's endings involved in pressure sensation. Myelinated A δ fibers are also involved in cold sensation. Epidermal nerve fibers are predominantly capsaicin-sensitive unmyelinated C-fibers, which are involved in the detection of thermal nociceptive pain (Nolano et al., 1999; Malmberg et al., 2004). C-fibers originate from small neurons in the dorsal root ganglia and form sub-epidermal bundles in the papillary dermis, immediately subjacent to the stratum basale of the epidermis. Individual fibers lose their Schwann cell ensheathment as axons cross the dermal-epidermal junction and weave through the keratinocytes of the epidermis (Wang et al., 1990; Kennedy and Wendelschafer-Crabb, 1993). These epidermal nerve fibers can be divided into two subsets, peptidergic and non-peptidergic. The peptidergic neurons are NGF-responsive and express CGRP, SP and the trkA receptor. The non-peptidergic nerves are GDNF-responsive and express GDNFR α and the P₂X₃ receptor (Snider and McMahon, 1998). Quantification of these epidermal nerve endings has proven to be a valuable diagnostic tool.

1.5 Epidermal Nerve Fiber Quantification

1.5.1 Evaluation of skin biopsies

Skin biopsies are emerging as a valuable means of diagnosing and staging peripheral nerve disorders. As a minimally invasive technique, skin biopsies allow for assessment of a variety of fiber types, including the small unmyelinated fibers that are difficult to evaluate by other means. There is

particular interest in using this technique to provide an assessment of distal symmetrical neuropathies, such as diabetic neuropathy, both to stage and evaluate progression of neuropathy, as well as to assess efficacy of potential therapeutics (Kennedy et al., 1996; Lauria et al., 1998; McArthur et al., 1999). Until recently, clinical studies have been restricted to using electrophysiologic and sensory testing as surrogate markers for nerve pathology, or to the evaluation of sural nerve biopsies, which are invasive and not approved as a diagnostic tool.

1.5.2 Techniques for assessment of intraepidermal nerve fibers

The development of several antibodies has allowed for the immunohistochemical assessment of intra-epidermal nerve fibers (IENFs). The most commonly used antibody is directed at PGP9.5, a cytosolic ubiquitin carboxyl-terminal hydroxylase that is found in all neurons and that, in skin biopsies, binds to dermal nerve bundles as well as both peptidergic and non-peptidergic epidermal nerve profiles (Dalsgaard et al., 1989; Wilkinson et al., 1989). Antibodies against neuropeptides, such as CGRP and SP, have also been used to selectively identify peptidergic nerve fibers (Bjorklund et al., 1986). Non-peptidergic nerve fibers can be identified with antibodies against the P₂X₃ receptor or through their ability to bind isolectin IB4 (Petruska et al., 1997). Antibodies against components of the cytoskeleton have also been used to identify IENFs. A study, comparing immunoreactivity using antibodies against various structural proteins and an antibody against PGP9.5 in skin from healthy subjects and patients with diabetic neuropathy, found similar IENF densities in

skin labeled with antibodies against PGP9.5, β -tubulin and microtubule-associated-protein-1B. IENF densities in skin labeled with antibodies against phosphorylated neurofilament, as well as 70 and 200 kDa neurofilament, were significantly lower than in the PGP9.5-labeled skin (Lauria et al., 2004).

The immunolocalization of transient receptor potential vanilloid receptor subtype 1 (TRPV1), the heat-sensitive receptor found on epidermal C-fibers (Caterina et al., 1997), has recently been examined in skin biopsies from patients with peripheral neuropathy. TRPV1-immunoreactive IENF densities have been quantified in biopsies from breast cancer patients (Gopinath et al., 2005) and patients with painful neuropathies (Lauria et al., 2006). However, epidermal nerve endings immunostained with TRPV1 receptor antibodies can be difficult to distinguish because TRPV1 immunoreactivity has also been observed in keratinocytes (Denda et al., 2001). Confocal microscopy studies examining co-localization of TRPV1 and other IENF markers have shown there to be a loss of TRPV1 immunoreactivity in patients with painful diabetic neuropathy (Lauria et al., 2006). A more recent study of skin from patients with diabetic neuropathy found a loss of TRPV1-expressing epidermal and sub-epidermal fibers, as well as a down-regulation of TRPV1 in surviving fibers (Facer et al., 2007).

Skin samples can be obtained through either punch biopsies or the blister method. Removal of punch biopsies, the more commonly used technique, is minimally invasive and generally does not require a suture (Kennedy, 2004). The even less invasive blister method involves applying a suction capsule to the skin,

which separates the epidermis from the dermis and creates a blister. The epidermis can then be removed with the epidermal innervation remaining intact (Kennedy et al., 1999).

Once removed, biopsies must be fixed and processed. Commonly used fixatives include paraformaldehyde and Zamboni's solution (Kennedy et al., 1996). If embedded in paraffin, tissue can be cut at a thickness of around 5 microns. Frozen tissue embedded in OCT can be cut to around 100 microns after cryoprotection (Kennedy et al., 1996). After sectioning, the tissue may then be mounted on glass slides. If thick sections are cut, they can be stained as 'free floating' sections, which allows the antibody to penetrate deeper into the tissue. Thin tissue sections are appropriate for quantification of immunoreactive profiles. However, for analysis of nerve length, thicker sections are often required (Kennedy et al., 1996).

Immunoreactive IENF profiles can be visualized through conventional light microscopy, fluorescence microscopy or confocal microscopy (Kennedy et al., 1996; Periquet et al., 1999). Methods for quantifying IENF density include manual counting of immunoreactive profiles, stereology and color subtractive-computer-assisted analysis (Underwood et al., 2001). Manual determination of linear density, which is perhaps the most commonly used method, has been shown to significantly correlate with stereology and has a diagnostic efficiency of 88% (McArthur et al., 1998).

There are 2 methods that are commonly used to visually quantify IENF density. The first involves counting all immunoreactive profiles that fall within the

epidermis, even those that represent nerve fragments. The second method involves counting only the nerve fibers that can be seen crossing the dermal-epidermal border, excluding branches within the epidermis. Both methods have been successfully used to quantify reductions in IENF density. However, a recent study found that the first method is more sensitive to capsaicin-induced fiber loss (Smith et al., 2007).

When compared to other widely used endpoints, IENF density measurements were found to be more reproducible than motor and sensory amplitude measurements, with the relative inter-trial variability similar to that of nerve conduction velocity measurements (Smith et al., 2005). As a measure of small fiber neuropathy, IENF density quantification is less invasive and more sensitive than sural nerve biopsy (Herrmann et al., 1999). In diabetic patients, IENF density correlates with warm and cold threshold, heat pain, pressure sense and total neurological disability score (Pittenger et al., 2004; Shun et al., 2004). These findings suggest that measurement of IENF density is a reliable means of evaluating diabetic neuropathy.

1.5.3 Cutaneous innervation in diabetic humans

Initial studies assessing cutaneous innervation in the skin of diabetic subjects found reduced immunoreactivity to PGP9.5, along with reduced immunoreactivity to the neuropeptides CGRP, SP, vasoactive intestinal polypeptide (VIP) and neuropeptide Y (NPY) (Levy et al., 1989; Lindberger et al., 1989). Multiple subsequent studies have confirmed the decrease in PGP9.5-immunoreactive IENFs (Levy et al., 1992; Properzi et al., 1993; Kennedy et al.,

1996; Lauria et al., 1998; Hirai et al., 2000; Gibran et al., 2002; Pittenger et al., 2004; Shun et al., 2004; Koskinen et al., 2005). A reduction in PGP9.5 immunoreactive profiles has been observed in patients suffering from both type 1 (Properzi et al., 1993; Boucek et al., 2005) and type 2 (Shun et al., 2004; Pittenger et al., 2005) diabetes, as well subjects with impaired glucose tolerance (Smith et al., 2005). In a recent study comparing patients with metabolic syndrome to patients with both metabolic syndrome and type 2 diabetes, changes in IENF density were only observed in patients with both afflictions (Pittenger et al., 2005).

In studies examining biopsies from multiple locations, a decrease in IENF density from proximal to distal sites has been observed (Holland et al., 1997; Pittenger et al., 2004), suggesting that loss of small fibers occurs in a length-dependent manner. In addition to the loss of IENFs, diabetic subjects also have a slower rate of nerve regeneration after C-fiber damage induced by topical application of capsaicin compared to non-diabetic subjects, and this impaired regeneration is most marked in patients exhibiting symptomatic neuropathy (Polydefkis et al., 2004).

1.5.4 Correlation with other indices of diabetic neuropathy

Recent studies have also focused on correlating the diabetes-induced reduction in cutaneous nerve fiber density with indices of sensory dysfunction. A quantitative analysis determining both nerve fiber number and length in the epidermis and dermis showed a significant correlation between reduced nerve length in the dermis and slowing of sural nerve conduction velocity, in addition to

an overall decrease in both dermal and epidermal nerve counts and lengths in diabetic patients (Hirai et al., 2000). In another study, IENF density in the distal leg showed a significant negative correlation with warm and cold thermal threshold, heat pain, pressure sense and total neurological disability score (Pittenger et al., 2004). A third study, examining distal leg biopsies from type 2 diabetic patients, found a strong negative correlation between IENF density and warm temperature threshold (Shun et al., 2004). These authors also reported a negative correlation between duration of diabetes and IENF density. A comparison of diabetic patients with and without neuropathic pain found a significant inverse correlation between IENF density and vibration perception threshold, as well as between IENF density and neuropathy status determined with a Michigan Neuropathy Screening Instrument in both groups. However, a significant correlation between IENF density and cold perception threshold was only observed in the group without pain (Sorensen et al., 2006). Correlations between IENF density and other measures of diabetic neuropathy, even those that do not measure small fiber dysfunction specifically, could be useful for staging neuropathy and provide a means of assessing efficacy of potential therapeutics in clinical trials. It has been reported that there is loss of epidermal fibers in patients with impaired glucose tolerance but without overt diabetes (Smith et al., 2001). Another study comparing patients with impaired glucose tolerance to patients with diabetes found that the reduction in IENF density in the group with impaired glucose tolerance was less severe (Sumner et al., 2003). Reductions in IENF density have also been reported in diabetic patients that do

not yet show clinical or electrophysiological evidence of neuropathy (Umapathi et al., 2007). Together these studies suggest that skin biopsies may be able to detect neuropathy at its earliest stages.

1.5.5 Animal models

The literature describing cutaneous innervation in non-human primates with diabetes is currently limited to a single paper assessing innervation of glabrous skin from monkeys with naturally occurring type 2 diabetes (Pare et al., 2007). Biopsies from monkeys with short-term hyperglycemia showed a hypertrophy of epidermal nerve fibers. However, in monkeys that were diabetic for duration of 8 years or longer, a severe reduction in PGP9.5-immunoreactive IENFs was observed. CGRP- and TRPV1-immunoreactivity was also diminished in the epidermis of longer-term diabetic monkeys.

While diabetic rats form the most extensively studied model of diabetic neuropathy, the literature describing immunohistochemical assessment of skin biopsies from diabetic rats is less extensive than the clinical literature. One of the earliest studies (Karanth et al., 1990) assessed SP, CGRP, VIP, NPY and PGP9.5 immunoreactivity in skin from the lip and footpad of STZ-induced diabetic rats, a model of insulin-deficient type 1 diabetes, and found no change at 2, 4 and 8 weeks of diabetes. However, at 12 weeks of diabetes an increase in CGRP-reactive fibers was observed in both the dermis and epidermis, along with an increase in VIP around sweat glands and blood vessels. An increase in PGP9.5 immunoreactivity was also reported, while dermal or epidermal SP and NPY immunoreactivity was unchanged (Karanth et al., 1990). The early increase

in sweat gland associated VIP is similar to that seen in humans with diabetes for less than 3 years (Properzi et al., 1993).

At the time that I began this dissertation, no other studies of epidermal innervation in diabetic rats had been published. Studies published during my dissertation work have been unable to confirm this apparent increase in epidermal and dermal innervation in diabetic rodents and instead have shown a reduction in epidermal innervation in rat models of diabetic neuropathy (Bianchi et al., 2004; Lauria et al., 2005; Leonelli et al., 2007; Roglio et al., 2007), which mirrors the reduction observed in human subjects with longer durations of diabetes. A correlation between decreased IENF density and tail sensory nerve conduction velocity slowing has also been observed in rats with STZ-induced diabetes (Lauria et al., 2005). Together, these data suggest that rats may be useful for modeling loss of cutaneous innervation in diabetic neuropathy and for investigating the pathophysiological mechanisms involved.

The immunohistochemical assessment of skin biopsies in diabetic mice was also limited when I began my research. In a study examining the cutaneous innervation of C57Bl/6 mice with STZ-induced diabetes of 7 week's duration, footpad and flank skin biopsies showed decreased immunoreactivity to CGRP, P₂X₃, and PGP9.5 when compared to non-diabetic controls (Christianson et al., 2003). However, it should be noted that this quantification included both dermal and epidermal profiles. Studies had also been performed in type 2 diabetic mouse models that spontaneously develop insulin resistance before ultimately progressing to insulin deficiency. Compared to their heterozygous non-diabetic

littermates, PGP9.5-immunoreactive epidermal fibers were significantly reduced in genetically diabetic C57BL/KsJ-m^{+/+}Lepr^{db}; db/db mice, and similar reductions were observed in the skin samples from human subjects evaluated in the same study (Gibran et al., 2002). These results agree with changes observed in both type 1 and type 2 diabetic patients and suggest that mice may also be a valuable model for the studying cutaneous innervation.

1.5.6 Therapeutic interventions

The effects of therapeutic intervention on cutaneous innervation in animal models of diabetes are largely unexplored. During the course of my dissertation work, a report was published on the neuroprotective properties of erythropoietin in the STZ-diabetic rat (Bianchi et al., 2004). While the density of PGP9.5-immunoreactive profiles in the epidermis was unchanged after 5 weeks of diabetes in this study, a significant reduction was observed after 11 weeks of diabetes and administration of erythropoietin from week 5 onwards prevented the epidermal nerve fiber deficit from developing. Thermal hypoalgesia, already present at week 5 of diabetes, was also reversed by erythropoietin treatment. Another study examining the effects of intrathecally delivered insulin and IGF-1 found an increase in IENF density and IENF length compared to the untreated diabetic group (Toth et al., 2006). However, the treatments were unable to increase IENF density or length to that of the non-diabetic control group. Recent evidence also suggests that progesterone and its reduced metabolites, as well as testosterone and its metabolites, may have protective effects against cutaneous nerve fiber loss (Leonelli et al., 2007; Roglio et al., 2007). In STZ-diabetic rats,

treatments with progesterone, dihydroprogesterone and tetrahydroprogesterone were able to prevent a reduction in IENF density and reverse established thermal hypoalgesia (Leonelli et al., 2007). Treatments with testosterone, dihydrotestosterone and $5\alpha,17\beta$ -diol prevented a reduction in IENF density. However, only dihydrotestosterone and $5\alpha,17\beta$ -diol were able to partially reverse thermal hypoalgesia (Roglio et al., 2007).

During my dissertation work, STZ-diabetic mice have also been used to assess efficacy of assorted therapies. Intrathecal treatment with NGF for 2 weeks stimulated axonal branching, but failed to improve cutaneous innervation, whereas intrathecal GDNF and NTN treatment increased both axonal branching and cutaneous innervation in diabetic mice (Christianson et al., 2003). Herpes-simplex-virus-mediated gene transfer of both vascular endothelial growth factor (VEGF) (Chattopadhyay et al., 2005) and neurotrophin-3 (NT-3) (Chattopadhyay et al., 2007) has been shown to prevent reductions in proportional area of footpad skin and subcutaneous tissue occupied by PGP9.5-immunoreactive nerve fibers in STZ-diabetic mice. In the ob/ob mouse model, treatment with an aldose reductase inhibitor was able to prevent both onset of thermal hypoalgesia and IENF loss (Drel et al., 2006). Peroxynitrite decomposition catalysts have also shown efficacy in the prevention of IENF loss (Drel et al., 2007). However, in none of these studies was the therapy used against established loss of epidermal fibers and, while the data are encouraging for the development of prophylactics, whether these or any other agents have the

capacity to promote functional re-innervation of the epidermis remains to be established.

1.5.7 Pathogenic mechanisms of epidermal fiber loss

In most clinical studies of IENF loss, distinctions have not been made between patients with insulin-dependent type 1 diabetes and patients with insulin-resistant type 2 diabetes. However, whether or not IENF loss is affected by the presence or absence of insulin is an important question. While several studies have reported a reduction in IENF density in rat models of type 1 diabetes (Bianchi et al., 2004; Lauria et al., 2005; Leonelli et al., 2007; Roglio et al., 2007), the effects of hyperglycemia on epidermal innervation in rat models of type 2 diabetes remain unexplored. Fiber loss has been reported in mouse models of type 2 diabetes (Gibran et al., 2002; Drel et al., 2006), although these models can show insulinopenia in later stages of the disease. Another study of STZ-induced type 1 diabetic mice found evidence of epidermal reinnervation in mice that had spontaneously regained islet cell function (Kennedy and Zochodne, 2005). The role that endogenous insulin plays in the preservation of cutaneous innervation is certainly worthy of further study.

Examination of the effects of various therapeutics on IENF density (see above) may also shed light on the pathogenic mechanisms underlying cutaneous nerve fiber loss. The efficacy of erythropoietin (Bianchi et al., 2004) and exogenous insulin (Toth et al., 2006), both of which have neurotrophic properties (Konishi et al., 1993; Fernyhough et al., 1993; Xu et al., 2004), as well as GDNF, NTN (Christianson et al., 2003), VEGF (Chattopadhyay et al., 2005) and NT-3

(Chattopadhyay et al., 2007) at preventing cutaneous nerve fiber loss in diabetic rodents suggests that diminished neurotrophic support may contribute to similar losses in patients with diabetes. The efficacy of aldose reductase inhibition (Drel et al., 2006) indicates that increased flux through the polyol pathway may also contribute to the pathogenic mechanisms involved.

Specific Aims

The following questions will be addressed in this dissertation:

1. Do rodent models mirror the epidermal nerve fiber loss observed in humans with diabetic neuropathy, and what other diabetes-induced changes develop in skin?
2. How do changes in epidermal nerve fiber density relate to alterations in thermal nociception?
3. What are the mechanisms involved in the development of epidermal nerve fiber loss and thermal hypoalgesia?

2 – GENERAL METHODS

2.1 Rodent Models of Diabetes

Experiments examining the effects of type 1 diabetes were performed on adult female rats of either the Wistar or Sprague-Dawley strains, or adult male mice of either the C57Bl/6 or Swiss Webster strains. Mice and rats were given an intraperitoneal injection of streptozotocin (STZ), an antibiotic that selectively targets insulin-producing beta cells by binding to the GLUT2 receptor (Schnedl et al., 1994). In cell culture, STZ reduces GLUT2 protein levels, but not mRNA levels, in a concentration-dependent manner (Gai et al., 2004). High doses of STZ result in beta cell toxicity. Multiple lower doses result in both beta cell toxicity and T-cell dependent immune reactions (Wang and Gleichmann, 1998). Injections of STZ cause an initial drop in blood glucose levels, followed by a permanent state of hyperglycemia. The STZ was dissolved in 0.9% sterile saline and administered at a dose of 55 mg/kg of body weight for rats and 180 mg/kg for mice. Prior to each STZ injection, rats and mice were fasted to limit the competition between endogenous glucose and STZ for the GLUT2 receptor. Hyperglycemia was confirmed after 3 days with a glucose-oxidase-strip-operated reflectance meter, and rodents with blood glucose levels above 15 mmol/l were considered diabetic. Blood glucose levels were monitored throughout the studies

Experiments examining the effects of type 2 diabetes were performed on db/db (B6.Cg-*m*+/*+**Lep*^{*db*}/*J*) mice obtained from Jackson Labs (stock #000697).

These mice are homozygous for the spontaneous G→T point mutation *Lepr^{db}*. As a result, they express an alternatively spliced transcript of the leptin receptor OB-R that lacks the long intracellular domain necessary for intracellular signal transduction (Chen et al., 1996). Leptin plays a central role in the regulation of metabolism, appetite and body weight. With a mutated leptin receptor, db/db mice become obese by 3 to 4 weeks of age and exhibit polydipsia, polyuria and polyphagia. Initially db/db mice exhibit hyperinsulinemia, but after prolonged periods of hyperglycemia many mice experience a drop in insulin levels (Hummel et al., 1966). Non-diabetic C57Bl/6 mice were used as age-matched controls. Blood glucose levels of the db/db mice were measured weekly for the duration of the study.

Rats and mice were housed in a vivarium with controlled temperature and humidity. The light/dark schedule was 12 hours of light followed by 12 hours of darkness. The rodents were given free access to food and water. In early studies, rats and mice were fed Harlan diet 8604. In later studies, the diet was switched to Harlan 7001, which has lower levels of several antioxidants (see Table 3.2). Body weights were monitored weekly. Low doses of insulin were given to rats whose body weights fell to below 200 grams.

2.2 Behavioral Assessment

2.2.1 Measurement of thermal response latency

Thermal response latency was measured using a slightly modified version of the method described by Hargreaves et al. (1998). Animals were placed in plexiglass enclosures with a warmed (30°C) glass floor and allowed to acclimate

for approximately 30 minutes. After the acclimation period, a mobile radiant heat source was applied to the heel portion of the hind paw from below the glass. The heat was increased at a rate of approximately 0.9°C per second to ensure that the animal's response was due to the activation of C-fibers (Yeomans et al., 1996; Yeomans and Proudfit, 1996). The latency from the initiation of heat to paw withdrawal was measured by movement sensors. The heat source was automatically cut off after 20 second to avoid tissue damage. Animals were observed during latency measurements to ensure that paw withdrawal movements were not part of normal movement or grooming behavior. All measurements were taken after a 30-minute acclimation period, with 5-minute intervals between each measurement. The initial measurement was discarded, and the median of the following 3 measurements was used for analysis. A calibration curve, representing the rate of heat increase, was also constructed for each group of animals to allow for conversion from withdrawal latency to the temperature applied at the time of withdrawal.

2.3 Rodent Physiology

2.3.1 Measurement of motor nerve conduction velocity

Motor nerve conduction velocity measurements were taken from control and diabetic mice of the C57Bl/6 and Swiss Webster strains. Mice were anesthetized with isoflurane and placed on a heating pad. A thermistor probe was inserted rectally, and a constant body temperature was maintained. Paws were immobilized and reference electrodes were inserted in the interosseous muscles. Mice were then stimulated with an electrode at the ankle followed by

stimulation at the sciatic notch. The difference in response latency between the 2 sites was recorded to obtain the time required for the motor nerve conduction to travel from the ankle to sciatic notch. Calipers were then used to measure the distance between the 2 areas stimulated. The distance was divided by the difference in response latencies to obtain the nerve conduction velocity.

2.3.2 Measurement of Blood Flow

Blood flow was measured by laser Doppler. A low power laser was used to illuminate the foot pad skin, and an optical probe collected backscattered light. A percentage of that light was scattered by red blood cells, and Doppler shift was derived by comparing emitted and returned signal. Prior to measurement, animals were anesthetized with isoflurane and placed on a heating pad. A cylindrical laser probe was then applied directly above the skin for 20 seconds before the blood flow, expressed in arbitrary units, was recorded. The probe was applied to 5 separate points on the plantar surface of the hind paw, starting at the tubercles and continuing down toward the heel, and the average of these 5 measurements was used for analysis.

2.4 Immunohistochemical Assessment of Skin Biopsies

2.4.1 Immunohistochemistry

Skin biopsies were taken from the plantar surface of the hind paw. The tissue was immediately submerged in 4% paraformaldehyde in 0.1M sodium phosphate buffer and fixed for 24 hours. Tissue samples were then dehydrated and embedded in paraffin blocks. 6 μm thick sections were then cut transversely so that both the dermal and epidermal layers were visible and collected onto

glass slides. The slides were incubated with either an antibody against the pan-neuronal marker PGP9.5 (1:1000, Chemicon International, Temecula, CA or Biogenesis Ltd., UK), an antibody against substance P (SP) to visualize peptidergic innervation (1:50, Abcam Inc, Cambridge, MA) or an antibody against growth associated protein-43 (GAP-43, 1:1000, Abcam, UK) in order to visualize regenerating fibers. The primary antibody incubation was followed by an incubation with a secondary biotinylated antibody. Next, the slides were incubated with a peroxidase-conjugated avidin-biotin enzyme complex (Vector Laboratories, Burlingame, CA). Immunoreactive profiles were visualized by adding a substrate containing hydrogen peroxide (Vector Laboratories, Burlingame, CA), which produced a red reaction product. Specificity was confirmed by omitting the primary antibody on certain sections.

2.4.2 Quantification of innervation

Immunoreactive profiles were viewed and quantified using a light microscope at 400x magnification by an observer who was unaware of the treatment groups. The total number of immunoreactive profiles throughout the epidermis was then normalized to the length and area of the section. Immunoreactive profiles in the immediately subjacent papillary dermis were also quantified. Figure 2.1 contains a representative micrograph demonstrating PGP9.5-immunoreactive nerve fiber profiles.

In initial experiments, length was traced and measured using a computerized system (ImagePro). In later experiments, point-counting methods using a grid reticle (Microscope Depot, Tracy, California) containing 100 squares

each 25 μm were used to determine both the length and area of the sections analyzed. For measurement of length, the number of intersections between the epidermis, measured along the base of the stratum granulosum, and the grid lines was quantified. Length was calculated using a previously derived formula (Kalichman et al. 1995): $\text{Length} = \text{no. of intersections} \times 1/2 \times (\pi/2 \times 25 \text{ micrometers})$.

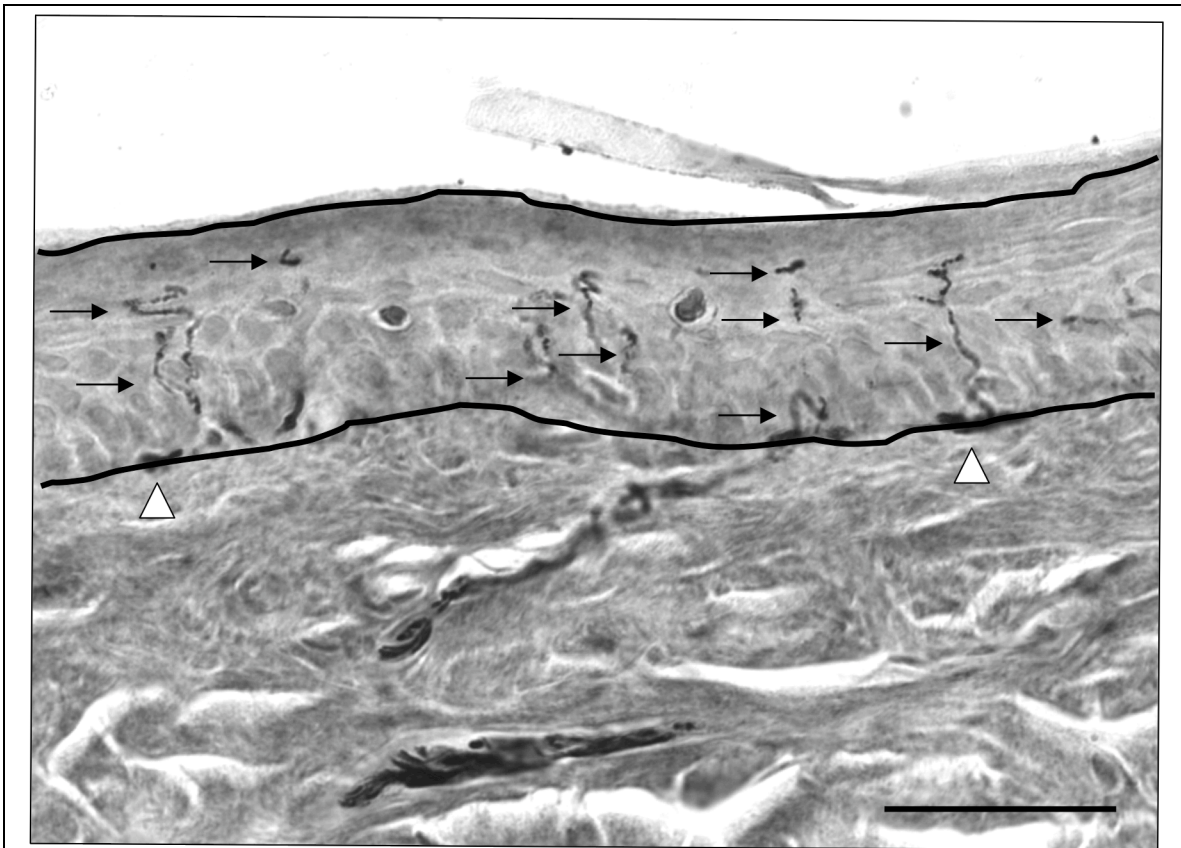


Figure 2.1. A micrograph of PGP9.5-immunostained rat skin. Arrows identify immunoreactive IENF profiles, arrowheads identify sub-epidermal nerve plexuses and black lines mark the upper and lower boundaries of the epidermal area analyzed. Bar, 40 μm .

Epidermal area was quantified by counting the number of lattice points contained within the epidermis, excluding the stratum lucidum and the stratum corneum.

The total number of points was then multiplied by the area of each individual square within the grid to calculate the total area of the section analyzed.

Epidermal thickness was determined by dividing the area of each section by its length. However, due to the undulating nature of the dermal-epidermal junction, our calculation was an estimation of the average thickness, rather than the exact thickness at any given point.

2.5 ELISA Assays

2.5.1 Measurement of serum insulin levels

Blood was collected at the time of sacrifice and allowed to clot. Serum was then separated by centrifugation. Samples were stored at -20°C until time of use. Insulin levels were measured using an ultrasensitive mouse insulin ELISA kit (Merckodia, Winston Salem, NC). Samples were added to a plate coated with monoclonal anti-insulin antibodies and incubated for 2 hours with a solution containing monoclonal peroxidase-conjugated anti-insulin antibodies that were directed against a separate epitope. Samples containing a known amount of insulin were also included. After washing to remove unbound antibodies, 3,3',5,5'-tetramethylbenzidine was added to allow for colorimetric detection. After 30 minutes, 0.5M H_2SO_4 was added to stop the reaction. Spectrophotometric readings of plates were made using a wavelength of 450 nm. The known samples were used to construct a standard curve, and the insulin levels of the unknown samples were then extrapolated.

2.5.2 Measurement SP

SP was first extracted from sciatic nerves by boiling the tissue in a media consisting of 2M glacial acetic acid, 10mM hydrochloric acid, 1mM ethylene diamine tetraacetic acid and 1mM DL-dithiothreitol. After the nerves were homogenized and centrifuged, the supernatant was extracted and freeze dried. SP content of the reconstituted supernatant was later measured using a competitive enzyme immunoassay (Substance P EIA, Cayman Chemical Co., Ann Arbor, MI).

2.6 Measurement of Protein Oxidation

Foot skin samples were homogenized in PBS buffer, pH 7.4 containing 5 mM butylated hydroxytoluene (Sigma-Aldrich) and 0.4% protease inhibitor cocktail (Sigma-Aldrich). Samples were then centrifuged at 10,000g for 15 minutes at 4°C and supernatants were collected. The levels of oxidatively modified proteins were measured by immunoblotting using an assay kit (Chemicon International., CA, USA; OxyBlot Protein Oxidation Detection assay).

3 - Assessment of Epidermal Innervation in Rodent Models of Diabetes

3.1 Introduction

3.1.1 Immunohistochemical assessment of epidermal innervation

The immunohistochemical assessment of skin biopsies, which are relatively non-invasive and easy to obtain, is emerging as a valuable means of diagnosing and staging clinical neuropathy. However, certain aspects of this technique still require validation. This chapter describes my work investigating the nature of changes in epidermal innervation in various rodent models of diabetes and identifying other diabetes-induced changes in skin.

The development of several neuron-specific antibodies has made the visualization of epidermal innervation possible. Antibodies against protein gene product 9.5 (PGP9.5), an ubiquitin carboxyl-terminal hydroxylase that is found in the cytoplasm of nerve fibers, are most commonly used in the identification and quantification of epidermal nerve fibers. However, questions have been raised as to whether changes in PGP9.5 immunoreactivity reflect a loss of innervation, or simply a downregulation of PGP9.5 expression in otherwise intact nerves. Comparisons between PGP9.5-immunoreactivity and immunoreactivity to other neuronal proteins in skin from both diabetic and non-diabetic rodents may help to address this question. High molecular weight (HMW) Tau is a microtubule-associated protein that is expressed in peripheral nerves, and antibodies against this protein also identify epidermal nerve fibers (Georgieff et al., 1993; Nothias et

al., 1995). In order to validate the use of the PGP9.5 antibody, we compared immunoreactivity in PGP9.5-immunostained skin sections to immunoreactivity in HMW Tau-immunostained skin sections from both control and diabetic rats.

3.1.2 Epidermal innervation in animal models of diabetic neuropathy

Although changes in epidermal innervation have been observed in primate (Pare et al., 2007), rat (Bianchi et al., 2004; Lauria et al., 2005; Leonelli et al., 2007; Roglio et al., 2007) and mouse (Gibran et al., 2002; Christianson et al., 2003;) models of diabetes, the techniques used to quantify epidermal innervation in these studies have varied. In some studies, both epidermal and dermal innervation were quantified (Christianson et al., 2003), while in other studies, only fibers observed crossing the dermal-epidermal junction were considered (Bianchi et al., 2004; Lauria et al., 2005; Leonelli et al., 2007; Roglio et al., 2007). Rodent strain and methods of induction of diabetes also vary. STZ-diabetic rats of the Sprague-Dawley strain have been evaluated (Bianchi et al., 2004; Lauria et al., 2005; Leonelli et al., 2007; Roglio et al., 2007), but innervation in rat models of type 2 diabetes remains unexplored. STZ-diabetic mouse models of the C57BL/6 strain (Christianson et al., 2003) have also been studied, but the majority of literature has focused on type 2 diabetic mouse models (Gibran et al., 2002; Drel et al., 2006; Vareniuk et al., 2007). It has recently been suggested that the effects of diabetes can vary greatly between various strains of mice (Sullivan et al., 2008). Although epidermal innervation has been examined in multiple strains of rats and mice, the effects of diabetes on epidermal nerve fiber density have yet to be assessed using a consistent method of quantification that

would allow for comparisons to be drawn between rats and mice of various strains. In the following experiments we sought to evaluate and compare diabetes-induced changes in epidermal innervation in various strains of rats and mice using a consistent method of quantification. We also examined the effect of diets containing different amounts of anti-oxidant vitamins on epidermal nerve fiber density in non-diabetic and STZ-diabetic rats.

3.1.3 Other diabetes-induced changes in skin

While there has been increasing interest in evaluating epidermal innervation in both human patients and animal models of diabetes, the effects of diabetes on other characteristics of skin remain largely unexplored. Glucose, insulin and IGF-1 all play a role in keratinocyte differentiation and proliferation (Spravchikov et al., 2001; Wertheimer et al., 2001). However, to date no attempts have been made to examine the effects of hyperglycemia and insulin-deficiency on keratinocytes and epidermal thickness in rodent models of diabetes. In the following experiments, epidermal thickness was also assessed in a variety of rodent models of diabetes.

3.2 Methods

3.2.1 Rodent models of diabetes

Type 1 diabetes was induced in rats of both the Wistar and Sprague-Dawley strains by a 50mg/kg injection of streptozotocin (STZ), an antibiotic that selectively targets and destroys insulin-producing beta cells. Mice of C57Bl/6 and Swiss Webster strains were injected with 180mg/kg of STZ to induce type 1 diabetes. Hyperglycemia was confirmed 3 days later, and only the rodents with

blood glucose levels exceeding 15 mmol/l were included in the diabetic groups. In order to study the effects of type 2 diabetes, db/db mice were purchased from Jackson Labs. db/db mice are homozygous for a leptin receptor mutation that results in hyperphagia and obesity, eventually leading to the development of hyperglycemia. Blood glucose levels were monitored throughout the study.

3.2.2 Analysis of skin samples

Plantar foot skin was removed from both non-diabetic control and STZ-diabetic rats of the Sprague-Dawley and Wistar strains, and non-diabetic control and STZ-diabetic mice of the C57Bl/6 and Swiss Webster strain. Plantar foot skin was also obtained from type 2 diabetic db/db mice. Skin samples were then processed and immunostained with antibodies against either PGP9.5 (Chemicon International, Temecula, CA or Biogenesis Ltd., UK) or HMW Tau (obtained from Dr. I Fischer) using the methods described in section 2.4.1. Both epidermal and sub-epidermal nerve fiber density were then assessed as described in section 2.4.2.

3.2.3 Measurement of epidermal thickness

Section area and section length were measured using the point counting methods described in the section 2.4.2. By dividing the epidermal area by the length of the epidermis, we derived an estimation of epidermal thickness. Given the undulating nature of the dermal-epidermal interface, our calculations did not necessarily reflect the precise thickness of the epidermis at any given point, but rather an estimation of the average distance between the dermal-epidermal interface and the stratum granulosum. The total number of nuclei observed

within the epidermis was also quantified and normalized to section length.

Although the epidermis contains melanocytes and Langerhans cells, the majority of the cells are keratinocytes. Hence, we assumed that the majority of the nuclei counted belonged to keratinocytes.

3.2.4 The effects of diet on epidermal innervation

Female Sprague Dawley rats were used to examine the effect of diet on epidermal nerve fiber density. Type 1 diabetes was induced using the methods described in section 3.2.1. Immediately following the confirmation of hyperglycemia, 1 group of diabetic rats and 1 group of non-diabetic control rats were placed on a diet with lower levels of several antioxidant vitamins (Harlan Diet, 7001), while another group of diabetic rats and another group of non-diabetic control rats were given the standard diet (Harlan Teklad Diet 8604, see table 3.3 for a comparison). After 12 months, the rats were sacrificed and foot skin was collected, immunostained and analyzed using the methods described in sections 2.4.1 and 2.4.2.

3.3 Results

3.3.1 Comparison of PGP9.5 and Tau immunoreactivity

Skin sections from Sprague-Dawley rats immunostained with antibodies against either PGP9.5 (Figure 3.1A) or HMW Tau (Figure 3.1B) contained multiple branched profiles, with the varicosities that are indicative of epidermal nerve fibers. The immunoreactive IENF profile densities were similar in both the control (Figure 3.1C) and diabetic (Figure 3.1D) groups. However, the HMW Tau

antibody did not appear to stain the Langerhans cells that are often stained by antibodies against PGP9.5 (see Figure 3.2).

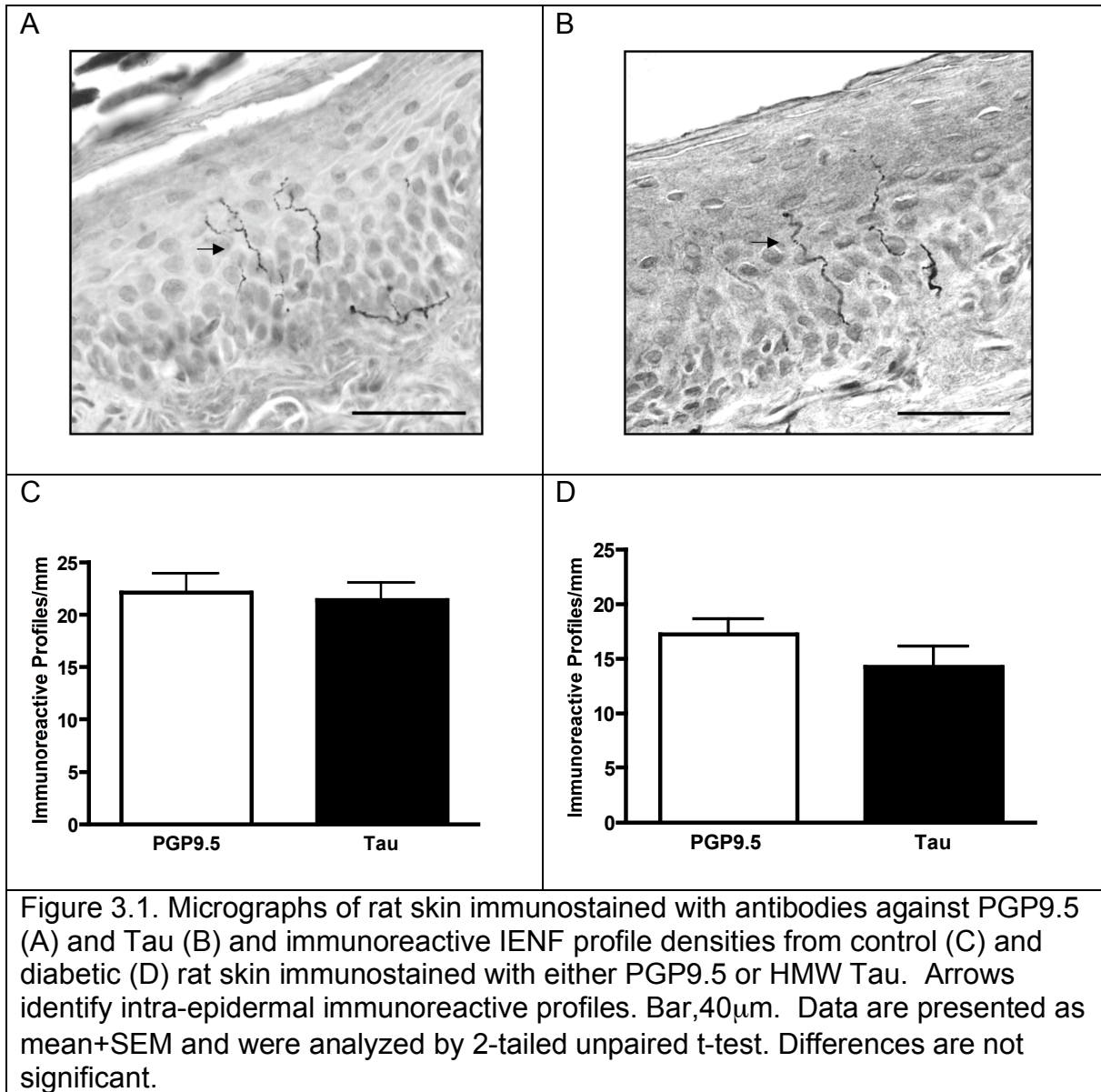
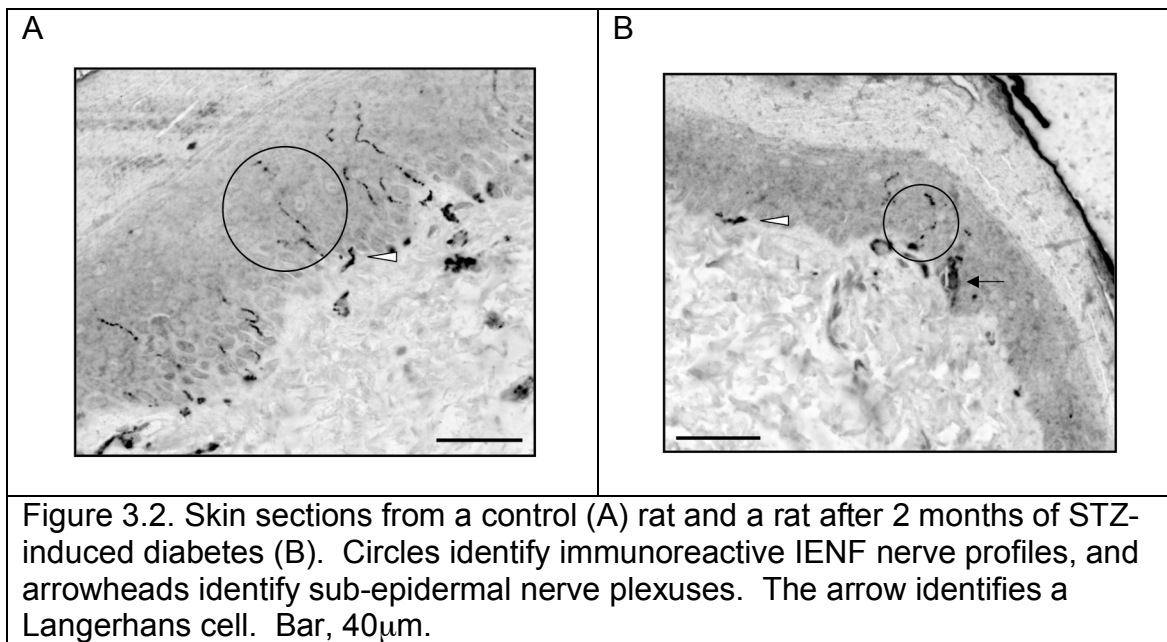


Table 3.1. Strain, gender, duration of diabetes, final body weight and final blood glucose levels for the rats and mice described in this chapter.				
Strain/Species	Gender	Treatment/Duration	Final Body Weight (g)	Final Blood Glucose (mmol/l)
Wistar/Rat (N=9)	Female	Control	unavailable	unavailable
Wistar/Rat (N=9)	Female	Diabetic/8 weeks	unavailable	unavailable
Sprague-Dawley/Rat (N=8)	Female	Control	unavailable	unavailable
Sprague-Dawley/Rat (N=8)	Female	Diabetic/8 weeks	218.8±32.2	unavailable
C57Bl/6/Mouse (N=8)	Male	Control	30.5±1.7	All<15
C57Bl/6/Mouse (N=7)	Male	Diabetic/4 weeks	18.6±1.9**	All>15
Swiss Webster/Mouse (N=8)	Male	Control	31.7±1.8	10.2±1.9
Swiss Webster/Mouse (N=8)	Male	Diabetic/4 weeks	23.2±3.2**	>33.3
C57Bl/6/Mouse (N=8)	Male	Control	26.1±1.7	6.7±0.6
db/db/Mouse (N=8)	Male	Diabetic/41 days	51.7±2.4**	18.2±5.1
Data are mean ± SEM. Statistical analysis was performed by unpaired t-test, **p<0.01.				

3.3.2 Immunoreactive IENF profile density in rat models of diabetes

Figure 3.2 contains representative micrographs of PGP9.5-immunostained skin from control and diabetic rats. We observed a significant ($p<0.05$) reduction in linear immunoreactive IENF profile density in female Wistar rats with STZ-induced diabetes of 2 month's duration (Figure 3.3A). A significant ($p<0.01$) reduction in linear immunoreactive IENF profile density was also observed in female Sprague-Dawley rats with STZ-induced diabetes for 2 month's duration

(Figure 3.3B). The density of sub-epidermal nerve profiles did not differ between diabetic and control rats of either strain (Figure 3.3C,D).



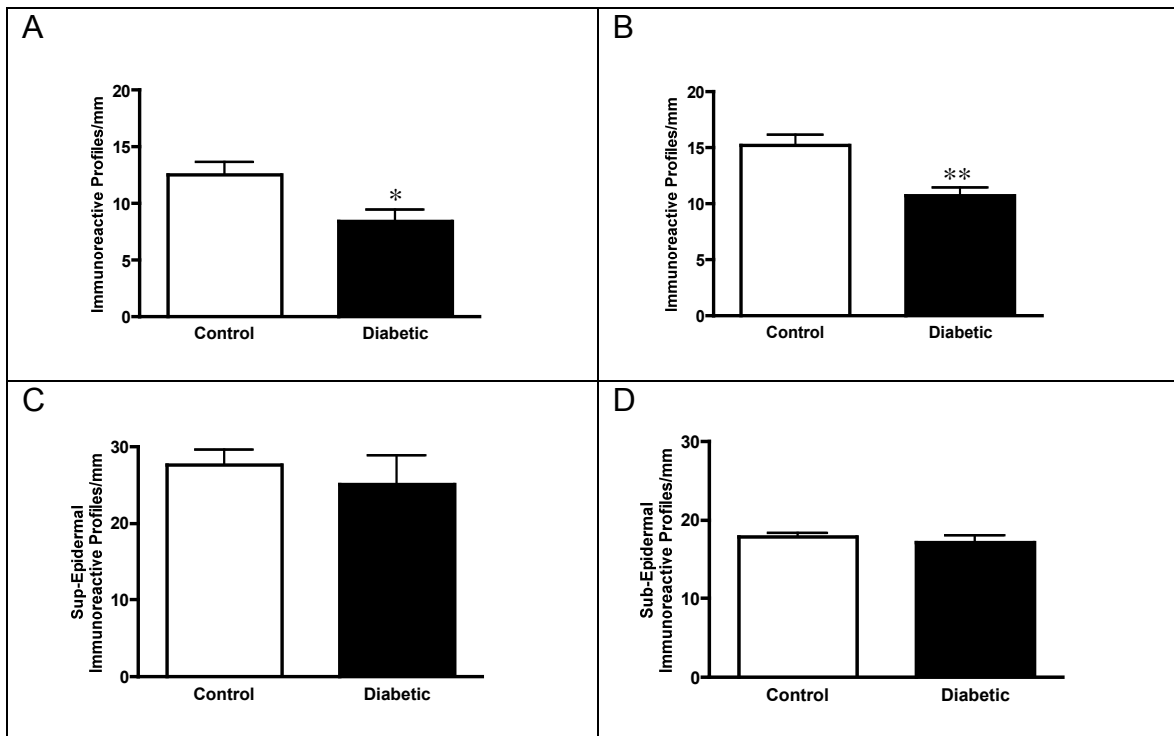
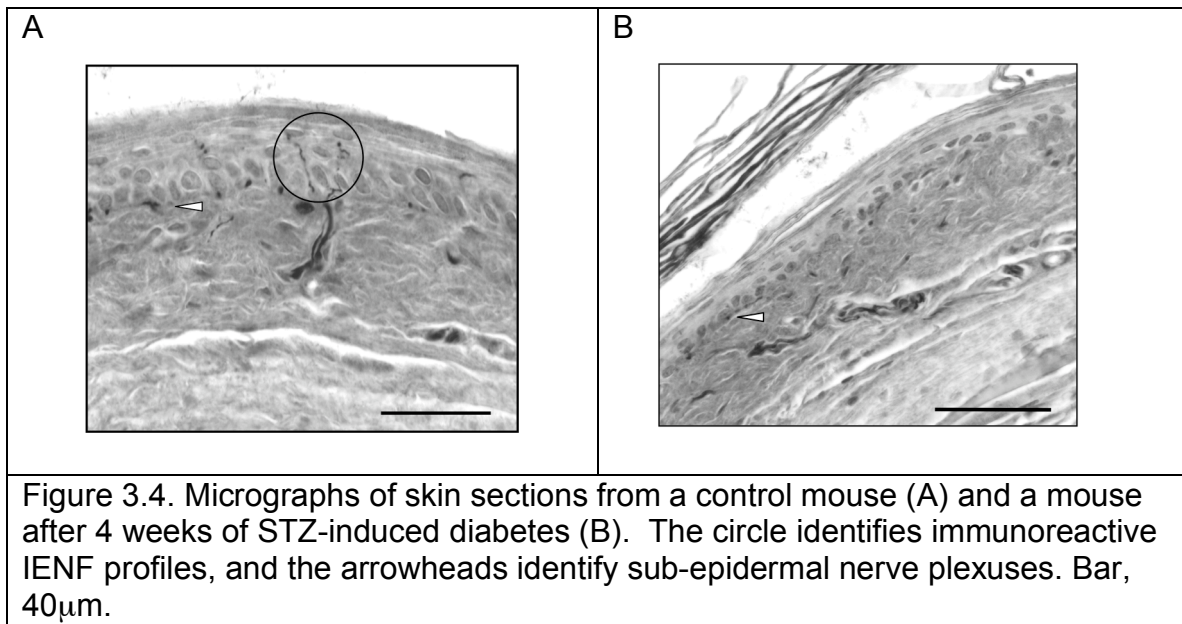


Figure 3.3. Immunoreactive IENF profile density was significantly reduced in female Wistar rats after 2 months of STZ-induced diabetes (A). A significant reduction was also observed female Sprague Dawley rats after 2 months of STZ-induced diabetes (B). The sub-epidermal immunoreactive nerve profile densities of both the Wistar (C) and Sprague-Dawley (D) rats were unchanged. Data are presented as mean+SEM and were analyzed by an unpaired 2-tailed t-test, * $p < 0.05$, ** $p < 0.01$.

3.3.3 Immunoreactive IENF profile density in mouse models of diabetes

Diabetic mice of both the C57BL/6 and Swiss Webster strains developed significant ($p < 0.01$) weight loss (Table 3.1) compared to control mice. Figure 3.4 contains representative micrographs of PGP9.5-immunostained skin from control and diabetic mice. In mice of the C57Bl/6 strain with STZ-diabetes for 4 week's duration, we observed a significant ($p < 0.01$) reduction in linear immunoreactive IENF profile density (Figure 3.5A). A significant ($p < 0.01$) reduction in linear



immunoreactive IENF profile density was also observed in Swiss Webster mice with diabetes for 4 week's duration (Figure 3.5B). Type 2 db/db mice developed significant ($p < 0.01$) weight gain, compared to non-diabetic control mice (Table 3.1). The db/db mice also developed a significant ($p < 0.01$) reduction in linear immunoreactive IENF profile density after approximately 41 days of hyperglycemia (Figure 3.5C). Again, sub-epidermal nerve profile density did not differ between the diabetic and control mice of the C57Bl/6, Swiss Webster and db/db strains (Figure 3.5D,E and F, respectively).

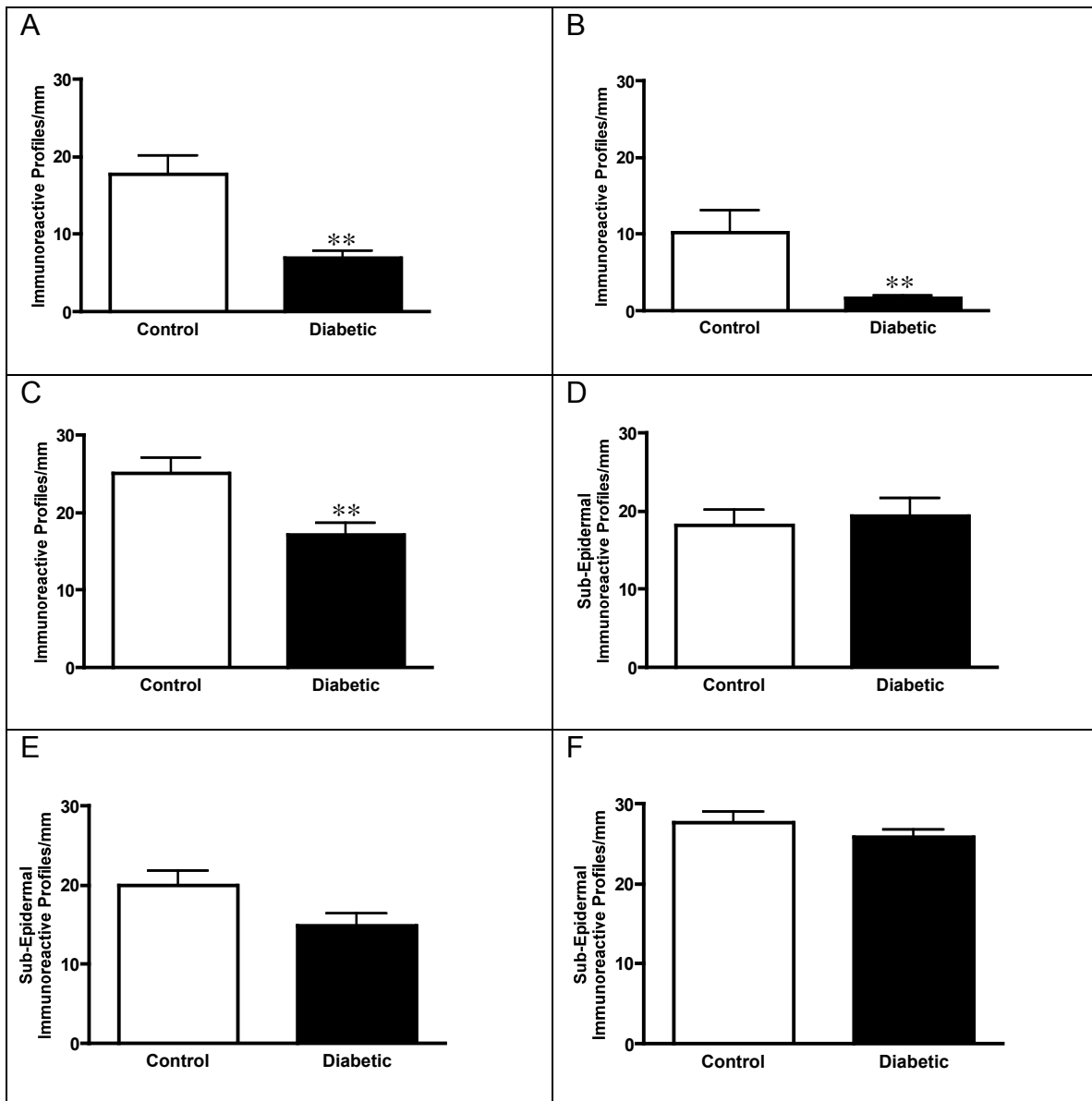


Figure 3.5. Immunoreactive IENF profile density was significantly reduced in STZ-diabetic mice of the C57BL/6 strain after 4 weeks (A). A reduction in immunoreactive IENF profile density was also observed in STZ-diabetic mice of the Swiss Webster strain after 4 weeks of diabetes (B). Genetically type 2 diabetic db/db mice developed a significant reduction in immunoreactive profile density after approximately 41 days of hyperglycemia (C). Sub-epidermal immunoreactive nerve profile density was unchanged in the C57BL/6 (D), Swiss Webster (E) and db/db (F) strains. Data are presented as mean+SEM and were analyzed by an unpaired 2-tailed t-test, ** $p < 0.01$.

3.3.4 The effect of diet on immunoreactive IENF profile density

At the conclusion of our study examining the effects of diet, diabetic rats had significant ($p < 0.05$) weight loss compared to control rats after 12 months. Body weight was unaffected by diet in both the control and diabetic groups (Table 3.2). The majority of the diabetic rats on both diets had blood glucose levels exceeding the upper limit of detection (Table 3.2). The levels of various nutrients in diets 8604 and 7001 are presented in Table 3.3. Diet 7001 had lower levels of the antioxidant vitamins E, B1, B6 and B12, compared to diet 8604. However, the levels of Niacin and Pantothenic Acid were higher in diet 7001. There were no significant differences in immunoreactive IENF density between the control and diabetic rats on Diet 8604 (Figure 3.6A). However, the diabetic rats on diet 7001 developed a significant ($p < 0.05$) reduction in immunoreactive IENF density compared to the control rats on diet 7001 (Figure 3.6B). Diabetic rats on diet 7001 also had increased levels of oxidatively modified proteins compared to both control rats ($p < 0.05$) and diabetic rats on diet 8604 ($p < 0.05$) (Figure 3.7).

Table 3.2. Final body weight and blood glucose levels for control and diabetic rats on either diet 8604 or diet 7001.		
Group	Final Body Weight (g)	Final Blood Glucose (mmol/L)
Control, Diet 8604 (N=8)	311.3±23.4	8.9±1.0
Diabetic, Diet 8604 (N=8)	251.5±4.2*	>33.3
Control, Diet 7001 (N=7)	322.9±34.3	7.2±0.5
Diabetic, Diet 7001 (N=6)	274.5±20.9*	>33.3

Data are mean±SD. Statistical analysis was performed by unpaired 2-tailed unpaired t-test. *p<0.05 vs. control.

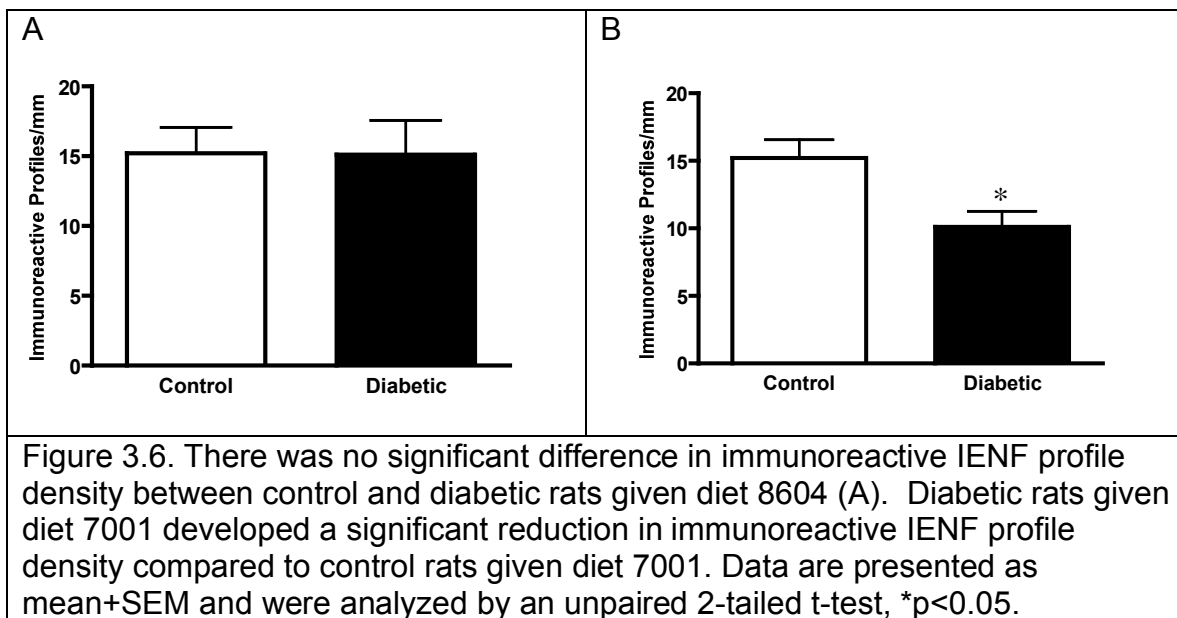
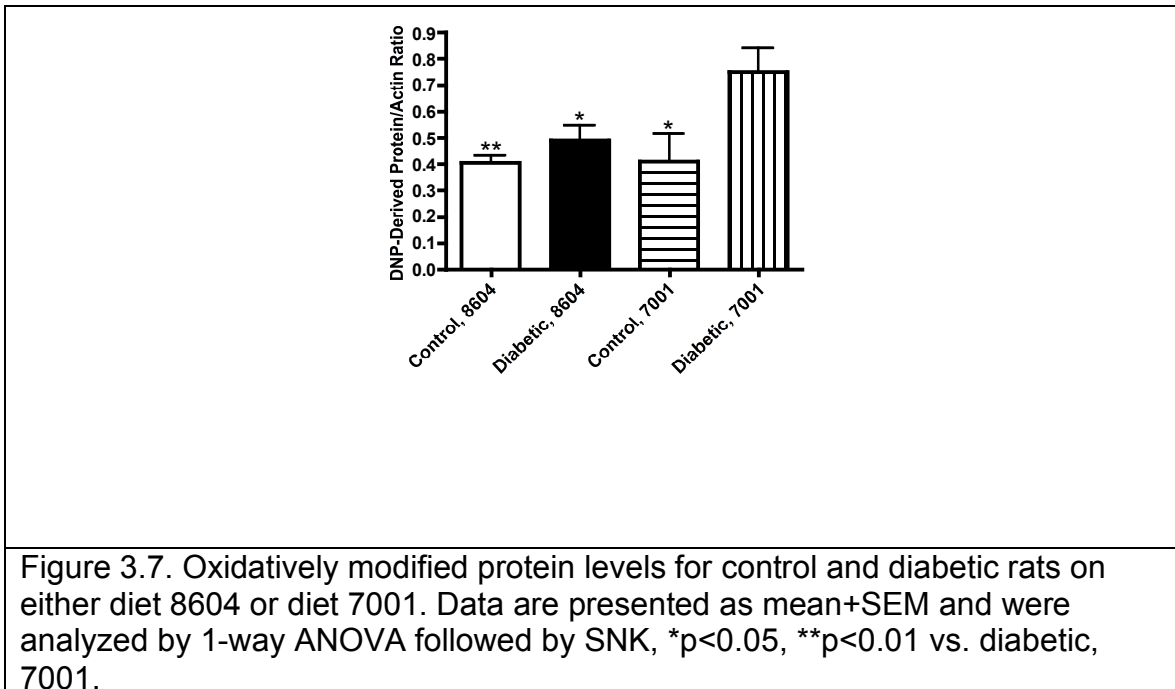


Table 3.3. A comparison of Harlan Teklad diets 8604 and 7001. Antioxidant vitamins are in bold.		
	Diet 8604	Diet 7001
Protein (%)	24.48	25.03
Fat (%)	4.40	4.25
Fiber (%)	3.69	4.67
Calcium (%)	1.36	1.85
Phosphorus (%)	1.01	0.89
Sodium (%)	0.29	0.44
Iron (mg/kg)	352.14	198.60
Manganese (mg/Kg)	105.39	87.60
Zinc (mg/Kg)	82.87	30.60
Copper (mg/Kg)	24.42	13.30
Iodine (mg/Kg)	2.46	2.00
Vitamin A (IU/g)	12.90	8.30
Vitamin D3 (IU/g)	2.40	5.05
Vitamin E (IU/g)	90.18	64.70
Niacin (mg/Kg)	63.42	80.00
Pantothenic Acid (mg/Kg)	21.03	33.40
Vitamin B6 (mg/Kg)	12.95	9.40
Vitamin B2 (mg/Kg)	7.85	7.80
Vitamin B1 (mg/Kg)	27.95	16.10
Vitamin K3 (mg/Kg)	4.11	9.00
Folic Acid (mg/Kg)	2.72	4.00
Biotin (mg/Kg)	0.39	0.31
Vitamin B12 (mcg/Kg)	51.20	29.20



3.3.5 Epidermal thickness in rat and mouse models of diabetes

In rats of the Sprague-Dawley strain with STZ-diabetes, we observed significant ($p<0.001$) epidermal thinning after 2 months (Figure 3.8A). Significant ($p<0.05$) epidermal thinning was also observed in STZ-diabetic C57Bl/6 mice after 4 weeks (Figure 3.8B). In STZ-diabetic Swiss Webster mice, significant ($p<0.001$ vs. control) epidermal thinning was observed as early as 1 week post-STZ injection (Figure 3.8C) and persisted after 4 weeks of diabetes ($p<0.01$) (Figure 3.8D). However, the mean epidermal thickness of type 2 diabetic db/db mice was significantly ($p<0.001$) thicker than that of the non-diabetic controls (Figure 3.8E). When the total number of nuclei observed throughout the epidermis was normalized to section area in Swiss Webster mice with diabetes for 2 weeks duration, no significant differences were observed between the diabetic and control groups (Figure 3.9A). However, when the nuclear counts

were normalized to section length, the control group had significantly ($p < 0.01$) more nuclei per mm than the group with diabetes for 2 weeks duration (Figure 3.9B).

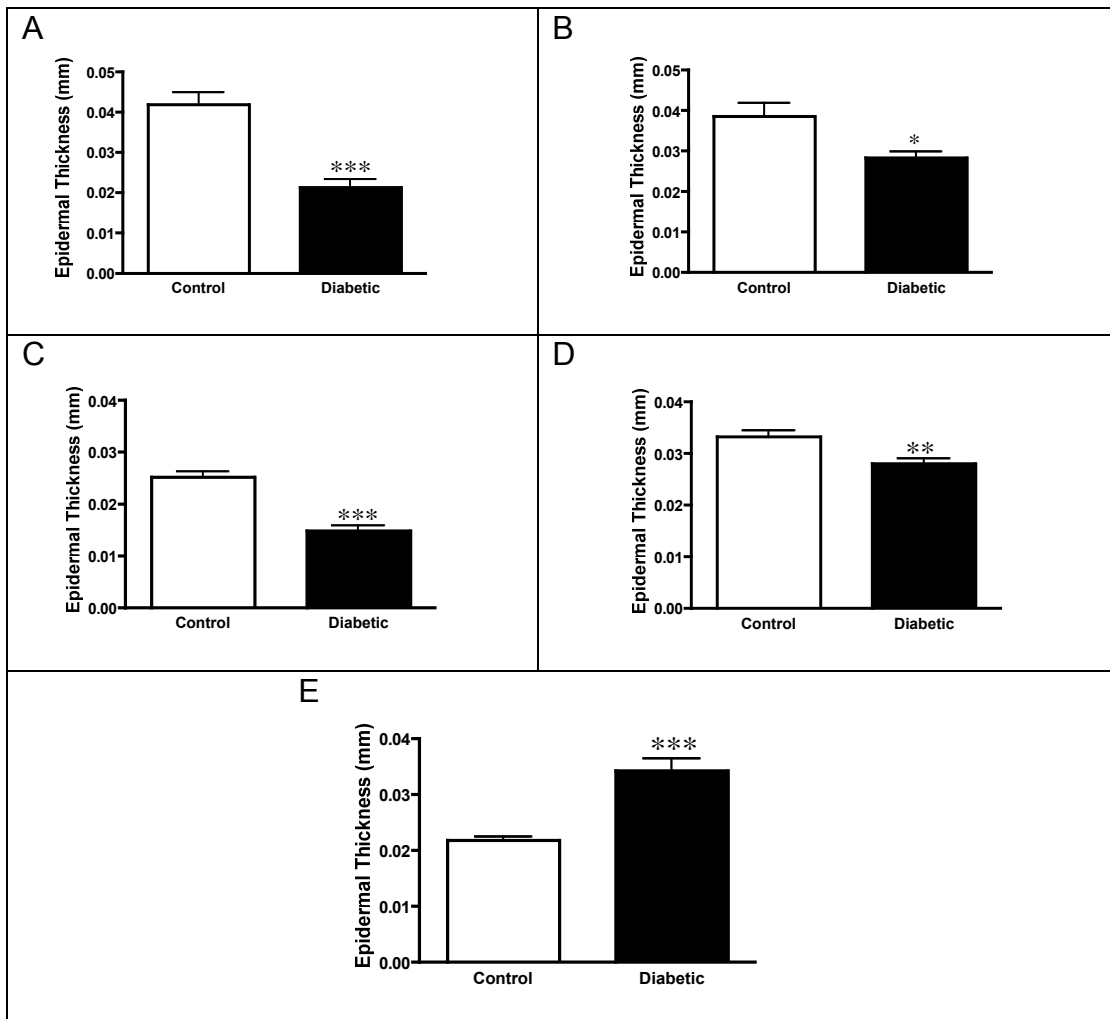


Figure 3.8. Significant epidermal thinning was observed in STZ-diabetic Sprague-Dawley rats after 8 weeks (A) and STZ-diabetic C57Bl/6 mice after 4 weeks (B). STZ-diabetic Swiss Webster mice developed significant epidermal thinning after 1 week (C) and this thinning persisted after 4 weeks (D). The mean epidermal thickness of the db/db mice was significantly thicker than that of the control mice (E). Data are presented as mean+SEM and were analyzed by 2-tailed unpaired t-test, * $p < 0.05$, ** $p < 0.01$, *** $p < 0.001$ vs. control.

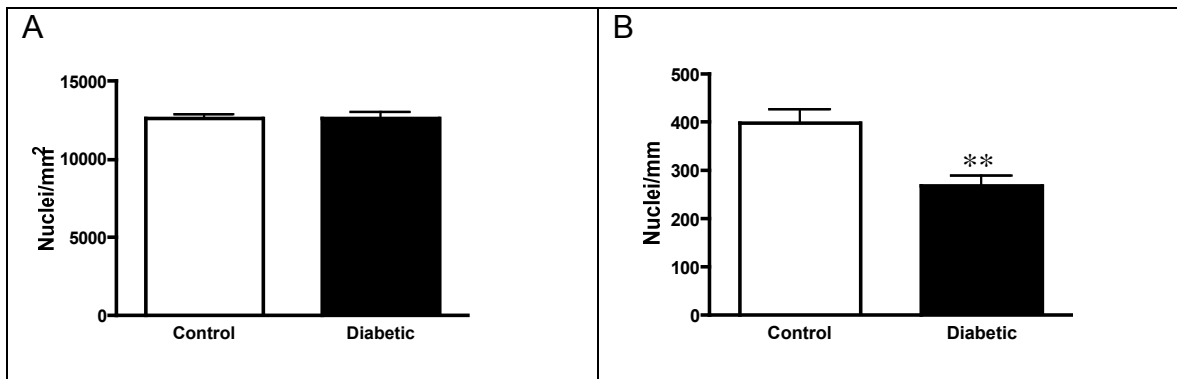


Figure 3.9. The number of nuclei counted within the epidermis was unchanged between Swiss Webster control mice and mice with STZ-induced diabetes for 2 weeks duration when normalized to section area (A). A significant reduction in linear nuclear density was observed in the diabetic group (B). Data are presented as mean+SEM and were analyzed by an unpaired 2-tailed t-test, ** $p < 0.01$.

3.4 Discussion

As demonstrated in Figures 3.2 and 3.4, immunoreactive IENF profiles are clearly present in skin samples from control and diabetic rats and mice after immunostaining with antibodies against the pan-neuronal marker PGP9.5. Through the analysis of similarly-immunostained skin samples, we were able to assess epidermal innervation using a consistent method in a variety of strains of both rats and mice. Our results, showing similar immunoreactivity in skin from control and diabetic rats immunostained with antibodies against either PGP9.5 or HMW Tau, indicate that the decrease in PGP9.5 immunoreactivity observed in skin from diabetic rodents is due to a loss or retraction of the epidermal C-fibers, rather than simply a reduction in PGP9.5 expression. Unfortunately, the antibody against HMW Tau does not cross-react with mice, so we were unable to compare PGP9.5 and HMW Tau immunoreactivity in this species.

There are 2 methods commonly used to quantify epidermal innervation. The first considers only immunoreactive nerve fibers that are observed crossing the dermal-epidermal junction. The second method, commonly referred to as the fragment-counting method, considers all immunoreactive nerve profiles observed from the lower edge of the stratum basale to the upper edge of the stratum granulosum of the epidermis. The majority of the studies examining epidermal innervation in STZ-diabetic Sprague-Dawley rats (Bianchi et al., 2004; Lauria et al., 2005; Leonelli et al., 2007; Rogilio et al., 2007) employed the first method. However, a recent study, comparing the method in which only nerves crossing the dermal-epidermal border are counted to the fragment-counting method, found that, while both methods were able to successfully discriminate reductions in IENF density, the fragment-counting method was more sensitive to capsaicin-induced fiber loss (Smith et al., 2007). If we assume that early degenerative and regenerative changes are occurring at the nerve terminals, a conclusion that is supported by our observation of reductions in epidermal innervation occurring before a decrease in sub-epidermal innervation is observed, one would expect the fragment-counting method to be more sensitive because it includes immunoreactive profiles observed in the outer layers of the epidermis. Therefore, we employed the fragment-counting method of analysis because it would be more likely to identify early signs of degeneration, as well as sprouting, in our subsequent studies evaluating therapeutics. However, when nerve fragments throughout the epidermis are counted, there is a high likelihood that portions of the same nerve fiber will be counted multiple times. Hence, we refer

to the fragments as immunoreactive IENF profiles, rather than considering each fragment as an individual nerve fiber.

Although reductions in epidermal innervation have been observed in rats of the Wistar strain with cisplatin or paclitaxel-induced neuropathy (Lauria et al., 2005), our observation of a reduction in epidermal innervation in Wistar rats with STZ-induced diabetes is novel. While the majority of studies examining diabetes-induced fiber loss have employed Sprague-Dawley rats (Bianchi et al., 2004; Lauria et al., 2005; Leonelli et al., 2007; Roglio et al., 2007), our results indicate that Wistar rats with STZ-induced diabetes could also serve as a model of epidermal nerve fiber loss. Our observation of similar diabetes-induced reductions in epidermal innervation in rats of both the Wistar and Sprague-Dawley strain also argues against the notion that strain plays a large role in the development of diabetic neuropathy.

There is a previous report describing a reduction in cutaneous innervation in STZ-diabetic C57BL/6 mice (Christianson et al., 2003). However, these researchers employed a different method of quantification. In their study, computer-imaging software was used to visualize each skin sample and calculate the section area. The immunoreactive axons throughout the dermis and epidermis were then traced using a graphics tablet, and the percentage of the total skin area occupied by axons was calculated. In our analysis, we made a distinction between epidermal and sub-epidermal profiles, which allowed us to demonstrate that there is a reduction in epidermal, but not sub-epidermal innervation in STZ-diabetic mice of the C57Bl/6 strain. We observed a similar

reduction in epidermal nerve profile density in STZ-diabetic Swiss Webster mice. Based on these results, STZ-diabetic mice of either the C57Bl/6 or Swiss Webster strains could serve as models of diabetes-induced changes in epidermal innervation.

Our observation of a reduction in epidermal innervation in type 2 diabetic db/db mice mirrors the deficit observed in db/db mice using a computer-assisted color-subtractive analysis to assess fiber density (Underwood et al., 2001). More recent studies have confirmed the usefulness of type 2 diabetic db/db mice (Gibran et al., 2002), as well as ob/ob mice (Drel et al., 2006), for the assessment of epidermal innervation.

The results of our study comparing control and diabetic rats receiving 2 separate diets for 12 months indicate that diet may play a role in the severity of neuropathy observed in diabetic rodents. One key difference between these diets was in the levels of the antioxidant vitamins E, B1, B6 and B12, with the diabetic rats receiving the diet lower in these antioxidants (diet 7001) appearing to be more susceptible to diabetes-induced IENF loss. This observation is in agreement with multiple studies reporting the efficacy of these vitamins in the prevention of neuropathy (Okada et al., 2000; Medina-Santillan et al., 2004; Haupt et al., 2005). Our observation of increased levels of oxidatively modified proteins in the skin of the diabetic rats receiving diet 7001 further indicates that oxidative stress may contribute to fiber loss. Although diet 7001 has higher levels of niacin and pantothenic acid, neither of these vitamins have been shown to improve neuropathy. In studies aimed at evaluating the effects of various

therapeutics on certain indices of diabetic neuropathy, it is advantageous to try to maximize the deficits observed in our untreated diabetic rodents. Therefore, based on the results of this study, the rodents used in the experiments described in the remainder of this dissertation were given the diet 7001.

While previous clinical studies have described either thickening (Forst et al., 1994) or thinning (Forst et al., 2006) of the skin in patients with diabetes, these measurements included both the dermal and epidermal layers. To date, the effects of diabetes on epidermal thickness in rodent models remains unexplored. Our observation of epidermal thinning in both rat and mouse models of diabetes is novel, but not entirely unexpected. Several mechanisms could be responsible for diabetes-induced changes in epidermal thickness.

In mouse models of skin denervation, the dying back of epidermal nerve fibers results in a reduction in epidermal thickness (Chiang et al., 1998). However, in our experiments, we observed epidermal thinning before a detectable reduction in epidermal innervation was observed. Also, in our study of type 2 diabetic db/db mice, we observed a thickening of the epidermis despite a robust reduction in epidermal nerve fiber density. These data suggest that factors other than fiber loss may contribute to the epidermal thinning observed in diabetic rodents.

In cultured keratinocytes, high glucose levels are associated with changes in cellular morphology and decreased proliferation (Spravchicov et al., 2001), and activation of both the insulin receptor and the IGF-1 receptor appear to be involved keratinocyte proliferation (Wertheimer et al., 2000). In insulin receptor

knockout mice, a decrease in keratinocyte proliferation is observed (Wertheimer et al., 2001). Insulin receptor substrate 1 (IRS-1) knockout mice, which lack a protein that acts as an interface between insulin and IGF-1 receptors and promotes various downstream signaling pathways (Myers et al., 1994), have a significantly thinner epidermis. Histological analysis of the IRS-1 knockout mice revealed that their stratum spinosum had fewer layers (Sadagurski et al., 2007). Our observation of a reduction in nuclear density in the diabetic mice when nuclei counts were normalized to section length, but not section area, indicates that this thinning of the epidermis is also the result of a reduction in the number of keratinocytes, rather than cell shrinkage. These reports raise the possibility that the epidermal thinning observed in STZ-diabetic rodents could be due to hyperglycemia, IGF-1 deficiency, insulin deficiency or a combination of these factors. The potential role of insulin in epidermal thinning is further supported by our observation of epidermal thickening in the hyperinsulinemic db/db mice.

Differences in epidermal thickness between non-diabetic and diabetic rodents should be considered when quantifying nerve profiles. When comparing linear density of profiles counted throughout the epidermis between a control group and a diabetic group with a thinner epidermis, a reduction in epidermal innervation expressed as linear IENF density may appear more exaggerated than if epidermal area had been incorporated into the measurement. The IENF data presented in the following chapters includes both linear and area densities.

In conclusion, STZ-diabetic rats of the Wistar and Sprague-Dawley strains, as well as STZ-diabetic mice of the C57Bl/6 and Swiss Webster strains, develop

epidermal nerve fiber loss. Type 2 diabetic db/db mice also develop epidermal nerve fiber deficits, indicating that each of these models could be useful for modeling the nerve fiber loss that has been observed clinically. The thinning of the epidermis observed in STZ-diabetic rats and mice, as well as the thickening observed in db/db mice, should be taken into account when analyzing cutaneous innervation.

4 – The relationship between thermal hypoalgesia and epidermal nerve fiber loss

4.1 Introduction

4.1.1 Thermal sensitivity in animal models and humans with diabetes

Changes in thermal sensitivity occur in both animal models and humans with diabetes. In clinical studies, both thermal hyperalgesia and thermal hypoalgesia have been reported, and these changes are viewed as an early indicator of diabetic neuropathy (Dyck et al., 2000). Thermal sensitivity has been studied in rodent models of diabetes with varying results. In the STZ-diabetic Sprague Dawley rat model, a period of thermal hyperalgesia has been observed approximately 4 weeks after induction of diabetes, which is followed by a progression to thermal hypoalgesia after 8 weeks (Calcutt et al., 2004). Both thermal hyperalgesia and hypoalgesia have been reported in mouse models of diabetes (Levine et al., 1982; Davar et al., 1995; Gabra and Sirois, 2005), but to date only a single study has reported a clear progression from one state to the other (Pabbidi et al., 2008). Differences in strain and method of induction of diabetes may be responsible for some of the variability observed in mouse models (Sullivan et al., 2008). Although changes in thermal sensitivity are present in humans and rodent models of diabetes, how these changes relate to other indices of diabetic neuropathy has not been addressed.

4.1.2 Epidermal innervation in animal models and humans with diabetes

The innervation of the epidermis consists primarily of unmyelinated C-fibers, which are involved in the sensation of noxious heat. Recent studies have focused on quantifying these intraepidermal nerve fibers (IENFs) as a measure of diabetic neuropathy. Diabetes-induced reductions in epidermal innervation have been observed in multiple clinical studies (Levy et al., 1989; Lindberger et al., 1989; Levy et al., 1992; Properzi et al., 1993; Kennedy et al., 1996; Lauria et al., 1998; Hirai et al., 2000; Gibran et al., 2002; Pittenger et al., 2004; Shun et al., 2004; Koskinen et al., 2005), as well as in diabetic primates (Pare et al., 2007) and rodents (Gibran et al., 2002; Bianchi et al., 2004; Chen et al., 2005; Lauria et al., 2005; Drel et al., 2006; Toth et al., 2006; Leonelli et al., 2007; Roglio et al., 2007; Obrosova et al., 2007; Vareniuk et al., 2007). Attempts have been made to correlate the loss of epidermal innervation with measures of nerve function to assess the predictive value of IENF loss for other aspects of diabetic neuropathy. In humans, reductions in IENF density have been correlated with changes in pressure and vibration perception, total neurological disability score and neuropathy status (Pittenger et al., 2004; Sorensen et al., 2006). In a rat model of type 1 diabetes, loss of IENF density was correlated with sensory nerve conduction velocity slowing determined by antidromic tail stimulation (Lauria et al., 2005).

4.1.3 The relationship between epidermal innervation and thermal sensitivity

One would logically expect that loss of thermal sensation is a consequence of a loss of epidermal innervation. Indeed, reductions in IENF

density induced by topical application of capsaicin to the skin of normal volunteer subjects have been associated with a loss of heat and heat pain sensitivity (Simone et al., 1998; Nolano et al., 1999; Malmberg et al., 2004). However, only a few studies of diabetic humans have reported any correlation between loss of epidermal innervation and changes in heat sensitivity (Pittenger et al., 2004; Shun et al., 2004; Quattrini et al., 2007). The relationship between thermal hypoalgesia and IENF density in animal models of diabetes also remains largely unexplored. The aim of the following experiments was to examine the relationship between changes in heat sensitivity and changes in epidermal innervation in a mouse model of diabetes.

4.2 Methods

4.2.1 Experimental design

Type 1 diabetes was induced in male Swiss Webster mice by intraperitoneal injection of 180 mg/kg of streptozotocin (STZ). Hyperglycemia was confirmed 3 days later, and only mice with blood glucose levels exceeding 15 mmol/l were included in the diabetic groups. Two weeks after STZ injection, the thermal withdrawal latencies of 8 diabetic mice and 8 age-matched controls were assessed using the methods described in section 2.2.1. Hind paw cutaneous blood flow was also assessed using the methods described in section 2.3.2. Mice were then sacrificed and plantar foot skin was removed from the same region of the paw where the thermal stimulus was applied during the measurement of thermal withdrawal latency. Skin samples were later immunostained using the methods described in section 2.4.1. An antibody

against the pan-neuronal marker PGP9.5 was used to visualize the innervation of the skin. In earlier studies, the antibody was obtained from Chemicon International (Temecula, CA). Later studies used an antibody from Biogenesis Ltd. (UK). Skin sections from control mice and mice that had been diabetic for 2 weeks were also immunostained with antibodies against either substance P (SP) (Abcam Inc., Cambridge, MA) or GAP-43 (Abcam Inc., Cambridge, MA). Immunoreactive nerve profile density and epidermal thickness were then determined using the methods described in section 2.4.2. Sciatic nerves were also removed from control and diabetic mice after 2 weeks of diabetes and immediately frozen in liquid N₂. SP was later extracted and levels were measured using the methods described in section 2.5.3.

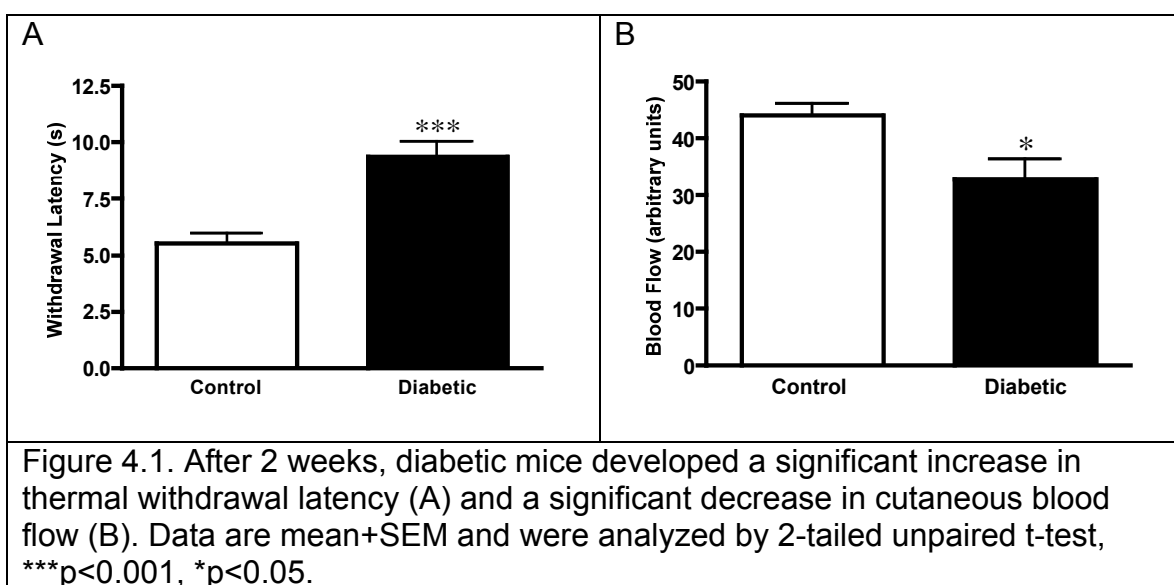
4.3 Results

4.3.1 The impact of 2 weeks of diabetes

After 2 weeks, the diabetic mice were hyperglycemic and had a significant ($p < 0.001$) weight loss (Table 4.1). There was a significant ($p < 0.001$) increase in paw thermal withdrawal latency in the diabetic mice compared to the control mice (Figure 4.1A) and a significant decrease in hind paw cutaneous blood flow (Figure 4.1B). The linear densities of PGP9.5-immunoreactive IENF profiles and sub-epidermal PGP9.5-immunoreactive nerve profiles of control and diabetic mice were not significantly different (Figure 4.2A, E). However, when PGP9.5-immunoreactive IENF counts were normalized to epidermal area, the diabetic group had a significantly ($p < 0.05$) increased profile density compared to the control group (Figure 4.2B), reflecting the significant ($p < 0.001$) thinning of the

Table 4.1. Final body weight and blood glucose levels for STZ-diabetic and control mice after 2 weeks.		
Group	Final Body Weight (g)	Final Blood Glucose (mmol/l)
Control, 2 Weeks (N=8)	31.5±0.6	13.0 (9.9-17.6)
Diabetic, 2 Weeks (N=8)	21.4±0.7***	>33.3

Data are presented as mean±SEM (body weight) or median(range) (blood glucose). Statistical analysis of body weights was performed by unpaired t-test.***p<0.01 vs. control.



epidermis in skin from diabetic mice (Figure 4.2C). There was no correlation between thermal withdrawal latency and PGP9.5-immunoreactive IENF profile density after 2 weeks of diabetes (Figure 4.2D). Both linear and area densities of SP-immunoreactive IENF profiles were significantly (both p<0.01) increased in diabetic mice compared to controls (Table 4.2). With respect to GAP-43, there

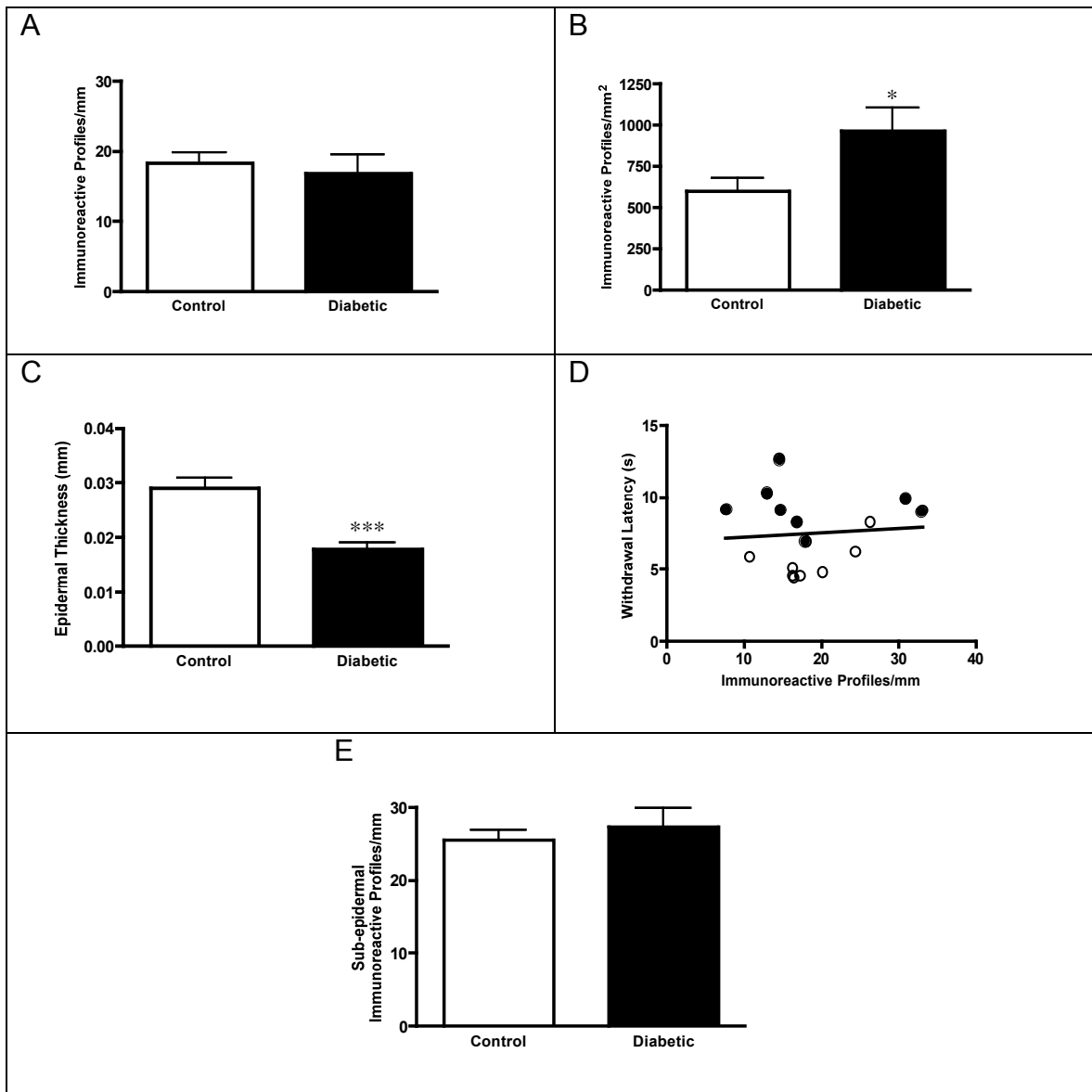


Figure 4.2. After 2 weeks of diabetes, linear immunoreactive IENF profile density was unchanged (A) and when immunoreactive profile counts were normalized to epidermal area, the density was significantly increased (B). The epidermis of the diabetic mice was significantly thinner (C). Withdrawal latency did not correlate with linear immunoreactive profile density (D), and sub-epidermal immunoreactive nerve profile density was unchanged (E). Data are mean+SEM and were analyzed by 2-tailed unpaired t-test, *** $p < 0.001$, * $p < 0.05$. In the linear regression analysis, closed circles represent diabetic mice and open circles represent control mice, $r^2 = 0.0063$.

was a nonsignificant increase in linear density and a significant ($p < 0.05$) increase in area density of immunoreactive IENF profiles (Table 4.2). The densities of

either SP or GAP-43-immunoreactive IENF profiles were markedly lower than the corresponding values obtained using PGP 9.5 (Figure 4.2A). No significant differences in either sub-epidermal SP- or GAP-43-immunoreactive nerve profile densities were evident between the diabetic and control groups (Table 4.2). There was a significant ($p=0.05$) decrease in SP levels in the sciatic nerves of mice after 2 weeks of diabetes compared to controls (Table 4.2).

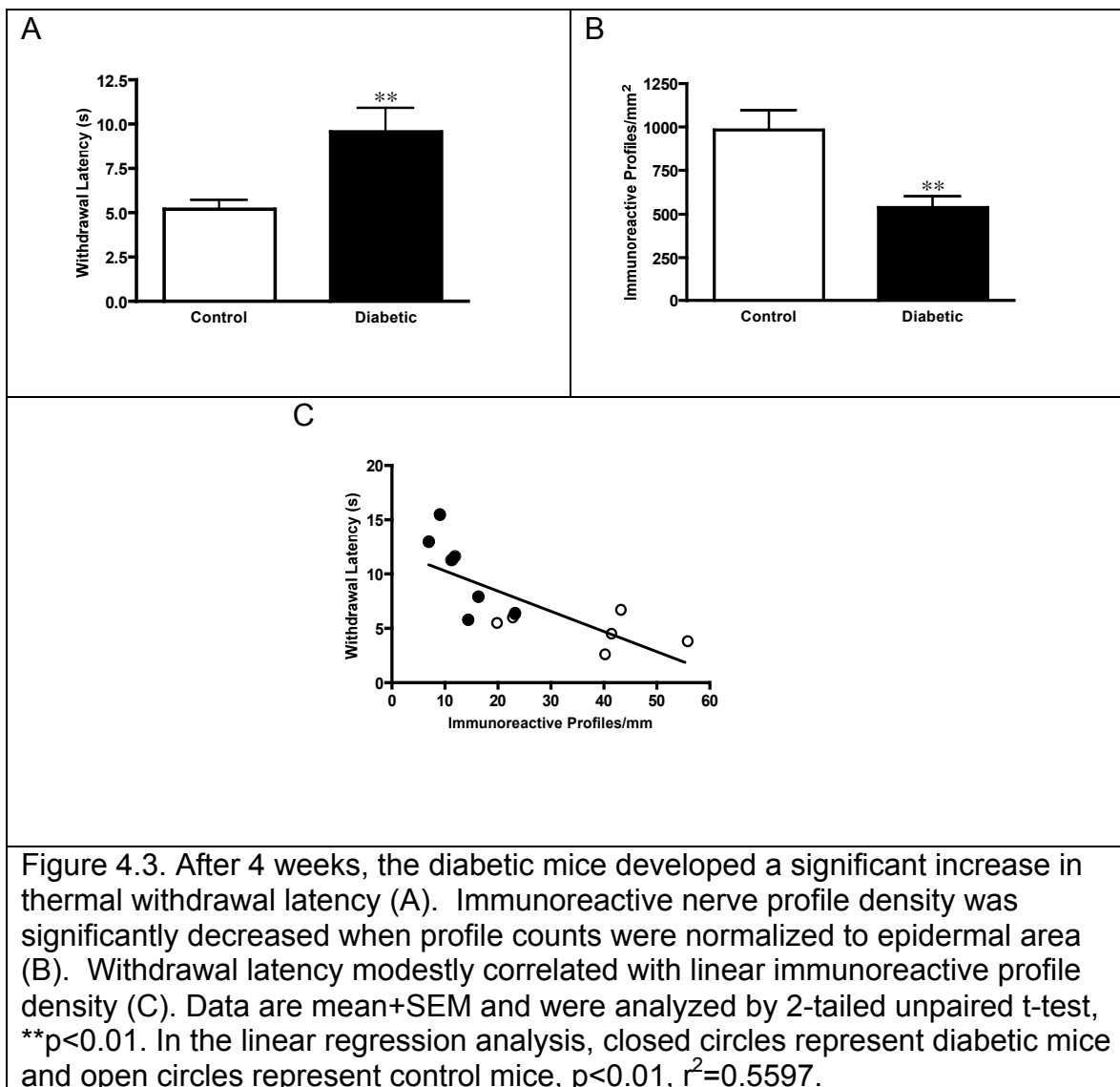
Table 4.2. Sciatic nerve (SN) levels of SP, and SP and GAP-43 immunoreactive epidermal and sub-epidermal nerve profile densities of foot pad skin from control and diabetic mice after 2 weeks of diabetes.							
SP					GAP-43		
Group	SN pg/mm	IENF Profiles #/mm	IENF Profiles #/mm ²	SNP Profiles #/mm	IENF Profiles #/mm	IENF Profiles #/mm ²	SNP Profiles #/mm
Control (N=7)	14.9±1.3	0.5±0.2	21.7±8.0	5.6±0.7	6.8±1.2	206±33.5	25.2±1.2
Diabetic (N=7)	11.3±1.5 [#]	1.1±0.3 ^{**}	96.1±21.2 ^{**}	4.6±0.7	9.4±1.8	507.2±101.5 [*]	28.1±1.3

Data are presented as mean±SEM and were analyzed by unpaired t-test, ^{**} $p<0.01$, ^{*} $p<0.05$, [#] $p=0.05$ vs. control.

4.3.2 The impact of 4 weeks of diabetes.

As was described in chapter 3, diabetic mice were hyperglycemic and developed significant ($p<0.05$) weight loss compared to control mice after 4 weeks (Table 3.2). We again observed a significant ($p<0.01$) increase in paw thermal withdrawal latency in the diabetic mice compared to the control mice (Figure 4.3A). As was reported in chapter 3, there was also a significant ($p<0.01$) reduction in linear PGP9.5-immunoreactive IENF profile density (Figure 3.5B) and a significant ($p<0.01$) thinning of the epidermis (Figure 3.7D). Despite this thinning, a significant ($p<0.01$) decrease in PGP9.5-immunoreactive IENF

profiles per section area was also detected (Figure 4.3B). Regression of paw thermal withdrawal latency against paw PGP9.5-immunoreactive IENF profile

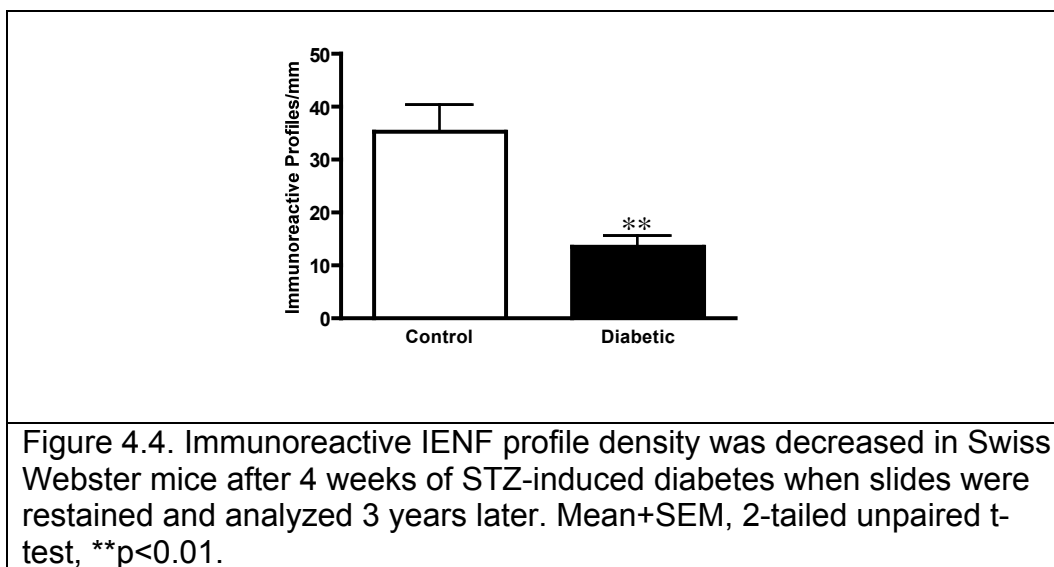


linear density demonstrated a significant (p<0.01; r²=0.5597) inverse relationship (Figure 4.3C). As described in chapter 3, we did not detect a change in sub-epidermal PGP9.5-immunoreactive nerve profile density despite the significant

decrease in PGP9.5-immunoreactive IENF profile density after 4 weeks of diabetes (Figure 3.5E).

4.3.3 Reanalysis of skin from mice with diabetes for 4 week's duration

Three years after our initial analysis, we repeated our immunostaining of skin from mice that had previously shown an epidermal nerve fiber deficit, using the PGP9.5 antibody that was used in our more recent experiments (Biogenesis Ltd.). We again observed a significant ($p < 0.01$) decrease in immunoreactive IENF profile density in the diabetic mice (Figure 4.3).



4.4 Discussion

The present time-course study of sensory fiber function and structure has identified a disassociation between thermal sensitivity and IENF density in the paw of diabetic mice. It is plausible that immunostaining with PGP9.5 does not

identify early structural damage to IENFs, as PGP9.5 is a cytoplasmic enzyme also known as ubiquitin hydroxylase (Wilkinson et al., 1989). However, our comparison of linear IENF density measured using PGP9.5 to that measured using the structural protein HMW Tau found that similar values were obtained with antibodies directed at either antigen (see section 3.3.1). The early loss of thermal sensation could also reflect loss of a small sub-population of IENFs subsumed within the total PGP9.5-immunoreactive population. To begin to address this possibility, we measured epidermal and dermal fibers expressing SP, as this neuropeptide is associated with thermal nociception (Mantyh et al., 1997; Cao et al., 1998; Laneuville et al., 1998; Nichols et al., 1999; Vierck et al., 2003). However, we did not detect any loss of SP-containing fibers in the paw of diabetic mice but instead found a statistically significant increase in IENF linear and area density. It is possible that this increase reflects sprouting to compensate for early damage or dysfunction of sensory fibers. Therefore, epidermal fibers immunoreactive to an antibody against GAP-43, which is expressed by developing and regenerating nerve fibers (De Graan et al., 1985), were quantified. GAP-43 immunoreactive profiles were detected in the skin of control mice, likely reflecting epidermal neural plasticity and remodeling resulting from continuous migration of basal keratinocytes to more superficial layers of the epidermis (Verze et al., 1999; Verze et al., 2003). The modest trend towards an increase in linear density coupled with a significant increase in area density of GAP-43-immunoreactive IENF profiles in mice that had been diabetic for 2 weeks

suggests that IENFs, prior to subsequent degeneration, may experience an early period of sprouting in response to the onset of diabetes.

Our time course data suggest that heat-sensitive IENFs may be subject to a diabetes-induced disruption of function that precedes the loss of PGP9.5-immunoreactive profiles. The coefficient of determination (r^2) for the regression of paw thermal withdrawal latency against linear IENF density after 4 weeks of diabetes indicates that only 56% of the variation in withdrawal latency can be attributed to changes in immunoreactive IENF profile density. Therefore, factors other than fiber loss must contribute to thermal hypoalgesia, even when IENF loss is detected. These functional disorders could include impairment of heat detection at peripheral terminals or mechanisms involved in central nociceptive processing. TRPV1 is a heat-sensitive receptor found on C-fiber terminals (Caterina et al., 1997) and a reduction in TRPV1-immunoreactive IENF density has recently been reported in skin biopsies from patients with diabetic neuropathy (Facer et al., 2007). TRPV1 expression is also decreased in the cell bodies of the small, unmyelinated neurons of diabetic rats (Hong and Wiley, 2005) and in the spinal cord, dorsal root ganglia and paw skin of diabetic mice (Pabbidi et al., 2008). A similar loss of TRPV1 could plausibly contribute to the thermal hypoalgesia in our diabetic mice. Unfortunately, keratinocytes also express the TRPV1 receptor (Denda et al., 2001). Immunostaining of skin sections with commercially available TRPV1 antibodies results in high levels of background staining in the epidermis, which makes the identification and

quantification of TRPV1-immunoreactive nerve fibers within the epidermis difficult.

Changes in expression of SP may also affect C-fiber nociceptive function. In STZ-diabetic rats, reduced SP levels have been reported in dorsal root ganglia (Willars et al., 1989; Kanbayashi et al., 2002) and both the peripheral (Robinson et al., 1987; Willars et al., 1989) and central (Calcutt et al., 2000) projections of primary afferents. Reductions in SP reflect reduced synthesis of this neuropeptide and consequent decreases in the amounts undergoing axonal transport (Tomlinson et al., 1988) and released in the spinal cord after peripheral noxious stimulation (Calcutt et al., 2000). Our present finding of a similar decline in sciatic nerve SP content in mice after 2 weeks of diabetes suggests that diminished synthesis, transport and spinal release of SP may contribute to early thermal hypoalgesia.

Given that the epidermis is avascular and depends on dermal vessels for oxygenation and removal of waste, we hypothesized that epidermal nerve endings may be particularly vulnerable to diabetes-induced changes in dermal blood flow. In clinical studies, both increases (Edmonds et al., 1982; Archer et al., 1984) and decreases (Rendell et al., 1989; Jorneskog et al., 1995) in cutaneous blood flow have been observed. A relationship between impaired vasomotion and thermal sensitivity has also been reported in diabetic patients (Stansberry et al., 1996). We measured cutaneous blood flow in our control and diabetic mice as a means of identifying an early physiological change that may also contribute to the loss of function and eventual retraction of epidermal C-

fibers. Our observation of a decrease in blood flow to the skin of mice that had been diabetic for 2 weeks suggests another potential mechanism of C-fiber dysfunction and may also provide evidence of dysfunction in another subset of nerve fibers. Thermoregulation of the skin relies on arteriovenous shunts that bypass the capillary bed, and sympathetic nerves direct the opening and closing of these shunts. Diabetes-induced sympathetic neuropathy may result in increased opening of these shunts and the subsequent diversion of blood away from the papillary dermis. In clinical studies, increased shunting of blood flow appeared to contribute to the development of diabetic foot ulcers (Boulton et al., 1982; Edmonds et al., 1982). In our mice, it is possible that dysfunction of the sympathetic nerve fibers may have resulted in the opening of the arteriovenous shunt and a consequent reduction in blood flow to the capillaries subjacent to the epidermis, which may have contributed to the dysfunction of the epidermal C-fibers.

The degeneration of C-fibers may also further contribute to reduced cutaneous blood flow through disruption of nerve axon reflex-related vasodilation. Stimulation of epidermal C-fibers results in the antidromic stimulation of adjacent C-fibers leading to a release of the neuropeptides SP and CGRP, which act as potent dilators. In patients with diabetes, reductions in acetylcholine and sodium nitroprusside-induced vasodilatory response have been observed (Parkhouse and LeQuesne, 1988; Hamdy et al., 2001; Caselli et al., 2003). Our observation of an increase in SP-immunoreactive nerve endings in skin from diabetic mice could be viewed as evidence that a reduction in SP-induced vasodilation of the

dermal blood vessels is not involved in the reduction of cutaneous blood flow. However, the possibility remains that impaired release of SP from the peripheral terminals could contribute to reduced blood flow, especially given the impaired spinal release of SP that has been observed in diabetic rats (Calcutt et al., 2000). Regardless of the mechanisms of dysfunction, our observation of a reduction in cutaneous blood flow after 2 weeks of diabetes provides evidence of an early physiological change that may contribute to the loss of thermal sensitivity and the eventual degeneration of epidermal C-fibers.

Our observation of epidermal thinning in diabetic mice presents issues of both IENF quantification, further discussed in section 3.4, and the physical and functional contribution of epidermal cells to heat transduction and sensation during diabetes. As noted in section 3.4, epidermal thinning in our insulin-deficient and hyperglycemic mice is consistent with reports that insulin and IGF-1 are involved in keratinocyte proliferation and differentiation (Wertheimer et al., 2000; Wertheimer et al., 2001) and that high glucose levels decrease proliferation of cultured keratinocytes (Spravchicov et al., 2001). Further, it has been suggested that epidermal nerve fibers and keratinocytes make synaptic connections (Chateau and Misery, 2004). Given that keratinocytes express a variety of heat-sensitive receptors (Denda et al., 2001; Peier et al., 2002; Chung et al., 2003), these cells may be involved in the detection of heat, and thinning of the epidermis during diabetes could contribute to thermal hypoalgesia, even when there is no loss of epidermal innervation.

The results of our subsequent studies described in chapters 5 and 6 confirm the dissociation between thermal nociception and epidermal innervation. In 3 separate studies, we observed significant ($p < 0.01$) thermal hypoalgesia (Figure 5.4, Figure 5.7, Figure 6.6) after 4 weeks of diabetes, although reductions in epidermal innervation had not yet developed (Figure 5.5, Figure 5.8, Figure 6.7). Given that these results disagree with our previous observation of a reduction in epidermal innervation after 4 weeks of diabetes, we addressed the possibility that the change of antibody vendor or unintentional changes in technique could be responsible for our failure to observe deficits in more recent experiments. As demonstrated in Figure 4.3, the deficit that we had observed 3 years ago was still observed in slides that were immunostained and analyzed more recently. Therefore, these results demonstrate that the lack of a decrease in epidermal innervation observed in our more recent experiments is not due to a failure of technique. Nevertheless, these more recent experiments, demonstrating a reduction in thermal sensation preceding epidermal nerve fiber loss, further support our hypothesis that functional changes precede structural changes.

In summary, diabetes-induced thermal hypoalgesia develops before a detectable reduction in linear PGP9.5-immunoreactive IENF profile density. While the appearance of thermal hypoalgesia before a reduction in IENF density was surprising, it is not entirely unprecedented as the onset of thermal hypoalgesia preceded a reduction in innervation of leg skin from diabetic mice (Chen et al., 2005) and was absent from mice fed a high-fat diet that displayed

thermal hypoalgesia (Obrosova et al., 2007). Neurochemical and functional disorders of epidermal nociceptors appear to contribute to early stages of diabetes-induced thermal hypoalgesia before the quantifiable loss of peripheral terminals.

5 – The Pathogenesis of Diabetic Neuropathy

5.1 Introduction

5.1.1 Mechanisms of development of diabetic neuropathy

Although neuropathy affects nearly 50% of patients with diabetes (Pirart et al., 1978), the pathogenesis is not fully understood. Without a clear understanding of the molecular pathways contributing to the development of diabetic neuropathy, effective therapies have been difficult to identify. Among the mechanisms thought to play a role in the development of diabetic neuropathy are increased flux through the polyol pathway and loss of neurotrophic support. The experiments described in the following chapter were designed to examine the contribution of both of these pathways by determining the effects an aldose reductase inhibitor and exogenous neurotrophic factors on several measures of diabetic neuropathy.

5.1.2 Polyol pathway flux

The polyol pathway involves the conversion of glucose to sorbitol by the enzyme aldose reductase with the consequent oxidation of NADPH, followed by the conversion of sorbitol to fructose by the enzyme sorbitol dehydrogenase with the resulting reduction of NAD⁺. Increased flux through this pathway is thought to contribute to the development of diabetic neuropathy by depleting myo-inositol levels and disrupting the sodium, potassium-ATPase (Gillon et al., 1983; Greene

and Lattimer, 1983). Polyol pathway activation generates oxidative stress as well through the depletion of NADPH, which is involved in the glutathione cycle and nitric oxide production (Lee and Chung, 1999) and may also contribute to loss of neurotrophic support in diabetic rodents (Mizisin et al., 1997; Ohi et al., 1998). Multiple studies have indicated that inhibitors of aldose reductase show therapeutic potential (Tomlinson et al., 1982; Yue et al., 1982; Mayer and Tomlinson, 1983; Calcutt et al., 1994; Mizisin et al., 1997; Cotter et al., 1998; Obrosova et al., 2002; Calcutt et al., 2004). In rats with streptozotocin(STZ)-diabetes, treatment with the aldose reductase inhibitor IDD 676 prevented both the onset of thermal hyperalgesia and the progression to hypoalgesia (Calcutt et al., 2004). However, the effects of this aldose reductase inhibitor on thermal hypoalgesia and epidermal nerve fiber density in a mouse model of diabetes have not thus far been explored.

5.1.3 Loss of neurotrophic support

Neurotrophic factors are vital for the development and maintenance of peripheral nerves and loss of neurotrophic support is thought to be a factor in the development of diabetic neuropathy (Hellweg and Hartung, 1990; Calcutt et al., 1992; Fernyhough et al., 1994; Hellweg et al., 1994). Treatment with neurotrophic factors such as CNTF or compounds that have neurotrophic factor-like properties, such as Neotrofin or TX14(A), may prove to be an effective means of preventing and reversing diabetes-induced degeneration of peripheral nerves.

Although treatment with NGF has shown efficacy in animal models (Apfel et al., 1994; Diemel et al., 1994; Christianson et al., 2003), clinical trials have been less successful, partially due to hyperalgesia at the site of injection (Apfel et al., 2000). Recent studies have focused on the purine derivative Neotrofin, also referred to as AIT-082, which may prove to have therapeutic potential similar to that of NGF, without inducing hyperalgesia. Neotrofin has been shown to enhance NGF-mediated neurite outgrowth in cultured PC12 cells (Middlemiss et al., 1995). In rat skin, injections of Neotrofin induced nerve sprouting without causing hyperalgesia (Holmes et al., 2003). Treatment with Neotrofin was able to prevent NGF depletion in muscle and foot skin, as well as substance P (SP) and CGRP depletion in the sciatic nerve and dorsal root ganglia of STZ-diabetic rats (Calcutt et al., 2006). Neotrofin treatment also prevented thermal hypoalgesia and improved sensory nerve conduction velocity in these rats.

Ciliary Neurotrophic Factor (CNTF), which is produced by Schwann cells, serves as a neurotrophic factor for sensory and motor neurons. CNTF-like activity was found to be reduced in the sciatic nerves of STZ-diabetic and galactose fed rats (Calcutt et al., 1992) and treatment with CNTF has been shown to prevent the development of thermal hypoalgesia (Calcutt et al., 2004), improve nerve conduction velocity and promote regeneration after nerve crush injury in STZ-diabetic rats (Mizisin et al., 2004).

Prosaposin peptides promote differentiation and prevent cell death in a variety of nerve cell types (Hiraiwa et al., 1997). Prosaposin mRNA levels are elevated in the peripheral nerve of STZ-diabetic rats (Calcutt et al., 1999), and

the prosaposin-derived peptide, TX14(A), has been shown to preserve both axon caliber and sodium, potassium-ATPase activity, attenuate reductions in SP levels and prevent the development of thermal hypoalgesia in STZ-diabetic rats (Calcutt et al., 1999). The peptide also prevents both formalin and SP-induced thermal hyperalgesia, alleviates tactile allodynia (Calcutt et al., 2000; Jolivald et al., 2006) and both prevents and reverses nerve conduction velocity slowing (Calcutt et al., 1999; Mizisin et al., 2001) in STZ-diabetic rats. Although Neotrofin, CNTF and TX(14)A all show therapeutic potential, their effects on thermal hypoalgesia and IENF loss in STZ-diabetic mice remain unexplored.

In the following experiments, we examined the effects of the aldose reductase inhibitor IDD 676, as well as Neotrofin, CNTF and TX14(A) on various functional and structural deficits in STZ-diabetic mice. Given that these compounds have already demonstrated efficacy in the prevention of thermal hypoalgesia in diabetic rats, the primary aim of these experiments was to examine their effects on IENF loss. Other measures of diabetes were included to confirm the efficacy of the treatments. A better understanding of the effects of these compounds is valuable not only for the identification of potential therapeutics, but also to further our understanding of the contribution of increased flux through the polyol pathway and loss of neurotrophic support to the development of diabetic neuropathy.

5.2 Methods

5.2.1 The effects of IDD 676 and Neotrofin on diabetic neuropathy

This study used Swiss Webster mice with STZ-induced diabetes and included an untreated diabetic group, a diabetic group receiving a 250mg/kg dose of the aldose reductase inhibitor IDD 676 (Institute for Diabetes Discovery, Branford, Conn., USA) administered by oral gavage, a diabetic group receiving a 150mg/kg intraperitoneal injections of Neotrofin (NeoTherapeutics Inc., Irvine, CA) and a non-diabetic control group. Treatments were initiated immediately following the confirmation of hyperglycemia and continued 6 days weekly for 4 weeks. At the conclusion of treatment period, the mice underwent thermal withdrawal latency testing and motor nerve conduction velocity (MNCV) was measured using the methods described in sections 2.2.1 and 2.3.1, respectively. Mice were then sacrificed and foot skin was taken for analysis of epidermal nerve fiber density and epidermal thickness, as described in section 2.4.2.

5.2.2 The effects of CNTF and TX14(A) on diabetic neuropathy

This study used STZ-diabetic Swiss Webster mice and included an untreated diabetic group, a diabetic group receiving 1mg/kg of CNTF (Regeneron, Tarrytown, NY), a diabetic group receiving 1mg/kg of TX14(A) (AnaSpec, San Jose, CA) and a non-diabetic control group. Subcutaneous injections of either CNTF or TX14(A) were administered immediately following the confirmation of hyperglycemia and continued 6 days weekly for 4 weeks. Thermal withdrawal latency was measured at the conclusion of the treatment period. Mice were then sacrificed and footpad skin was removed for analysis.

5.2.3 Reversal of diabetic neuropathy

Type 1 diabetes was induced in Swiss Webster mice by injection of STZ. After 4 weeks, thermal withdrawal latency and MNCV were measured. Mice were then divided into groups consisting of non-diabetic control mice, untreated diabetic mice, and diabetic mice treated with either 250mg/kg of IDD 676, 150mg/kg of Neotrofin, 5mg/kg of CNTF or 5mg/kg of TX14(A). Treatments were administered 6 days weekly and continued for 4 weeks. At the conclusion of the treatment period, thermal withdrawal latency and MNCV were again measured. Mice were then sacrificed and footpad skin was taken for analysis of epidermal nerve fiber density and epidermal thickness.

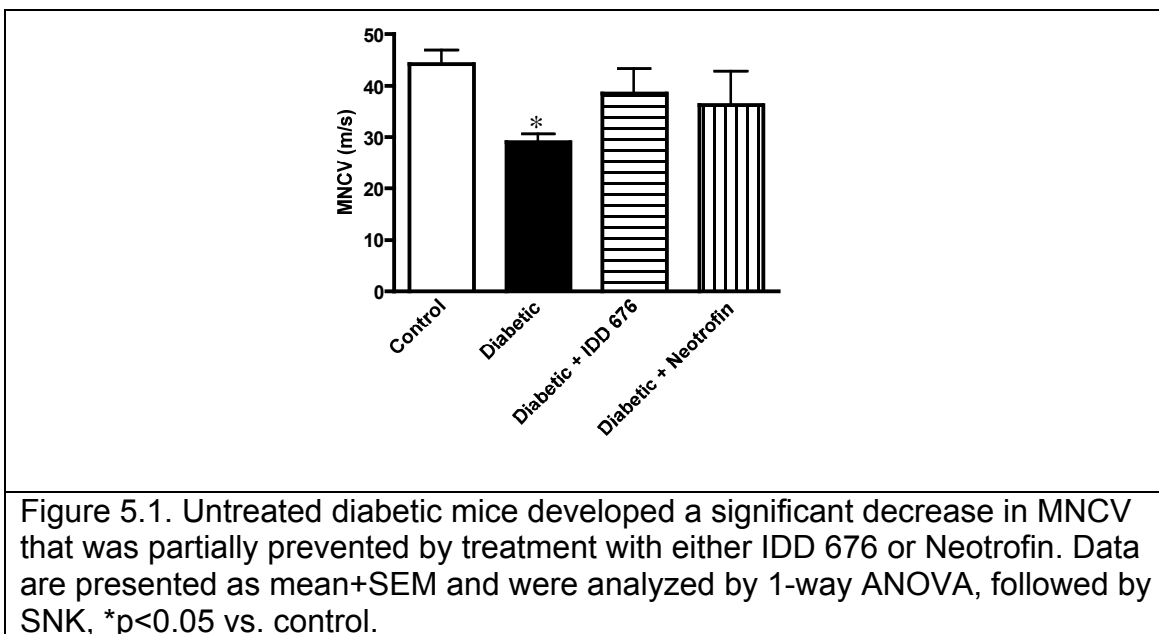
5.3 Results

5.3.1 The effects of IDD 676 and Neotrofin on diabetic neuropathy

After 4 weeks, untreated diabetic mice developed a significant ($p < 0.001$) weight loss, compared to the control mice. Neither IDD 676 nor Neotrofin affected body weight (Table 5.1). The untreated diabetic mice also developed significant ($p < 0.05$) MNCV slowing, compared to control mice. Treatment with either IDD 676 or Neotrofin resulted in a partial amelioration, with MNCV values not being significantly different from either the untreated diabetic mice or the control mice (Figure 5.1). Significant ($p < 0.001$ vs. control) thermal hypoalgesia was also observed in the untreated diabetic mice and was not prevented by either treatment (Figure 5.2). Significant changes in epidermal innervation (Figure 5.3) and epidermal thickness (Figure 5.4) were not observed in any of the groups.

Table 5.1. Final body weight and blood glucose levels for non-diabetic control mice, untreated diabetic mice and mice treated with either 250mg/kg of IDD 676 or 150mg/kg of Neotrofin 6 days weekly for 4 weeks.		
Group	Final Body Weight (g)	Final Blood Glucose (mmol/l)
Control (N=8)	31.7±2.3	10.7 (7.2-13.4)
Untreated Diabetic (N=11)	22.9±3.1***	>33.3
IDD 676-Treated Diabetic (N=7)	23.1±1.3***	>33.3
Neotrofin-Treated Diabetic (N=7)	22.3±2.6***	>33.3

Data are presented as mean±SD (body weight) or median(range) (blood glucose). Body weight was analyzed by 1-way ANOVA, followed by SNK, ***p<0.001 vs. control.



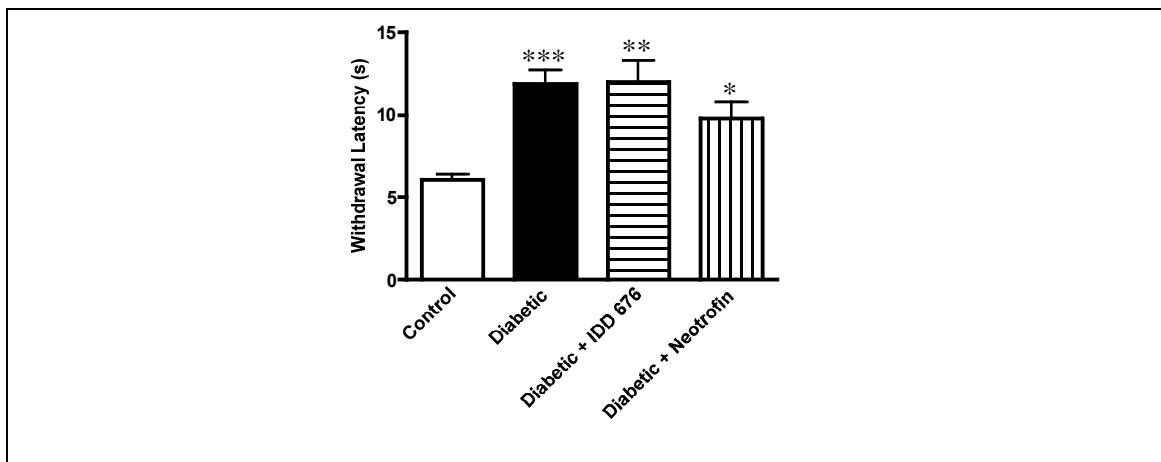


Figure 5.2. Untreated diabetic mice developed a significant increase in thermal withdrawal latency that was not prevented by treatment with either IDD 676 or Neotrofin. Data are presented as mean+SEM and were analyzed by 1-way ANOVA, followed by SNK, * $p < 0.05$, ** $p < 0.01$, *** $p < 0.001$ vs. control.

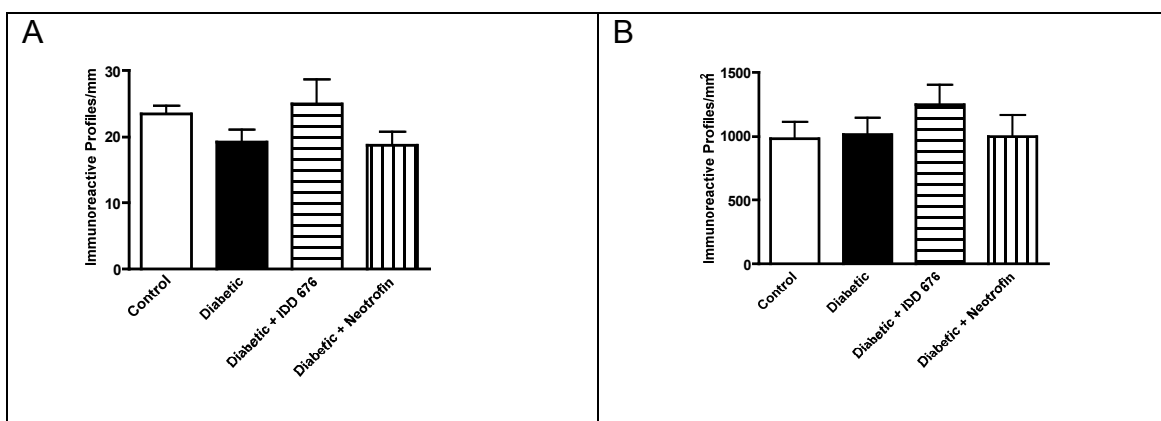
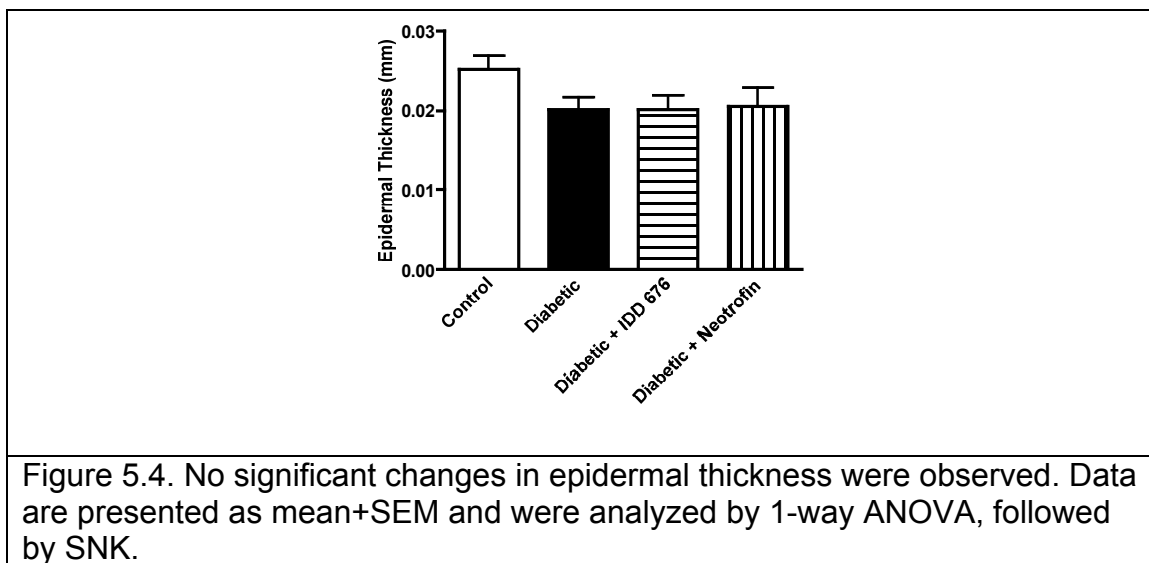


Figure 5.3. Significant changes in immunoreactive IENF profile density were not observed when profile counts were normalized to either epidermal length (A) or epidermal area (B). Data are presented as mean+SEM and were analyzed by 1-way ANOVA, followed by SNK.

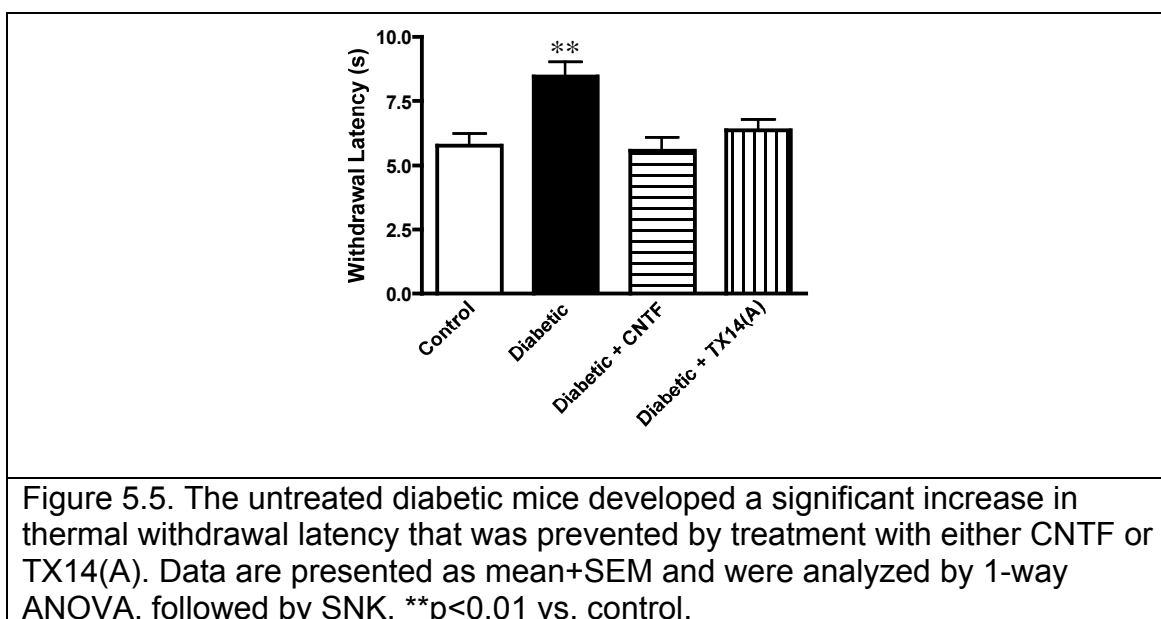


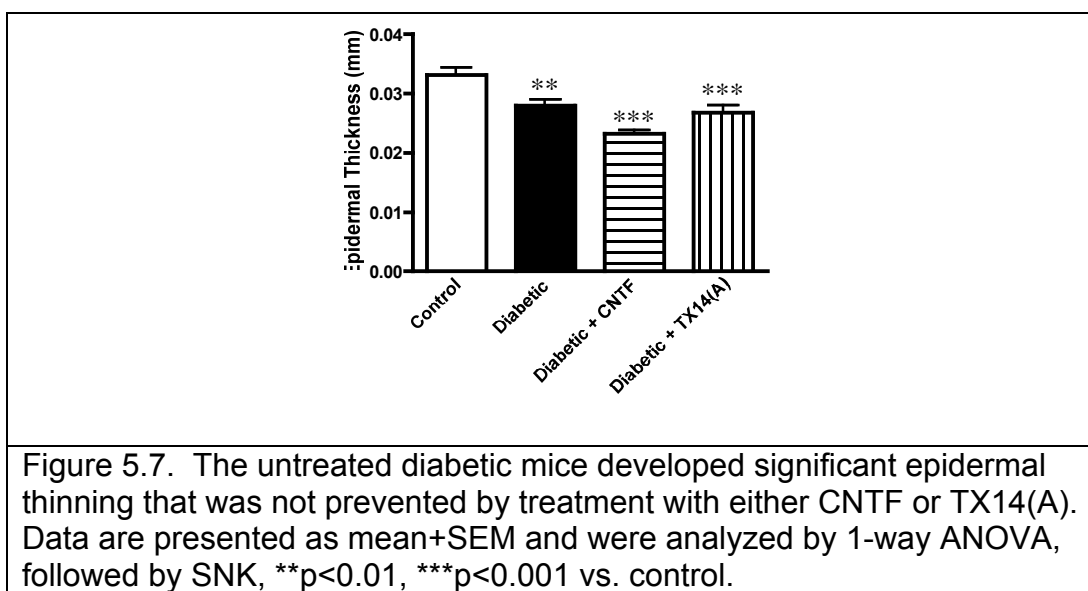
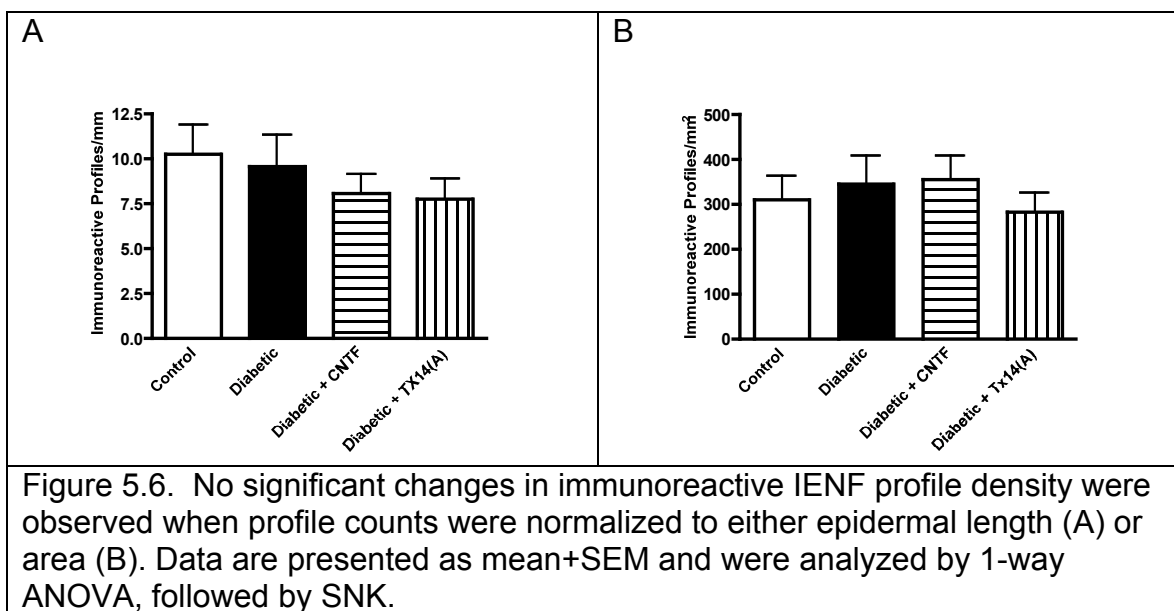
5.3.2 The effects of CNTF and TX14(A) on diabetic neuropathy

After 4 weeks, untreated diabetic mice experienced significant ($p < 0.01$) weight loss compared to control mice that was unaffected by treatment with TX14(A) (Table 5.2). Weight loss was more severe in CNTF-treated diabetic mice, which is consistent with a report that this factor has been associated with cachexia (Henderson et al., 1994). The untreated diabetic mice also developed significant ($p < 0.01$) thermal hypoalgesia, which was completely prevented by treatment with either CNTF or TX14(A) (Figure 5.5). Significant changes in epidermal nerve profile density were not observed in diabetic mice (Figure 5.6). However, the untreated diabetic mice developed significant ($p < 0.01$) epidermal thinning that was not prevented by either treatment (Figure 5.7).

Table 5.2. Final body weight and blood glucose levels for non-diabetic control mice, untreated diabetic mice and mice treated with either 1mg/kg of CNTF or 1mg/kg of Tx14(A), 6 days weekly for 4 weeks.		
Group	Final Body Weight (g)	Final Blood Glucose (mmol/l)
Control (N=8)	36.0±2.3	8.6 (4.0-12.2)
Untreated Diabetic (N=11)	30.6±2.6**	>33.3
CNTF-Treated Diabetic (N=13)	26.5±3.1**,#	>33.3
Tx14(A)-Treated Diabetic (N=12)	29.6±3.1**	>33.3

Data are presented as mean±SD (body weight) or median(range) (blood glucose). Body weight was analyzed by 1-way ANOVA, followed by SNK, **p<0.01 vs. control, #p<0.05 vs. untreated diabetic.

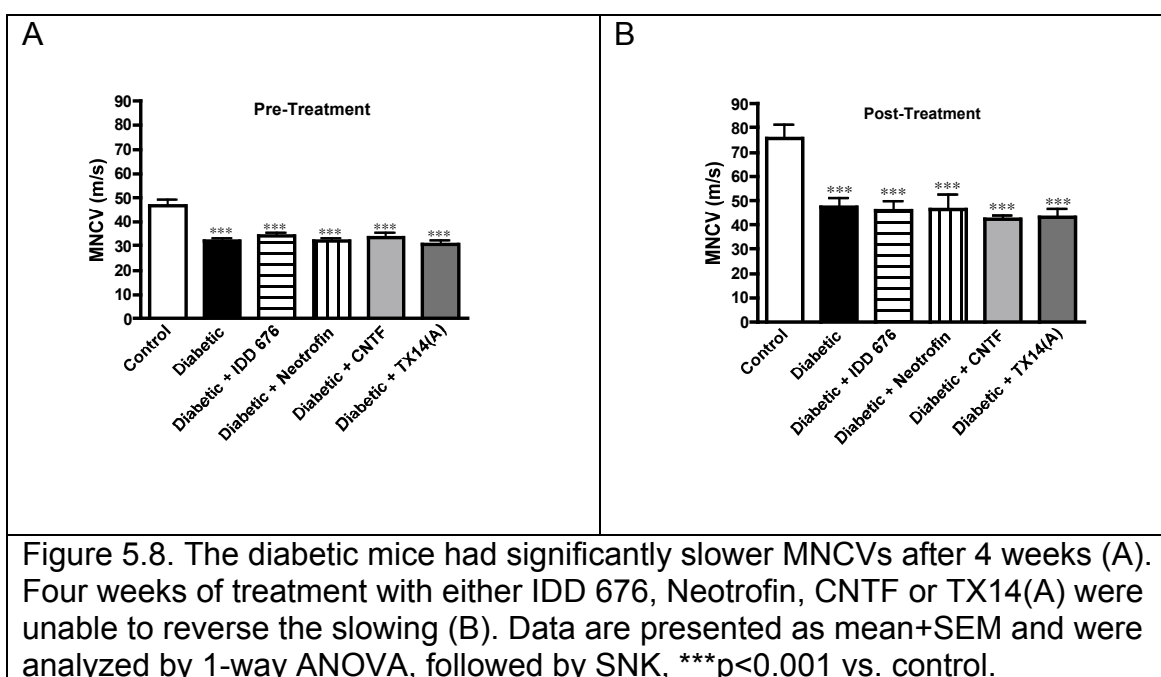




5.3.3. Reversal of neuropathy

After 4 weeks of untreated diabetes, diabetic mice had significantly ($p < 0.01$) slower MNCVs (Figure 5.8) and significantly ($p < 0.05$) higher thermal withdrawal latencies than control mice (Figure 5.9). Four subsequent weeks of treatment with either IDD 676, Neotrofin, CNTF or TX14(A) were unable to

reverse either deficit. Significant changes in immunoreactive nerve profile density (Figure 5.10) and epidermal thickness (Figure 5.11) were not observed in any of the groups. With the exception of CNTF, which again induced cachexia, none of the treatments had a significant effect on diabetes-induced weight loss (Table 5.3).



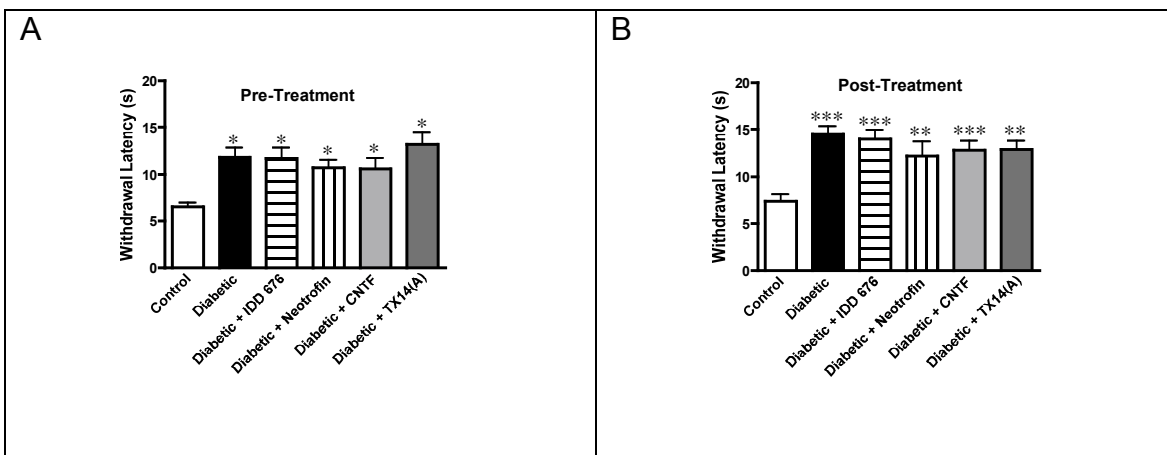


Figure 5.9. After 4 weeks, the diabetic mice developed a significant increase in thermal withdrawal latency (A). Four subsequent weeks of treatment were unable to reverse this increase (B). Data are presented as mean+SEM and were analyzed by 1-way ANOVA, followed by SNK, ** $p < 0.01$, *** $p < 0.001$ vs. control.

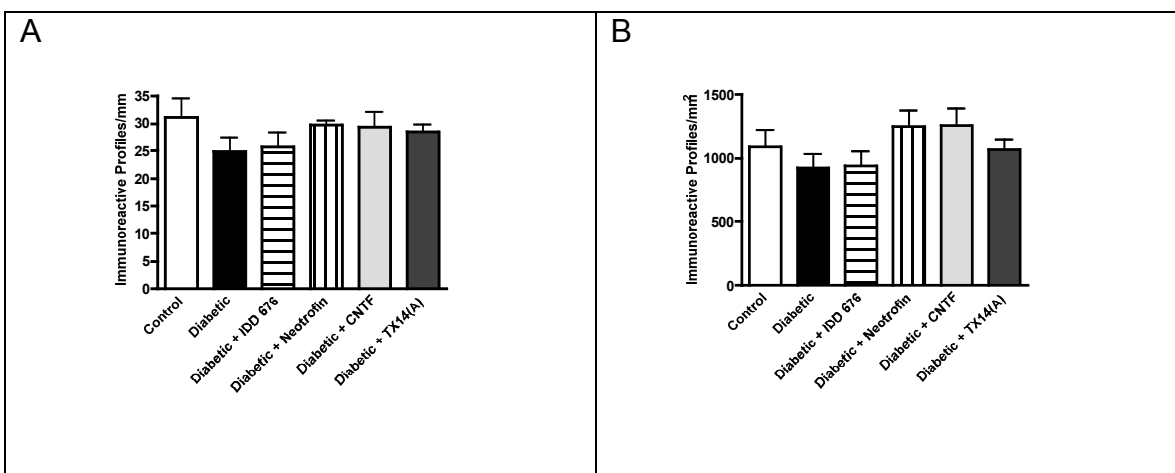


Figure 5.10. No significant changes in immunoreactive nerve profile density were observed when profile counts were normalized to either epidermal length (A) or area (B). Data are presented as mean+SEM and were analyzed by 1-way ANOVA, followed by SNK.

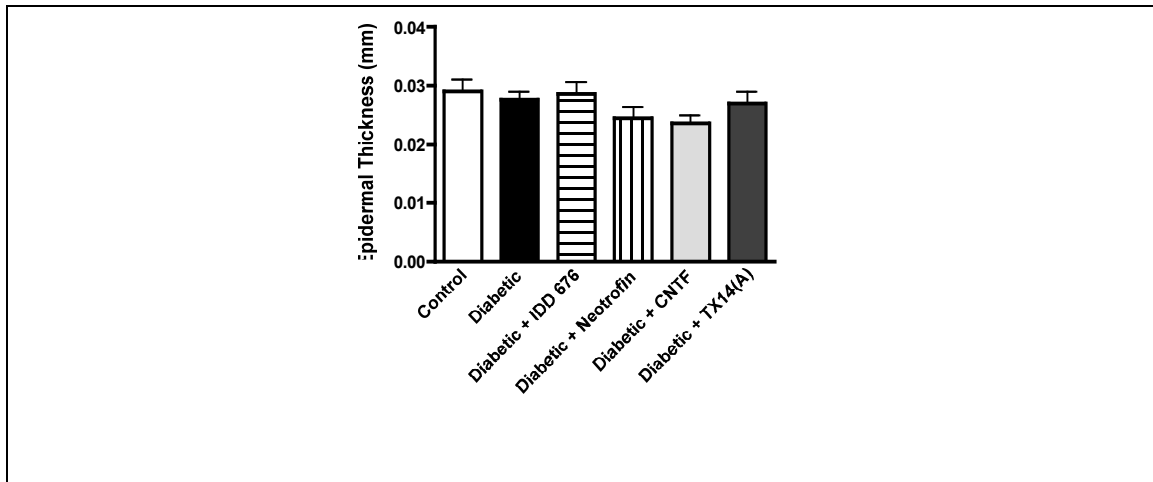


Figure 5.11. Significant changes in epidermal thickness were not observed between any of the groups. Data are presented as mean+SEM and were analyzed by 1-way ANOVA, followed by SNK.

Table 5.3. Final body weight and blood glucose levels for non-diabetic control mice, untreated diabetic mice and mice that were treated with either 250mg/kg of IDD, 150mg/kg of Neotrofin, 5mg/kg of CNTF or 5mg/kg of Tx14(A), 6 days weekly for 4 weeks following 4 weeks of untreated diabetes.

Group	Final Body Weight (g)	Final Blood Glucose (mmol/l)
Control (N=8)	32.7±2.3	9.2 (7.7-12.8)
Untreated Diabetic (N=10)	27.0±3.1**	>33.3
IDD 676-Treated Diabetic (N=14)	25.3±3.2***	>33.3
Neotrofin-Treated Diabetic (N=5)	25.2±3.2***	>33.3
CNTF-Treated Diabetic (N=9)	22.6±4.6***,#	>33.3
Tx14(A)-Treated Diabetic (N=9)	27.7±3.4**	>33.3

Data are presented as mean±SD (body weight) or median(range) (blood glucose). Body weight was analyzed by 1-way ANOVA, followed by SNK, **p<0.01, ***p<0.001 vs. control, #p<0.001 vs untreated diabetic.

5.4 Discussion

To explore the effects of aldose reductase inhibition, we examined the ability of IDD 676 to prevent several indices of diabetic neuropathy. The partial amelioration of MNCV slowing indicates that this dose was somewhat efficacious. However, we were unable to prevent the development of thermal hypoalgesia. Given that MNCV reflects the function of large nerve fibers, whereas thermal withdrawal latency is a measure of small fiber function, the possibility exists that large, myelinated fibers are more susceptible to the effects of increased polyol pathway flux and experience a greater benefit from aldose reductase inhibition. Indeed, aldose reductase has been localized to myelinating Schwann cells (Ludvigson and Sorenson, 1980; Powell et al., 1991). However, in STZ-diabetic rats, treatment with IDD 676 prevented both thermal hyperalgesia and thermal hypoalgesia (Calcutt et al., 2004). More recently, aldose reductase immunoreactivity has been reported in the sympathetic innervation of the dermal vasculature and therefore, could influence thermal sensitivity through disruption of blood flow (Jiang et al., 2006). The incongruity between our results and those observed in rats could be due to differences in the accumulation of polyol end products between the species. Indeed, diabetic mice neither accumulate sorbitol and fructose, nor experience a depletion of myo-inositol (Calcutt et al., 1988). These differences, along with other potentially unidentified species differences, may result in aldose reductase inhibition being less effective in the prevention of neuropathy in mouse models. Another potential reason for the limited efficacy of IDD 676 in our diabetic mice may be that the dose was insufficient. It has recently been reported that in order to achieve therapeutic efficacy, doses as

much as 10 times higher than those identified based on their ability to prevent polyol accumulation may be required (Oates, 2008). Perhaps, by treating the diabetic mice with a higher dose of IDD 676, we would have been able to replicate the degree of efficacy observed in rats. Future studies should involve further measures of efficacy, such as prevention of oxidative stress, to ensure that an adequate dose is administered.

Treatment with Neotrofin also resulted in a partial amelioration of MNCV. However, the development of thermal hypoalgesia was not prevented. In STZ-diabetic rats, injections of Neotrofin prevented both sensory nerve conduction velocity slowing and thermal hypoalgesia (Calcutt et al., 2006). The disconnect between our observations in STZ-diabetic mice and the effects of Neotrofin treatment in STZ-diabetic rats could be due to differences in drug metabolism between the species. Another possible explanation for Neotrofin's inability to prevent thermal hypoalgesia is that our dose of 150mg/kg, which was 5 times higher than the efficacious dose given to rats, was too high. Given that Neotrofin enhances endogenous NGF levels (Glasky et al., 1997; Calcutt et al., 2006) and that in cell culture excess NGF inhibits neurite outgrowth (Conti et al., 1997), the high doses of Neotrofin administered to our mice may have increased endogenous NGF to levels that were inhibitory. In future studies, NGF levels should be measured to determine efficacy and to ensure that they are within the range of non-diabetic mice.

The prevention of thermal hypoalgesia that we observed in STZ-diabetic mice receiving 1mg/kg treatments of either CNTF or TX14(A) is in agreement

with prior studies in STZ-diabetic rat models (Calcutt et al., 1999; Calcutt et al., 2000b; Calcutt et al., 2004). These results indicate that loss of neurotrophic support may play a role in the development of thermal hypoalgesia and suggest a similarity in the response to supplemental neurotrophic factors between rats and mice. Because we observed no change in epidermal nerve fiber density in the untreated diabetic mice, we were unable to assess the effects of CNTF and TX14(A) on epidermal innervation. However, these data further support the disconnect between thermal hypoalgesia and epidermal fiber loss discussed in chapter 4.

Although treatment with either IDD 676 or Neotrofin partially prevented MNCV slowing and treatment with either CNTF or TX14(A) prevented the development of thermal hypoalgesia, none of these treatments were successful in reversing either of these functional or behavioral deficits. These results are of clinical relevance because, although the prevention of various indices of neuropathy in animal models may increase our understanding of its pathogenesis, in order to successfully treat humans with diabetic neuropathy, potential therapeutics must be able to reverse established deficits.

Together, these data provide evidence of the involvement of polyol pathway flux in the development of MNCV slowing and the involvement of loss of neurotrophic support in the development of thermal hypoalgesia. Furthermore, these experiments highlight the importance of considering the differences between rats and mice when determining proper doses to administer. Given the apparent involvement of loss of neurotrophic support in the development of small

fiber neuropathy, our next set of studies focused on insulin as a neurotrophic factor and the role that insulin plays, beyond its effects on glycemic levels, in the development of diabetic neuropathy.

6 – Insulin as a Neurotrophic Factor

6.1 Introduction

6.1.1 Insulin as an in vitro neurotrophic factor

Recent evidence suggests that insulin deficiency may contribute to diabetic neuropathy, independent of its effects on glycemic levels. Multiple studies have confirmed that insulin is involved in the survival and maintenance of sensory neurons. In cultured human neuroblastoma cells, insulin increases both neurofilament and tubulin mRNA levels (Mill et al., 1985; Wang et al., 1992). Insulin also appears to be involved in tubulin stabilization and neurite outgrowth in cultured neuroblastoma cells (Ishii et al., 1985; Fernyhough et al., 1989). A more recent study, using cultured DRG neurons, indicates that the addition of insulin to the culture media can increase mitochondrial inner membrane potential (Huang et al., 2003). Given that mitochondrial dysfunction has been proposed as a mechanism of peripheral nerve degeneration (Nicholls and Budd, 2000) and that depolarization of the mitochondrial membrane has been observed in sensory neurons isolated from streptozotocin (STZ)-diabetic rats (Srinivasan et al., 2000), diabetes-induced insulin deficiency may lead to mitochondrial depolarization which could contribute to the development of diabetic peripheral neuropathy.

6.1.2 Insulin as an in vivo neurotrophic factor

Recent studies have examined the effects of low doses of insulin on peripheral neuropathy in rat models of diabetes. STZ-diabetic rats that were

given insulin at doses low enough to not affect glycosylated hemoglobin levels were protected against mitochondrial membrane depolarization and the development of nerve conduction velocity slowing (Huang et al., 2003). Another study, examining the effects of low doses of insulin delivered intrathecally, found that insulin treatment both prevented and reversed nerve conduction velocity slowing in STZ-diabetic rats, without influencing glycemic levels (Brussee et al., 2004). The insulin-treated rats also showed less axonal atrophy in the sural nerve than the untreated diabetic rats. Recently published studies have also explored the effects of low doses of insulin on epidermal innervation. One study, examining the effects of intrathecally delivered insulin in STZ-diabetic rats, found increases in IENF densities and IENF lengths in the treated diabetic rats (Toth et al., 2006). However, the IENF densities and lengths of the insulin-treated diabetic rats remained lower than those of the non-diabetic control group. Another study using STZ-diabetic mice found evidence of epidermal reinnervation in individuals that spontaneously regained islet cell function (Kennedy and Zochodne, 2005).

6.1.3 Comparisons of type 1 and type 2 rodent models

Given insulin's neurotrophic properties, one might expect the epidermal nerve fibers of humans and animals with type 2 diabetes to be protected from developing neuropathy. A recent study, using morphometric analysis to compare sural nerves from type 1 and type 2 diabetic rats, found that the type 1 diabetic rats showed signs of C-fiber degeneration sooner than the type 2 diabetic rats (Kamiya et al., 2005). While several studies have reported a reduction in IENF density in rat models of type 1 diabetes (Bianchi et al., 2004; Lauria et al., 2005;

Leonelli et al., 2007; Roglio et al., 2007), the effects of hyperglycemia on epidermal innervation in rat models of type 2 diabetes remain unexplored. Epidermal fiber loss has been reported in mouse models of type 2 diabetes (Gibran et al., 2002; Drel et al., 2006; Vareniuk et al., 2007). However, type 2 diabetic mouse models can show insulinopenia in later stages of the disease, and insulin levels were not reported by the authors of these studies. In the first study presented in this chapter, we compared changes in epidermal innervation in type 1 and type 2 diabetic mouse models of the same background strain. Our next studies examined the effects of various doses of insulin on certain measures of diabetic neuropathy in a type 1 diabetic mouse model. Lastly, we examined the effects of the systemic insulin release that occurs immediately following STZ-injection, as well as the effects of insulin injected directly into the paw, on heat sensitivity and epidermal innervation.

6.2 Methods

6.2.1 A comparison of type 1 and type 2 models

The type 1 diabetic group consisted of male C57Bl/6 mice that were given a single 180 mg/kg injection of STZ. Hyperglycemia was confirmed 3 days later, and only mice with blood glucose levels exceeding 15 mmol/l were included in the diabetic group. After 4 weeks of diabetes, thermal withdrawal latency was measured using the methods described in section 2.2.1. Mice were then sacrificed and plantar foot skin was taken. Skin samples were later immunostained and analyzed using the methods described in sections 2.4.1 and 2.4.2.

The type 2 diabetic group consisted of male db/db mice, which possess a leptin receptor mutation that results in the development of type 2 diabetes. These mice were generated by Jackson Labs (Bar Harbor, ME) using C57Bl/6 mice as the background strain (stock #000697). Blood glucose levels were monitored throughout the study. After the mice had been hyperglycemic for approximately 41 days, thermal withdrawal latency and motor nerve conduction velocity (MNCV) were measured using the methods described in sections 2.2.1 and 2.3.1, respectively. Mice were then sacrificed and plantar foot skin was removed from both the db/db mice and non-diabetic age-matched control mice. The skin samples were fixed, dehydrated, sectioned, immunostained and analyzed, as described in sections 2.4.1 and 2.4.2.

6.2.2 The effects of varied doses of insulin in type 1 diabetic mice

To examine the effects of varied doses of insulin, type 1 diabetes was induced in male Swiss Webster mice using the methods described in section 6.2.1. One group of diabetic mice was given a single Linbit Insulin Pellet (LinShin Inc., Canada). These implants release approximately 0.1 unit of insulin per day for at least 30 days. Another group of diabetic mice was given 3 Linbit Insulin Pellets.

After the mice had been diabetic for 4 weeks, thermal withdrawal latency and MNCV were measured using the methods described in sections 2.2.1 and 2.3.1, respectively. Plantar foot skin samples were removed at the time of sacrifice, and immunoreactive IENF profile density and epidermal thickness were then assessed in PGP9.5-immunostained skin sections, using the methods that

have been described in sections 2.4.1 and 2.4.2. Blood samples were also taken from the mice at the time of sacrifice and shipped to Biosafe Laboratories Inc. (Chicago, IL), where HbA1C levels were measured. A subsequent study was performed examining the effects of either 1 or 5 (3 initially, followed by 2 more after 4 weeks) insulin pellets on the same indices of neuropathy described above after 8 weeks of diabetes.

6.2.3 The acute effects of STZ-injection

To examine the effects of the systemic insulin release that occurs following STZ-injection and subsequent destruction of pancreatic beta cells, male Swiss Webster mice were given a 180 mg/kg intraperitoneal injection of STZ, using the same methods described previously. Blood glucose levels were monitored every 4 hours for the following 54 hours. After 54 hours, the STZ-injected mice and age-matched control mice, underwent thermal withdrawal latency testing and were sacrificed immediately thereafter. Footpad skin was then removed, immunostained and analyzed, using the methods described previously.

6.2.4 Effects of direct insulin injections

To examine the local effects of insulin, male Swiss Webster mice first underwent testing of baseline thermal withdrawal latency and were then injected with 0.1 unit of HumulinR insulin (Eli Lilly, Indianapolis) diluted in 20 microliters of saline into the plantar surface of the left hind paw. Age-matched control mice were given a 20 microliter injection of saline. After 54 hours, thermal withdrawal latency was again assessed. In order to draw comparisons between our

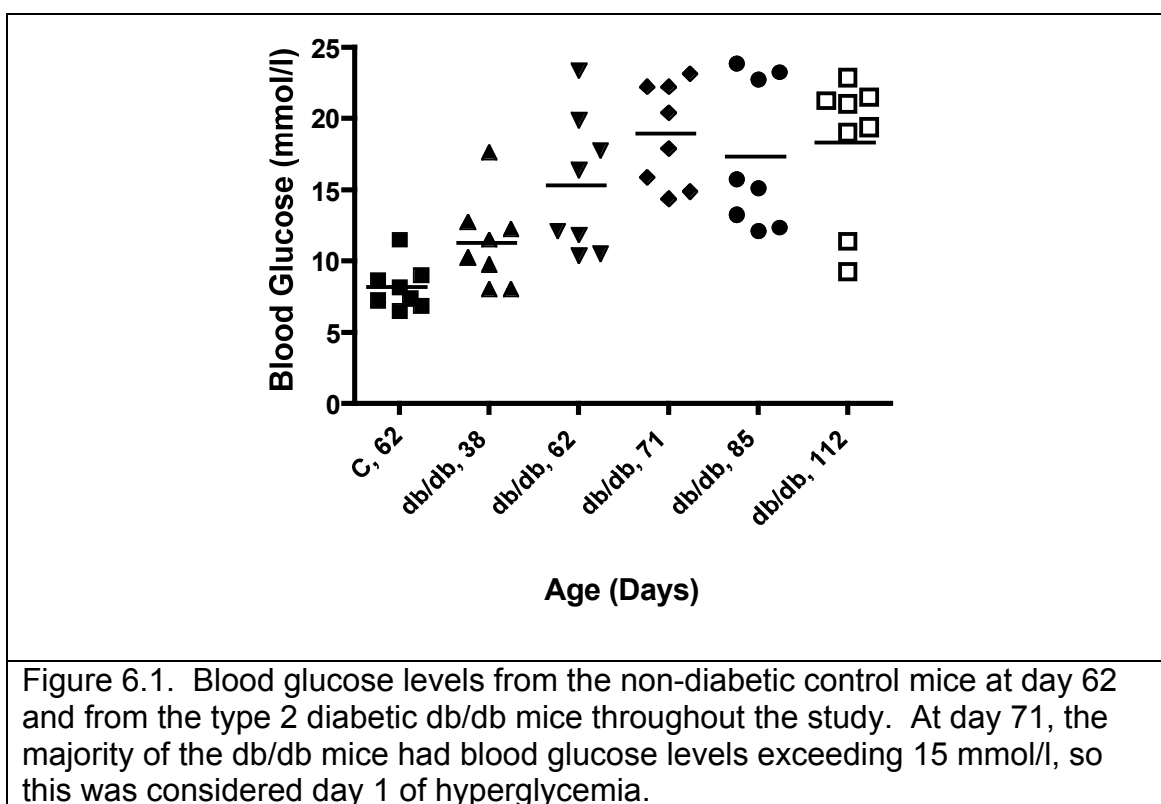
baseline withdrawal latency measurements and the measurements taken 54 hours later, we constructed a calibration curve, by plotting the rate of temperature increase. The calibration curve was used to convert latency measurements to the temperature at which the mouse reacted to the heat stimulus. Conversion from latency to temperature is necessary when comparing measurements taken on separate days, as the rate of heating is not always consistent. Immediately following thermal withdrawal latency assessment, the mice were sacrificed, and foot skin from both hind paws was removed. The skin samples were then immunostained and analyzed, using methods described previously. In addition to PGP9.5 immunohistochemistry, skin sections from these mice were also immunostained with an antibody against GAP-43 (Abcam, UK), a marker for regenerating nerve fibers. GAP-43-immunoreactive nerve profiles were quantified using the methods described previously.

6.3 Results

6.3.1 A comparison of type 1 and type 2 models of diabetes

The type 2 diabetic db/db mice developed a significant ($p < 0.001$) increase in body weight (see Table 3.1). The blood glucose levels of the db/db mice fluctuated throughout the study, so levels were measured frequently. Figure 6.1 shows the blood glucose levels at various time points throughout the study. By 71 days of age, the majority of the db/db mice had blood glucose levels exceeding 15 mmol/l, so this time point was considered to be the first day of hyperglycemia. Although glycemic levels continued to fluctuate throughout the study, the mice that were included in the diabetic group all possessed average

glycemic levels exceeding 15 mmol/l. At the time of sacrifice, the insulin levels of the db/db mice greatly exceeded ($p < 0.01$) those of the control mice (Figure 6.2). A significant ($p < 0.001$) decrease in MNCV (Figure 6.3) and a significant ($p < 0.01$) increase in thermal withdrawal latency (Figure 6.4A) developed in the db/db mice after 41 days of hyperglycemia. As was reported in chapter 3, a significant ($p < 0.01$) reduction in linear immunoreactive IENF profile density was observed (Figure 3.5C). A significant ($p < 0.001$) reduction in IENF density was also observed when profile counts were normalized to epidermal area (Figure 6.5A).



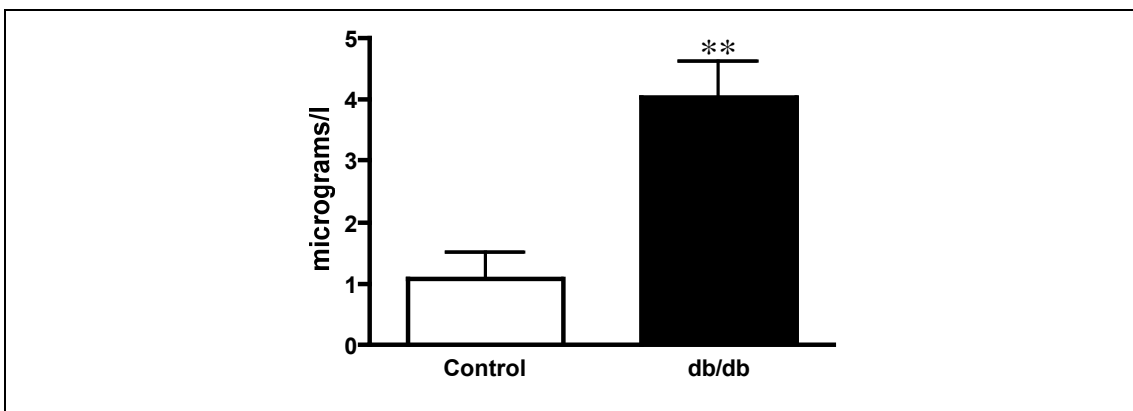


Figure 6.2. At the conclusion of the study, the insulin levels of the type 2 diabetic db/db mice were significantly higher than those of the non-diabetic control mice. Data are presented as mean+SEM and were analyzed by an unpaired 2-tailed t-test, ** $p < 0.01$.

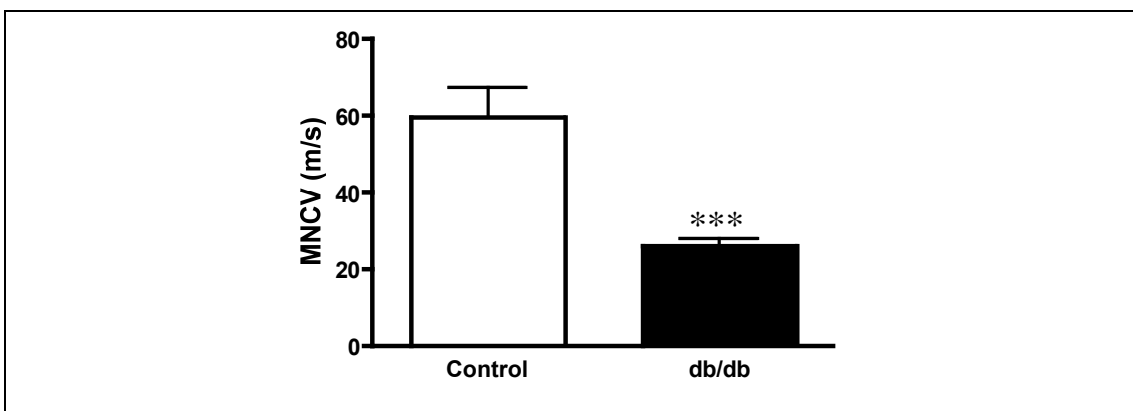


Figure 6.3. After 41 days of hyperglycemia, the MNCVs of the db/db mice were significantly slower than those of the control mice. Data are presented as mean+SEM and were analyzed by an unpaired 2-tailed t-test, *** $p < 0.001$.

After 4 weeks of diabetes, the STZ-injected C57Bl/6 mice had a significant ($p < 0.001$) weight loss (see Table 3.1) compared to control mice. The diabetic C57BL/6 mice also developed a significant ($p < 0.01$) increase in thermal withdrawal latency (Figure 6.4). As was reported in chapter 3, a significant ($p < 0.01$) reduction in linear immunoreactive IENF profile density was observed (Figure 3.5A), and immunoreactive IENF profile density was also reduced when counts were normalized to epidermal area (Figure 6.5B).

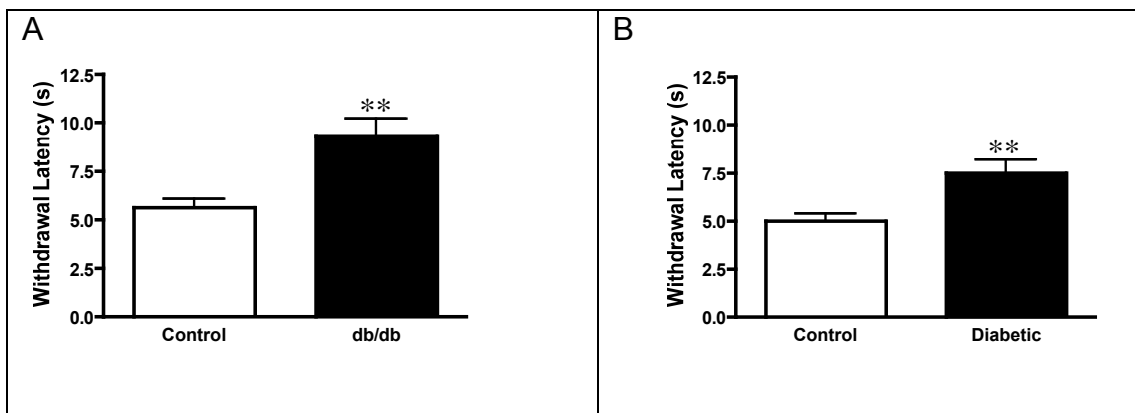


Figure 6.4. The thermal withdrawal latencies of db/db mice (A) and STZ-diabetic C57Bl/6 mice (B) were significantly increased compared to the control mice. Data are presented as mean+SEM and were analyzed by an unpaired 2-tailed t-test, ** $p < 0.01$.

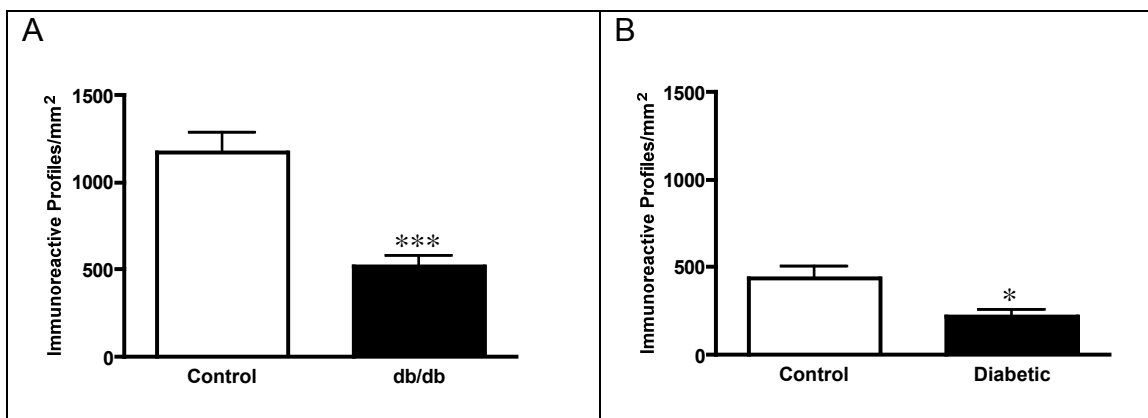


Figure 6.5. Both db/db (A) and STZ-diabetic C57Bl/6 (B) mice developed a significant decrease in immunoreactive IENF profile density when profile counts were normalized to epidermal area. Data are presented as mean+SEM and were analyzed by an unpaired 2-tailed t-test, * $p < 0.05$, *** $p < 0.001$.

6.3.2 The effects of varied doses of insulin

After 4 weeks, the untreated diabetic mice developed a significant ($p < 0.001$) weight loss compared to control mice, and the single insulin pellet did not significantly affect body weight. The diabetic mice that received 3 insulin pellets were significantly ($p < 0.01$) heavier than the untreated diabetic mice, yet still significantly ($p < 0.001$) lighter than the non-diabetic control mice (Table 6.1).

The blood glucose levels of both the untreated diabetic mice and the diabetic mice that received a single insulin pellet were at least 33.3 mmol/l. However, our method of detection was not sensitive enough to ascertain whether or not the low dose of insulin had an effect on blood glucose levels. The diabetic mice that received 3 insulin pellets had a lower median blood glucose level of 28.1 mmol/l (Table 6.1).

Table 6.1. Final body weight, blood glucose levels and HbA1C levels for mice treated with insulin pellets for 4 weeks.			
Group	Final Body Weight (g)	Final Blood Glucose (mmol/l)	Final HbA1C (%)
Control (N=10)	32.4±2.2	8.6 (5.6-18.1)	5.18±0.3
Untreated Diabetic (N=8)	25.6±3.0*	>33.3***	10.2±0.6*
Diabetic + 1 Insulin Pellet (N=11)	26.9±1.4*	>33.3***	8.8±1.0 [#]
Diabetic + 3 Insulin Pellets (N=9)	28.9±1.1 [#]	28.1 (24.4-33.3)	7.6±0.5 [#]
Data are mean ± SEM, except blood glucose levels, which are median (range). Statistical analysis was performed by 1 way ANOVA followed by SNK for final body weights and HbA1C levels and by Kruskal-Wallis followed by Dunn's for final blood glucose levels. *p<0.05, ***p<0.001 vs. control, [#] p<0.05 vs. untreated diabetic.			

The HbA1C levels of the untreated diabetic mice were also significantly ($p<0.001$) increased, compared to those of the non-diabetic control mice. Both the mice receiving the single implant and the mice receiving 3 implants had HbA1C levels that were significantly ($p<0.01$) lower than those of the untreated

diabetic mice, but these levels were still significantly ($p < 0.01$) higher than those of the non-diabetic control mice (Table 6.1).

The untreated diabetic mice developed significant ($p < 0.01$) MNCV slowing, compared to the non-diabetic control mice (Figure 6.6). Treatment with low doses of insulin appeared to have a partial effect, with the nerve conduction velocities of the mice that received a single insulin pellet not being significantly different from either the untreated diabetic mice or the non-diabetic control mice. The nerve conduction velocities of the diabetic mice that received 3 insulin pellets were completely normalized ($p < 0.05$ vs. untreated diabetic, $p > 0.05$ vs. control).

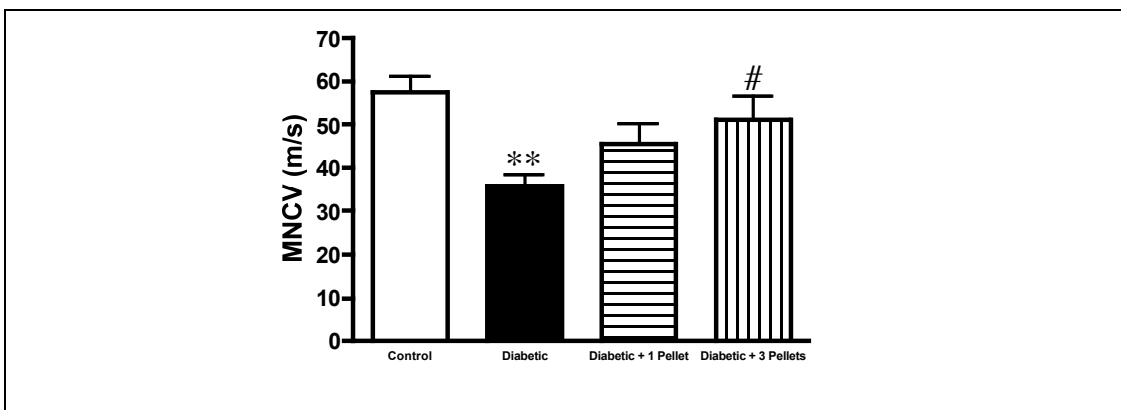
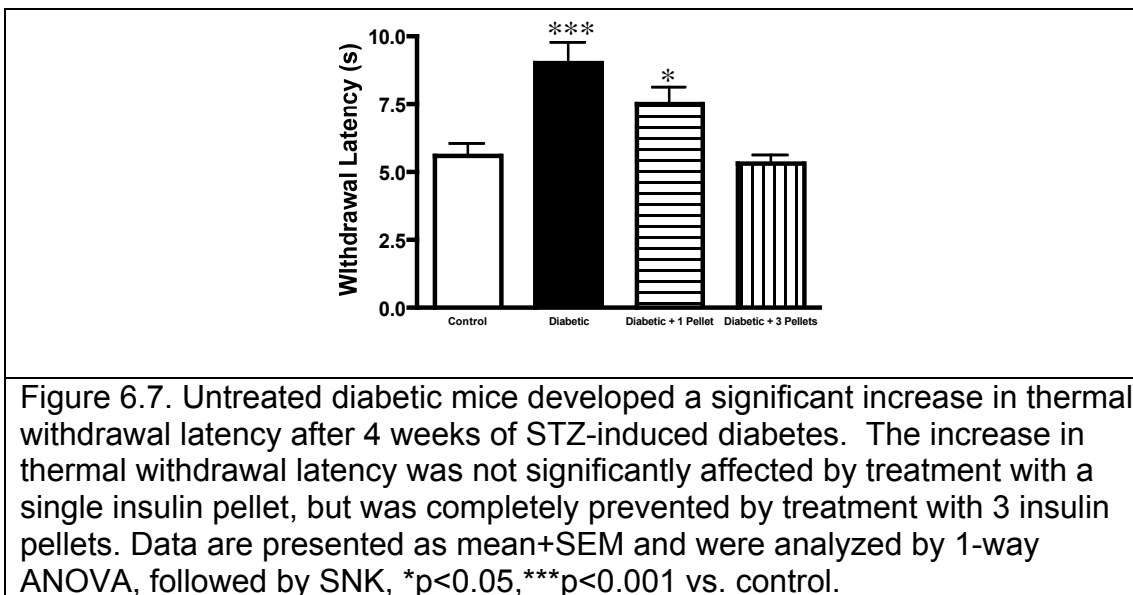


Figure 6.6. Untreated diabetic mice developed a significant decrease in MNCV after 4 weeks of STZ-induced diabetes. MNCV slowing was partially ameliorated by treatment with a single insulin pellet and completely prevented by treatment with 3 insulin pellets. Data are presented as mean+SEM and were analyzed by 1-way ANOVA, followed by SNK, ** $p < 0.01$ vs. control, # $p < 0.05$ vs. untreated diabetic.

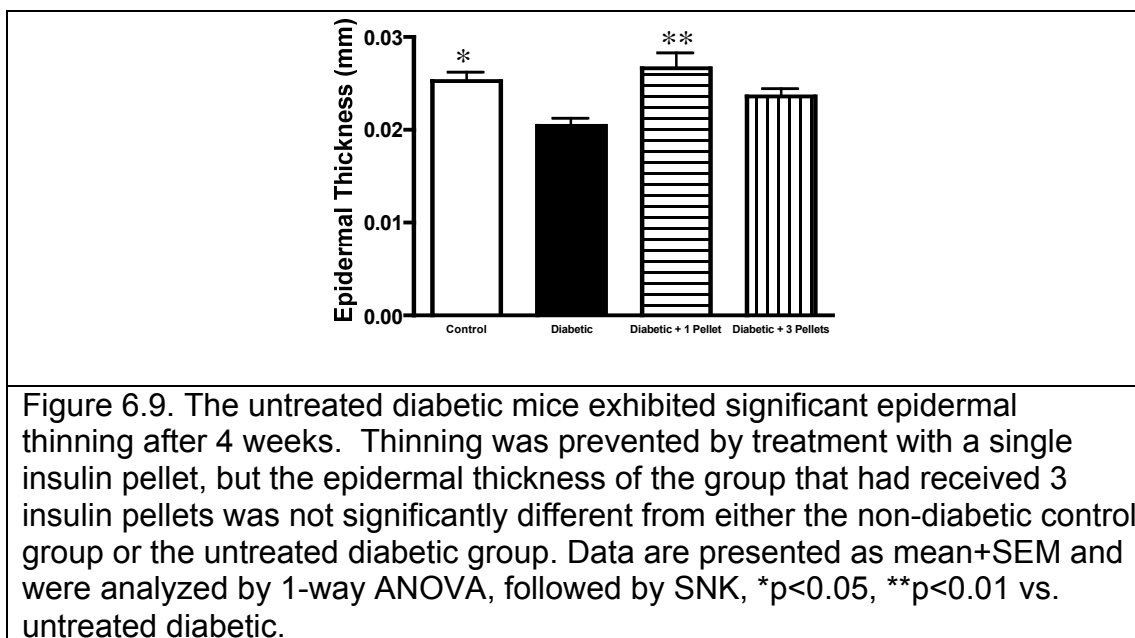
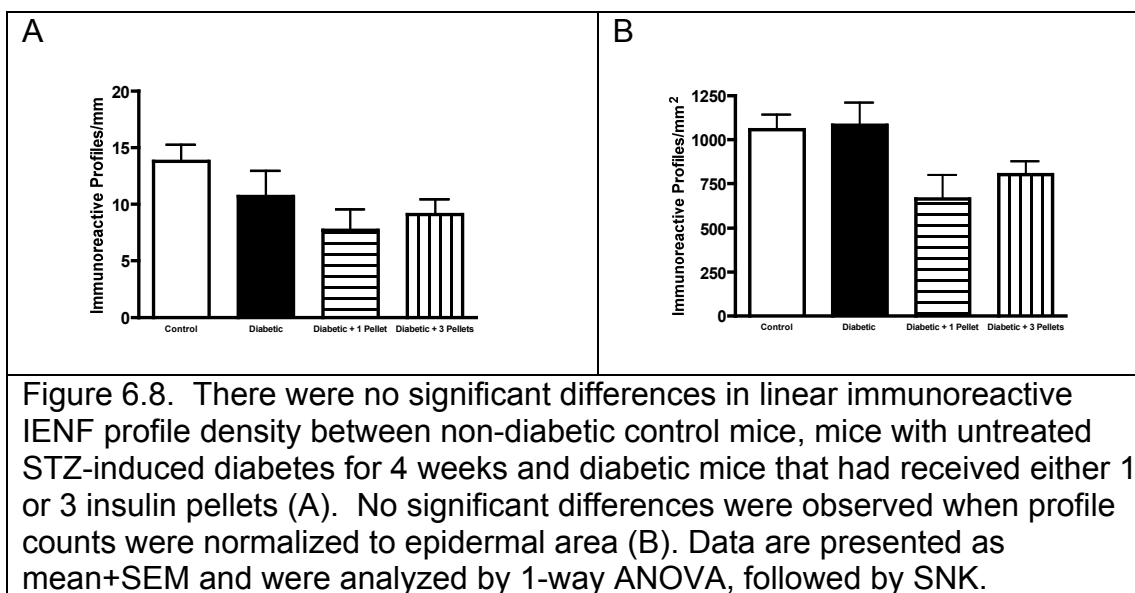
Untreated diabetic mice also developed a significant ($p < 0.01$) increase in thermal withdrawal latency after 4 weeks of diabetes (Figure 6.7). There was a partial alleviation of thermal hypoalgesia in the mice that received a single insulin

implant. However, values were not significantly different from the untreated diabetic mice and remained significantly ($p < 0.05$) higher than control mice. Treatment with 3 insulin pellets completely prevented the development of thermal hypoalgesia ($p < 0.01$ vs. untreated diabetic, $p > 0.05$ vs. control).



In our analysis of epidermal innervation, there were no statistically significant differences in immunoreactive IENF profile density between the control mice, the untreated diabetic mice, the diabetic mice that received 1 insulin pellet and the diabetic mice that received 3 insulin pellets (Figure 6.8), and this observation was true for profile counts normalized to both epidermal area and length. The untreated diabetic mice developed significant ($p < 0.05$) epidermal thinning (Figure 6.9). The thinning was completely prevented in the mice that received a single insulin pellet ($p < 0.01$ vs. untreated diabetic, $p > 0.05$ vs. control). However, the thickness of the epidermis of the mice that received 3 insulin

pellets was not significantly different from either the untreated diabetic mice or the non-diabetic control mice.



In our study examining the effects of varied doses of insulin after 8 weeks of diabetes, the final body weights of the untreated diabetic mice were significantly ($p < 0.001$) lower than those of the non-diabetic control mice. The

mice that were given a single insulin pellet were significantly ($p < 0.01$) heavier than the untreated diabetic mice, yet significantly ($p < 0.001$) lighter than the non-diabetic control mice. The mice that were given 5 insulin pellets were also significantly ($p < 0.001$) heavier than the untreated diabetic mice, but significantly ($p < 0.001$) lighter than the non-diabetic control mice (Table 6.2).

The final blood glucose levels for both the untreated diabetic mice and the mice that received a single insulin pellet were again above our limit of detection (33.3 mmol/l). The mice that received 5 insulin pellets had blood glucose levels that were lower than those of the untreated diabetic mice, yet still significantly ($p < 0.001$) higher than those of the non-diabetic control mice (Table 6.2).

The final HbA1C levels of the untreated diabetic mice were significantly ($p < 0.001$) increased, compared to those of the non-diabetic control mice. The HbA1C levels of the mice that received a single insulin pellet were significantly ($p < 0.05$) lower than those of the untreated diabetic mice, yet still significantly ($p < 0.001$) higher than those of the non-diabetic control mice. The diabetic mice that received 5 insulin pellets had significantly ($p < 0.001$) lower HbA1C levels than the untreated diabetic mice and the mice that received a single insulin pellet. However, the HbA1C levels of the mice that received 5 insulin pellets were still significantly ($p < 0.001$) higher than those of the non-diabetic control mice (Table 6.2).

After 8 weeks, the untreated diabetic mice had significantly ($p < 0.001$) slower nerve conduction velocities than those of the non-diabetic control mice (Figure 6.10). Treatment with either a single insulin pellet or 5 insulin pellets did

not have an effect on the MNCV slowing. The untreated diabetic mice also developed a significant ($p < 0.05$ vs. control) increase in thermal withdrawal latency (Figure 6.11). Treatment with a single insulin pellet had no effect on thermal withdrawal latency ($p < 0.05$ vs. control). However, treatment with 5 insulin pellets was able to prevent the development of thermal hypoalgesia ($p > 0.05$ vs. control).

Table 6.2. Final body weight, blood glucose levels and HbA1C levels for mice treated with insulin pellets for 8 weeks.			
Group	Final Body Weight (g)	Final Blood Glucose (mmol/l)	Final HbA1C (%)
Control (N=10)	34.5±2.6	10.6 (8.9-16.2)	4.5±0.2
Untreated Diabetic (N=8)	22.7±2.6*	>33.3***	11.3±0.3*
Diabetic + 1 Insulin Pellet (N=11)	27.3±3.5* [#]	>33.3***	10.2±1.0* [#]
Diabetic + 5 Insulin Pellets (N=11)	29.2±2.5* [#]	29.5 (4.1-33.3)	7.1±1.2* [#]
Data are mean ± SEM, except blood glucose levels, which are median (range). Statistical analysis was performed by 1-way ANOVA followed by SNK for final body weights and HbA1C levels and by Kruskal-Wallis followed by Dunn's for final blood glucose levels. * $p < 0.05$, *** $p < 0.001$ vs. control, [#] $p < 0.05$ vs. untreated diabetic..			

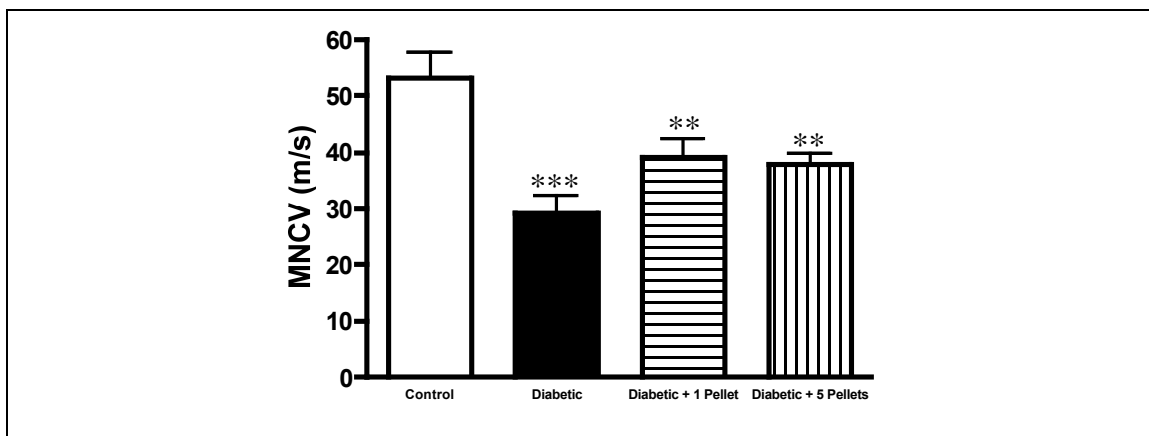


Figure 6.10. Untreated diabetic mice developed a significant reduction in motor nerve conduction velocity after 8 weeks of STZ-induced diabetes. Nerve conduction velocity slowing was not prevented by treatment with either a single insulin pellet or 5 insulin pellets. Data are presented as mean+SEM and were analyzed by 1-way ANOVA, followed by SNK, ** $p < 0.01$, *** $p < 0.001$ vs. control.

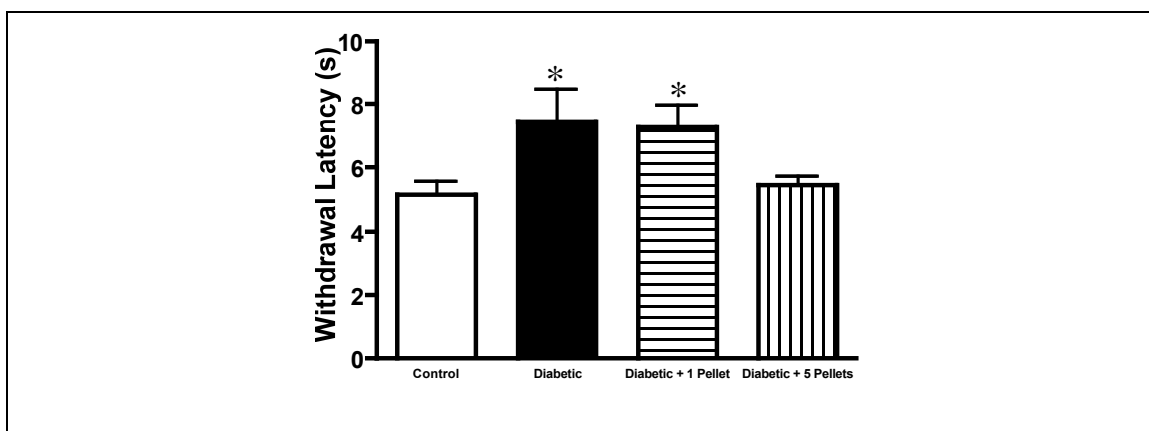


Figure 6.11. Untreated diabetic mice developed a significant increase in thermal withdrawal latency after 8 weeks of STZ-induced diabetes. The increase was not affected by treatment with a single insulin pellet, but was completely prevented by treatment with 5 insulin pellets. Data are presented as mean+SEM and were analyzed by 1-way ANOVA, followed by Dunnett's Multiple Comparison Test, * $p < 0.05$ vs. control.

No significant differences in immunoreactive IENF profile density were observed between the non-diabetic control mice, the untreated diabetic mice and either treatment group (Figure 6.12), and this observation was true for profile counts normalized to either epidermal area or length. There were also no significant differences in the thickness of the epidermis between the non-diabetic

control mice, the untreated diabetic mice and either treatment group (Figure 6.13).

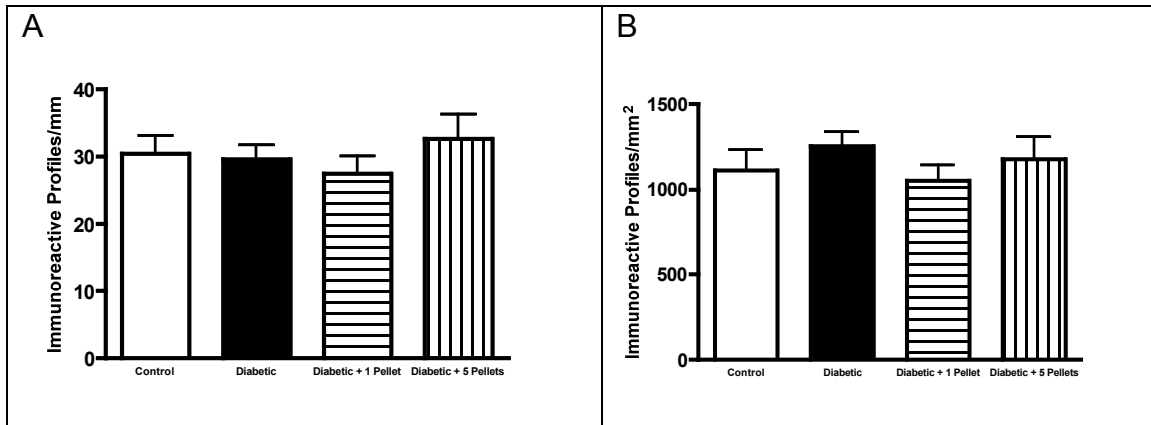


Figure 6.12. There were no significant differences in linear immunoreactive IENF profile density between non-diabetic control mice, mice with untreated STZ-induced diabetes for 8 weeks and diabetic mice that had received either 1 or 5 insulin pellets (A). Significant differences were also not observed when profile counts were normalized to epidermal area (B). Data are presented as mean+SEM and were analyzed by 1 way ANOVA, followed by SNK.

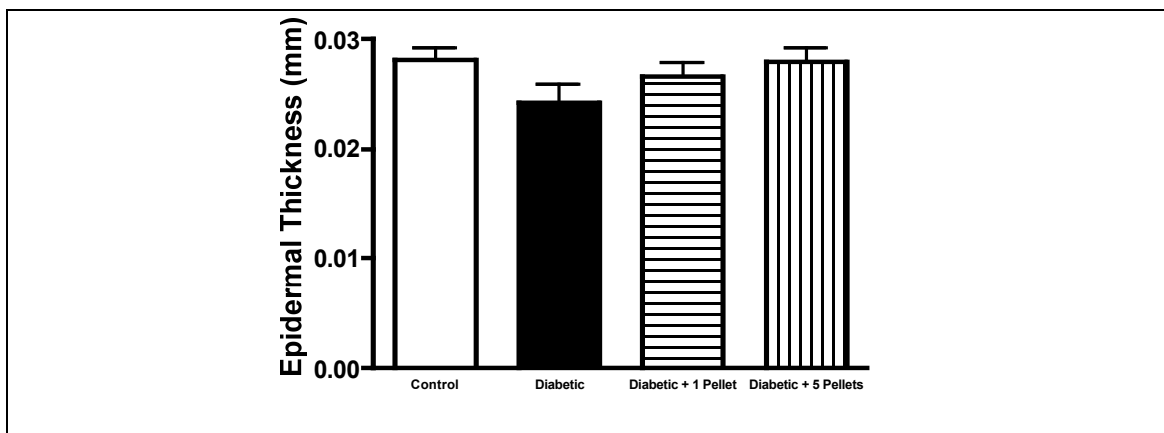


Figure 6.13. There were no significant differences in epidermal thickness between non-diabetic control mice, mice with STZ-induced diabetes for 8 weeks and diabetic mice that had received either 1 or 5 insulin pellets. Data are presented as mean+SEM and were analyzed by 1 way ANOVA, followed by SNK.

6.3.3 The short-term effects of STZ injection

The STZ-injected mice were hyperglycemic 4 hours post-injection (Figure 6.14). The increase in blood glucose levels was followed by a significant ($p < 0.001$) drop 8 hours post-injection. After 12 and 16 hours, blood glucose in the injected mice was again approaching hyperglycemic levels, and after 20 hours blood glucose exceeded 15 mmol/l. Hyperglycemia persisted in the injected mice for the duration of the study.

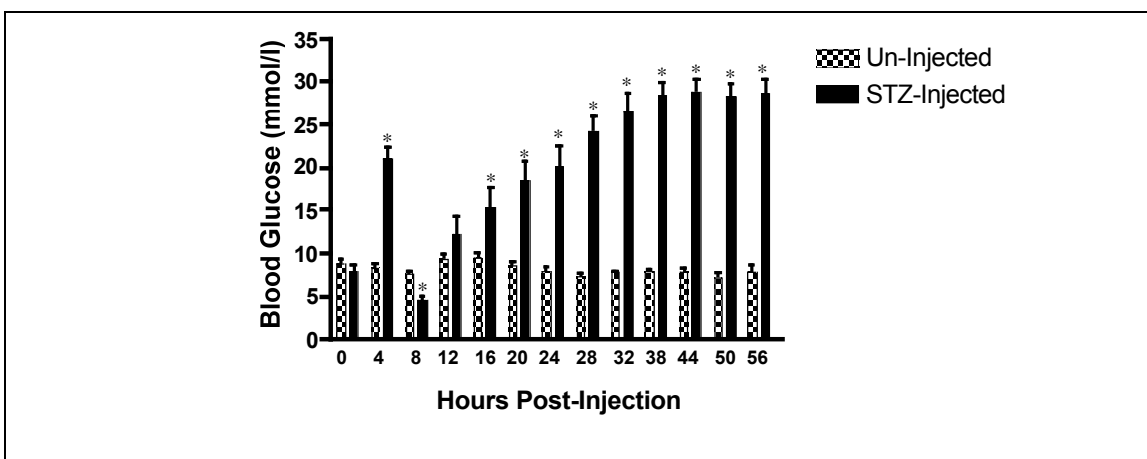


Figure 6.14. The blood glucose levels of the un-injected mice remained relatively consistent throughout the study. STZ-injected mice experienced an increase in blood glucose levels 4 hours post-injection that was followed by a transient decrease 8 hours post-injection. The mice eventually progressed to hyperglycemia. Data are presented as mean+SEM and were analyzed by an unpaired 2-tailed t-test, * $p < 0.001$ vs. un-injected mice.

After 54 hours, there were no significant changes in the thermal withdrawal latencies of the STZ-injected mice (Figure 6.15). There was a slight but not significant increase in the linear immunoreactive IENF profile density of the STZ-injected group (Figure 6.16A), and when profile counts were normalized to epidermal area, there was a significant ($p < 0.05$) increase in the density of the

STZ-injected group (Figure 6.16B). There was also an insignificant trend toward a thinning of the epidermis in the STZ-injected group (Figure 6.17).

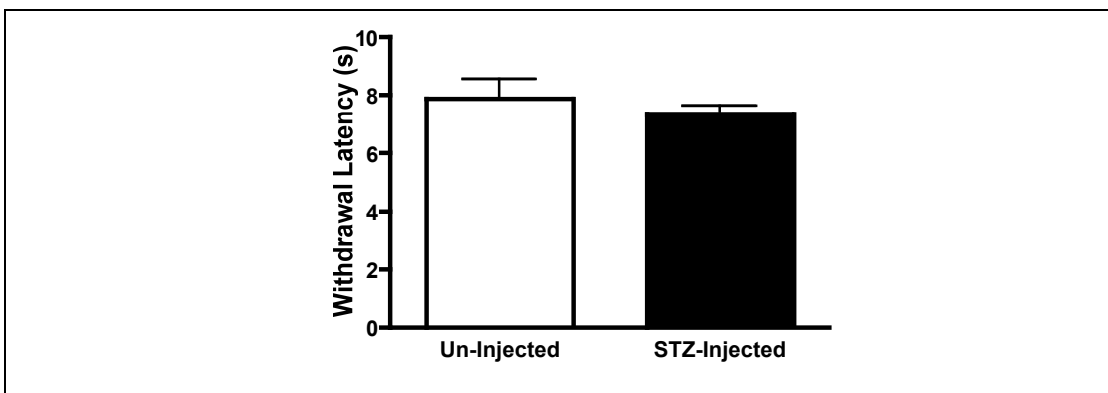


Figure 6.15. There were no significant changes in thermal withdrawal latency in the STZ-injected mice 54 hours post-injection. Data are presented as mean+SEM and were analyzed by an unpaired 2-tailed t-test.

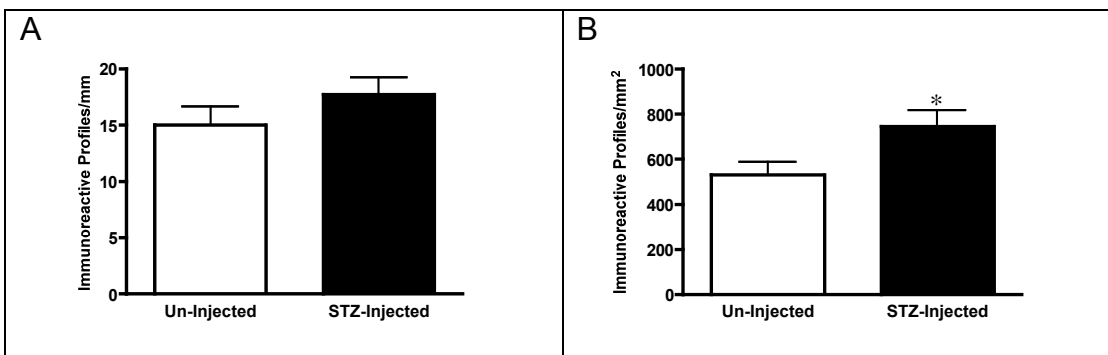


Figure 6.16. Immunoreactive IENF profile density was not significantly different in the STZ-injected mice when profile counts were normalized to epidermal length. However, the density was significantly increased in the STZ-injected group when profile counts were normalized to epidermal area. Data are presented as mean+SEM and were analyzed by an unpaired 2-tailed t-test, $p < 0.05$.



Figure 6.17. There were no significant differences in epidermal thickness between the un-injected mice and the STZ-injected mice, 54 hours post-injection. Data are presented as mean+SEM and were analyzed by an unpaired 2-tailed t-test.

6.3.4 Effects of direct insulin injections

There were no significant post-injection changes of thermal sensitivity in either the saline-treated or the insulin-treated mice, and this observation was true for both the injected and un-injected paws (Figure 6.18). There were also no significant changes in epidermal innervation between the insulin-injected mice and the saline-injected mice as measured using PGP9.5-immunoreactivity (Figure 6.19). Again, the lack of change was true for both the injected and un-injected paws of each group. Changes in epidermal thickness were also not observed (Figure 6.20). Although the GAP-43 antibody clearly identified immunoreactive IENF profiles (Figure 6.21A), no significant changes in GAP-43 immunoreactive nerve profile density were observed (Figure 6.21B).

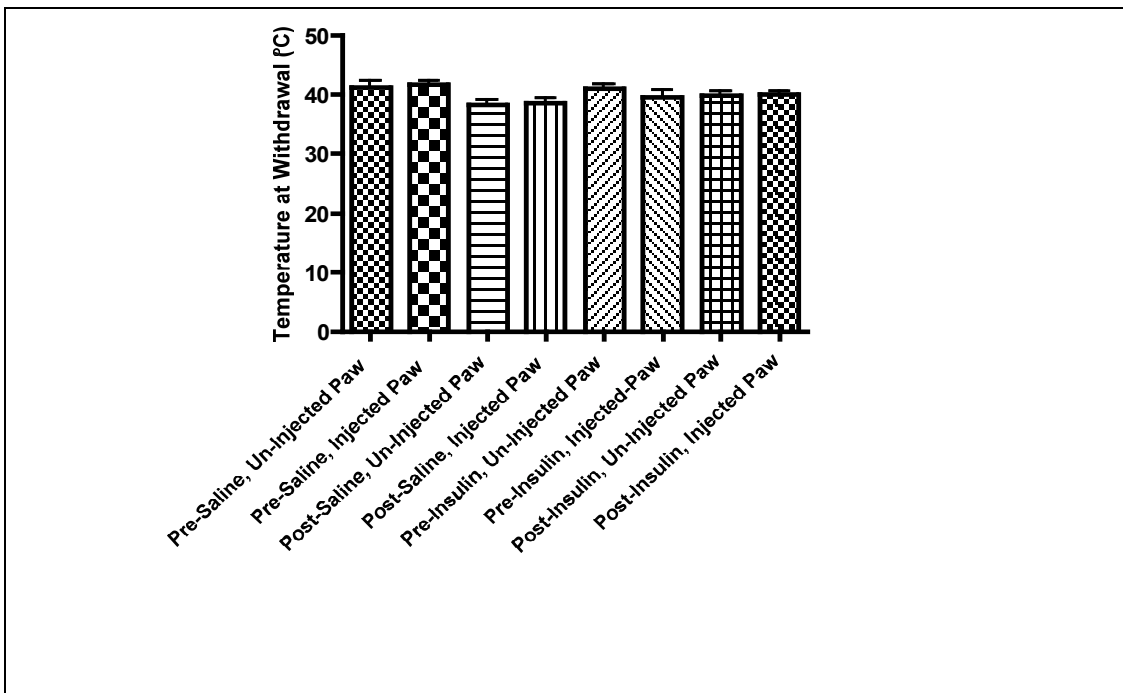


Figure 6.18. There were no significant differences in thermal sensitivity between any of the groups. Data are presented as mean+SEM and were analyzed by 1-way ANOVA, followed by SNK.

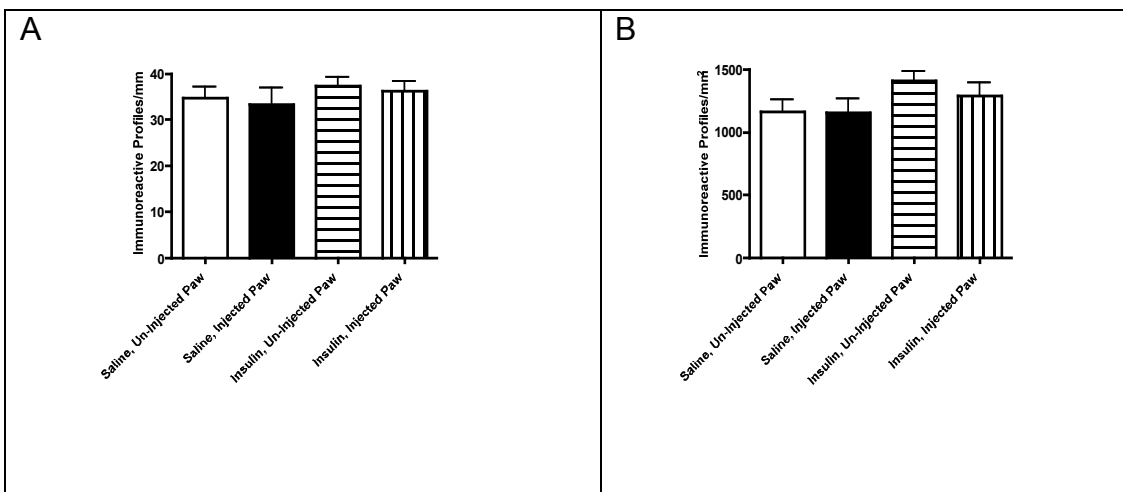


Figure 6.19. No significant differences in immunoreactive nerve profile density were observed between the insulin-injected and saline-injected mice when counts were normalized to either epidermal length (A) or epidermal area (B). Data are presented as mean+SEM and were analyzed by 1-way ANOVA, followed by SNK.

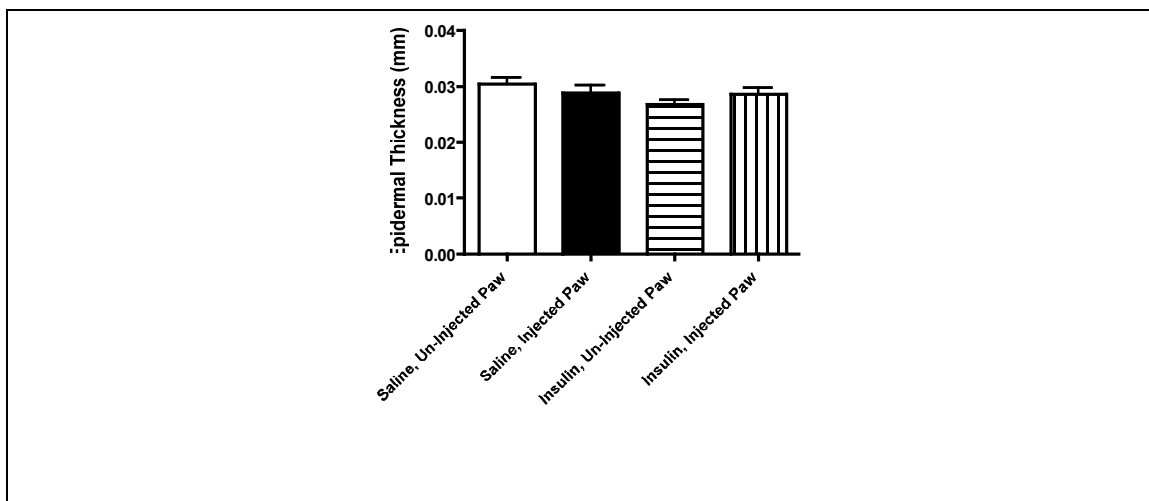


Figure 6.20. No significant differences in epidermal thickness were observed between the insulin-injected and saline-injected mice. Data are presented as mean+SEM and were analyzed by 1-way ANOVA, followed by SNK.

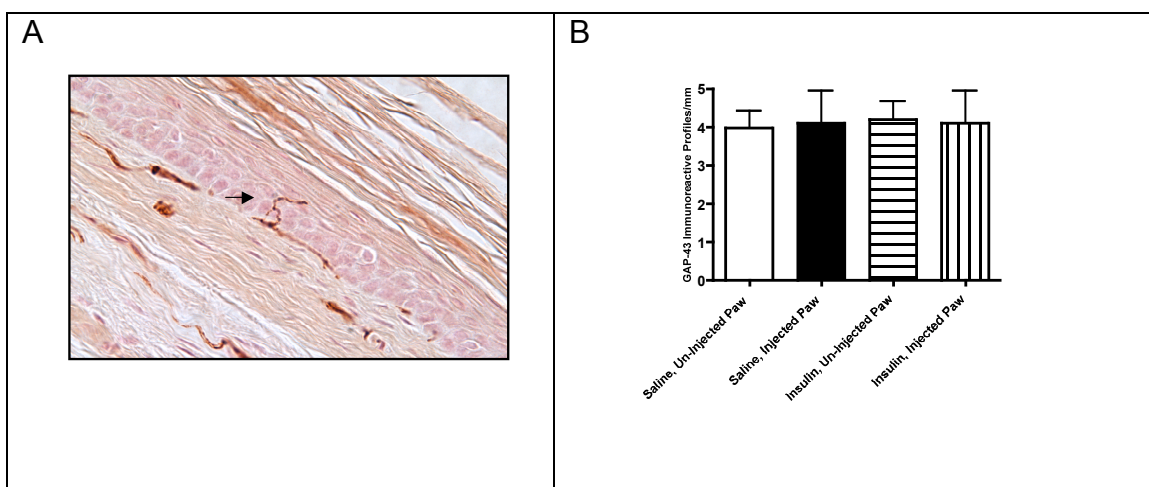


Figure 6.21. An GAP-43-immunoreactive IENF profile is identified with an arrow (A). There were no significant differences in GAP-43 immunoreactive IENF profile density between the insulin-injected and saline-injected mice. Data are presented as mean+SEM and were analyzed by 1-way ANOVA, followed by SNK.

6.4 Discussion

Our comparison of type 1 and type 2 diabetic mouse models demonstrated that both STZ-injected C57Bl/6 mice and db/db mice develop thermal hypoalgesia and reductions in epidermal innervation. We also observed

a decrease in the MNCVs of the db/db mice, and although we did not measure the MNCVs of our STZ-diabetic C57Bl/6 mice, reductions in MNCV velocity have previously been reported in STZ-diabetic mice of this strain (Obrosova et al., 2005). Together, these results indicate that neuropathy is present in both type 1 and type 2 mouse models of diabetes. Our observation of decreases in epidermal innervation in insulin-resistant type 2 mice agrees with reports published during my studies using leptin deficient db/db and ob/ob strains (Gibran et al., 2002; Drel et al., 2006). However, unlike these previous studies, we have demonstrated that the type 2 diabetic db/db mice develop a reduction in epidermal innervation, despite having insulin levels greatly exceeding those of the non-diabetic control mice. Our results, along with clinical studies reporting decreases in epidermal innervation in type 2 diabetic patients (Pittenger et al., 2004; Shun et al., 2004), appear to indicate that the presence of insulin per se does not play a protective role in the development of neuropathy in type 2 diabetic patients and mouse models. However, the observation of neuropathy in type 2 diabetic patients and mouse models does not necessarily negate a role for insulin in the maintenance of sensory neurons. Neurons may develop a resistance to insulin through mechanisms similar to those that cause insulin resistance in other cell types. Indeed, the PI3K signaling pathway through which insulin exerts its neurotrophic effects (Huang et al., 2005) is also involved in GLUT4 receptor translocation (Cheatham et al., 1994). A defect in the PI3K signaling pathway could contribute to the development of both hyperglycemia

and neuropathy. Further examination of insulin signaling in nerves from type 2 diabetic rodent models may shed additional light on this issue.

In our experiments examining the therapeutic effects of treatment with a single insulin pellet in STZ-diabetic Swiss Webster mice, the initial intention was to provide background levels of insulin, without altering hyperglycemia. Unfortunately, based on our HbA1C measurements, the amount of insulin released from a single pellet was enough to significantly lower glycated hemoglobin levels. By treating mice with either 3 or 5 insulin pellets, our intention was to normalize glycemic levels. Again, based on our HbA1C measurements, we were not completely successful. However, our experiments still provide valuable data on the effects of varied doses of insulin on several measures of diabetic neuropathy in Swiss Webster mice with STZ-diabetes for 4 or 8 weeks. The slight increase in MNCV and decrease in thermal withdrawal latency in the mice that were treated with a single pellet suggests that low doses of insulin are mildly efficacious after 4 weeks of diabetes. However, we were unable to determine whether the improvements were due to insulin's neurotrophic properties or its effect on blood glucose levels. The complete prevention of MNCV slowing and thermal hypoalgesia in the mice that received higher doses of insulin for 4 weeks, despite the persistence of hyperglycemia, suggests that insulin-deficiency, rather than hyperglycemia, may be the cause of these deficits.

When we examined the effects of 8 weeks of insulin treatment, both the low- and high-dose treatments were unable to prevent MNCV slowing. However,

the higher dose of insulin was still able to prevent the development of thermal hypoalgesia. Our results may indicate that different mechanisms are involved in the progression of these defects. Perhaps, although treatment with high doses of insulin prevents MNCV slowing during the early stages of diabetes, the effects of hyperglycemia overcome the therapeutic effects of insulin in later stages. Our observation of the prevention of thermal hypoalgesia, despite hyperglycemia, in the mice treated with higher doses of insulin for 8 weeks again indicates that insulin-deficiency may be a more prominent cause of this deficit.

Because no significant changes in immunoreactive IENF profile density were observed in the untreated diabetic mice, we were unable to assess the effects of varied doses of insulin on epidermal innervation after 4 and 8 weeks. These results further support the dissociation between thermal nociception and epidermal fiber loss discussed in chapter 4. Potential reasons for the variability in the timing of epidermal nerve fiber loss in STZ-diabetic mice will be further discussed in chapter 7. Our analysis of epidermal thickness indicates that insulin-deficiency may play a role in epidermal thinning after 4 weeks of diabetes. The greater effect of a single insulin pellet, compared to 3 insulin pellets, may indicate that there is an upper limit to the dose of insulin required to prevent epidermal thinning.

The purpose of our experiment examining the short-term effects of STZ injection was to assess the effects of systemic insulin release on thermal withdrawal latency and epidermal innervation. When STZ destroys the pancreatic beta cells, there is a release of insulin, which was confirmed in our

mice by the transient period of hypoglycemia that we observed 8 hours post-injection. We hypothesized that the burst of insulin released by the dying beta cells may induce sprouting of the epidermal nerves and could potentially result in transient thermal hyperalgesia prior to the onset of thermal hypoalgesia that we routinely measured after 4 and 8 weeks of diabetes. Our observation of an increase in PGP9.5-immunoreactive IENF profile density when immunoreactive nerve profile counts were normalized to epidermal area supports this hypothesis. However, when the immunoreactive IENF profile counts were normalized to epidermal length, the increase was not significant. The insignificant trend toward a decrease in epidermal thickness observed in the STZ-injected mice could account for the increase in epidermal nerve fiber density when immunoreactive nerve profile counts were normalized to epidermal area. The results of this experiment highlight the importance of normalizing immunoreactive IENF profile counts to both epidermal length and area. Although the release of insulin did not appear to have any effect on thermal withdrawal latency, the possibility remains that the excess insulin resulted in the sprouting of epidermal fibers that were not yet functional. Our data suggests the possibility that the STZ-induced systemic release of insulin has slight neurotrophic effects.

To further explore this possibility, we examined the effects of insulin injected directed into the paw. Our results showing no effect on either thermal withdrawal latency or epidermal innervation in mice injected with insulin again suggests a lack of neurotrophic properties. However, there are several other possibilities for why insulin appeared to have no effect that have to be

considered. We selected a dose of 0.1 insulin units because studies of the neurotrophic properties of insulin in diabetic rats that were published during my dissertation research reported this dose to be efficacious in the amelioration of nerve conduction velocity slowing and epidermal fiber loss when delivered to the spinal cord (Brussee et al., 2004; Toth et al., 2006). However, both of these studies involved continuous treatment, rather than a single injection. Another possible reason for the lack of neurotrophic effects observed when insulin was injected directly into the paw could be that the insulin may have to bind to receptors in the central terminals or DRG, rather than the peripheral nerve terminals, to be efficacious. The studies that reported therapeutic effects of low doses of insulin delivered the protein intrathecally (Brussee et al., 2004; Toth et al., 2006) and demonstrated that the insulin was binding to receptors found in the DRG (Brussee et al., 2004). It is quite possible that either the dose of insulin injected into the paw was too small, or that the binding of insulin to peripheral receptors was less effective.

Together, the results of these experiments indicate that although insulin may have neurotrophic properties, it does not appear to play a major role in the protection or sprouting of epidermal nerve fibers. Indeed, a study published during my dissertation research reporting protective effects of intrathecal insulin indicated that this approach was unable to completely restore epidermal innervation in STZ-diabetic rats (Toth et al., 2006). However, our results do indicate that insulin depletion may be involved in the early stages of MNCV slowing and in the development of thermal hypoalgesia.

The results of our studies examining the effects of low or high doses of insulin further highlight the dissociation between structural changes and functional deficits that was described in chapter 4. As in previous studies, an increase in thermal withdrawal latency was observed after both 4 and 8 weeks of diabetes. However, epidermal nerve fiber density was unchanged at both time points. As was discussed in chapter 4, this disconnect between structure and function could be due to early biochemical changes, including reduced receptor and neuropeptide expression, at either the distal or proximal regions of the sensory nerves.

7 – Discussion

7.1 Summary of Results

In light of the numerous reports of PGP-immunoreactive epidermal nerve fiber loss in skin biopsies from humans with diabetes (Kennedy et al, 1996; Pittenger et al., 2004; Shun et al., 2004), the first aims of this dissertation were to validate the use of antibodies against PGP9.5 in the quantification of epidermal innervation and to establish whether or not rodent models exhibit a similar fiber loss. We indeed confirmed that antibodies against PGP9.5 demonstrate similar immunoreactivity to antibodies against the structural protein HMW Tau, and therefore, a reduction in PGP9.5 immunoreactivity likely reflects a loss of epidermal innervation, rather than a downregulation of PGP9.5 content in otherwise intact fibers. We also demonstrated that streptozotocin(STZ)-diabetic rat models of the Wistar and Sprague-Dawley strains, as well as STZ-diabetic mouse models of the C57Bl/6 and Swiss Webster strains, also experience reductions in epidermal innervation and confirmed a previous report describing epidermal nerve fiber loss in type 2 diabetic db/db mice (Gibran et al., 2002). In addition to these results, we observed epidermal thinning the in STZ-diabetic rats and mice and epidermal thickening in type 2 diabetic db/db mice.

Given that the majority of the nerve fibers terminating in the epidermis are heat-sensitive C-fibers, the next series of experiments focused on examining the relationship between changes in heat sensitivity and loss of epidermal

innervation. After 2 weeks of diabetes, we observed a significant increase in thermal withdrawal latency. However, epidermal nerve fiber density was unchanged. Thermal hypoalgesia persisted after 4 weeks when a significant reduction in epidermal innervation was finally observed. These results indicate that early biochemical or physiological changes may contribute to the loss of thermal sensation before the C-fibers begin to retract. To further explore this issue, we examined epidermal and sub-epidermal substance P (SP)-immunoreactivity. Although there was no change in sub-epidermal SP-immunoreactivity, we observed a significant increase in epidermal SP-immunoreactivity, a possible indication of sprouting nerves. To further explore this possibility, we examined GAP-43 immunoreactivity and indeed observed an increase in GAP-43-immunoreactive epidermal nerve fibers. These results demonstrate that the thermal hypoalgesia observed after 2 weeks of diabetes is not due to distal changes in SP expression. To explore the possibility that changes in SP expression occurring more proximally could be involved in the loss of heat sensation, we measured SP content in the sciatic nerve. The decrease in sciatic nerve SP levels indicates that reductions in SP synthesis, transport or spinal release may contribute to the development of thermal hypoalgesia. Our observation of reduced cutaneous blood flow in mice that had been diabetic for 2 weeks identifies another factor that may contribute to the development of thermal hypoalgesia.

The next set of experiments were aimed at identifying potential mechanisms involved in the pathogenesis of diabetic neuropathy by examining

the effects of various therapeutics. Aldose reductase inhibition partially ameliorated motor nerve conduction velocity (MNCV) slowing, yet was unable to prevent thermal hypoalgesia. Neotrofin also had a partial effect on MNCV, but did not affect thermal withdrawal latency. Both CNTF and TX(14)A prevented increases in thermal withdrawal latency, indicating that loss of neurotrophic support may be involved in the development of thermal hypoalgesia. However, none of these compounds were able to reverse established deficits in MNCV or increases in thermal withdrawal latency.

The final set of experiments were aimed at examining the neurotrophic properties of insulin. First we compared mouse models of insulin-deficient type 1 diabetes and insulin-resistant type 2 diabetes. In addition to a similar loss of epidermal innervation, we observed an increase in thermal withdrawal latency in both models. Despite being hyperinsulinemic, the type 2 diabetic mice also developed significant MNCV slowing. These results indicate that insulin does not provide protection against the development of neuropathy in type 2 diabetic mice.

Next we examined the effects of varied doses of insulin after both 4 and 8 weeks of type 1 diabetes. High doses of insulin prevented both an increase in thermal withdrawal latency and MNCV slowing after 4 weeks. Lower doses of insulin had no effect on withdrawal latency, but partially ameliorated MNCV slowing. Both low and high doses of insulin prevented epidermal thinning. After 8 weeks, neither dose of insulin was able to prevent MNCV slowing, but the high dose of insulin prevented the development of thermal hypoalgesia.

Our next experiment assessed the impact of physiologic changes that occur immediately following injection of STZ, which include a release of insulin that results in a brief period of hypoglycemia before the progression to hyperglycemia. Three days after the injection of STZ, thermal withdrawal latency and linear immunoreactive IENF profile density were unaffected in STZ-injected mice. However, we did observe a significant increase in PGP9.5-immunoreactive IENF profile density when profile counts were normalized to epidermal area.

Lastly, we examined the effects of insulin injected directly into the paw. No changes in thermal withdrawal latency, immunoreactive IENF profile density or epidermal thickness were observed. To explore the possibility of nerve sprouting, we quantified GAP-43-immunoreactive nerve profiles and also observed no change.

7.2 Clinical and Experimental Relevance of Epidermal Nerve Fiber Assessment

When I began my dissertation research, the quantification of epidermal innervation in skin biopsies was being developed as a means of diagnosing and staging diabetic neuropathy, and as an outcome measure for clinical trials. Previous methods relied primarily on behavioral assessments, which can be highly subjective, or on electrophysiological studies, which only reflect the function of large nerve fibers. Sural nerve biopsy was the primary means of assessing structural changes. However, not only is this method highly invasive, it also does not allow for differentiation of autonomic and sensory nerve fibers.

The publication of several studies reporting a reduction in PGP9.5-immunoreactive IENFs identified the assessment of epidermal innervation in skin biopsies as practical means of evaluating peripheral small-fiber neuropathy (see table 7.1 for a summary). During the course of my research, more clinical studies were published, many examining the correlation between reductions in IENF density and other measures of diabetic neuropathy (Pittenger et al., 2004; Shun et al., 2004; Sorensen et al., 2006). However, questions still remain as to whether or not the evaluation of skin biopsies is the best way of diagnosing neuropathy in the clinical setting. Furthermore, whether or not rodents are the most appropriate choice for modeling diabetes-induced epidermal nerve fiber loss requires further consideration.

7.3 The Dissociation of Thermal Nociception and Epidermal Innervation: Clinical Implications

The assessment of epidermal innervation in skin biopsies initially showed promise as a diagnostic tool because IENF density was thought to be one of the earliest indicators of neuropathy (Lauria and Devigili, 2007) and was assumed to correlate with changes in heat pain sensitivity (Pittenger et al., 2004; Shun et al., 2004). However, based on our observations in mouse models, it appears that the retraction of epidermal nerve fibers is preceded by the loss of thermal sensitivity. If these results extend to humans, quantitative sensory testing, or more specifically the assessment of thermal sensitivity, may be able to identify diabetic neuropathy at an earlier stage. Given that therapeutics with the ability to reverse epidermal nerve fiber loss have not yet been identified, the ability to

diagnose small fiber neuropathy before reductions in IENF density are detectable could have implications for the successful treatment of diabetic neuropathy. It has recently been reported that when mice are fed a high fat diet for 16 weeks, their epidermal innervation remains intact. However, they develop thermal

Table 7.1. A comparison of cutaneous nerve fiber density assessment in various clinical and animal models of diabetes.

Species	Type	Duration	IENF Loss	SNP Loss	Source
Human	1	10-27 years	Yes	NA	Properzi et al., 1993; Kennedy et al., 1996; Boucek et al., 2005
Human	2	5-14 Years	Yes	NA	Lauria et al., 1998; Hirai et al., 2000; Shun et al., 2004; Pittenger et al., 2005
Human	Both	5-18 years	Yes	NA	Levy et al., 1989; Levy et al., 1992; Gibran et al., 2002; Pittenger et al., 2004; Koskinen et al., 2005; Polydefkis et al., 2004; Sorensen et al., 2006
Rhesus Monkey	2	8+ Years	Yes	NA	Pare et al., 2007
Rat (Sprague Dawley)	1	11-12 Weeks	Yes	NA	Bianchi et al., 2004; Leonelli et al., 2007; Roglio et al., 2007
Rat (Sprague-Dawley)	1	8 Weeks	Yes	No	Figure 3.3
Rat (Wistar)	1	8 Weeks	Yes	No	Figure 3.3
Mouse (ob/ob)	2	11 Weeks of Age (Duration of hyperglycemia not specified)	Yes	NA	Drel et al., 2006; Vareniuk et al., 2007
Mouse (db/db)	2	Not Specified	Yes	NA	Underwood et al., 2001; Gibran et al., 2002
Mouse (db/db)	2	41 days	Yes	No	Figure 3.5
Mouse (C57Bl6/J)	1	6 weeks	Yes	NA	Drel et al., 2007
Mouse (C57Bl/6)	1	4 weeks	Yes	No	Figure 3.5
Mouse (Swiss Webster)	1	4 weeks	Yes	No	Figure 3.5

hypoalgesia that can be reversed if mice are returned to a normal diet (Obrosova et al., 2007). Again, if these results can be extended to humans, pre-diabetic patients may show early changes in heat sensation that precede reductions in IENF density, and these sensory deficits may be reversible through lifestyle intervention. In a clinical study, lifestyle intervention was associated with a slight increase IENF density in pre-diabetic patients, but once fiber loss had extended to the sub-epidermal nerve plexus, epidermal reinnervation was unlikely (Smith et al., 2006). These results further highlight the importance of detecting nerve fiber degeneration at the earliest stages. In the very early detection of small fiber loss, corneal confocal microscopy, which involves the non-invasive monitoring of corneal nerve fibers, may prove to be a more suitable alternative. Indeed, in a recent study comparing corneal nerve fiber quantification to IENF quantification, corneal confocal microscopy was able to detect nerve damage at earlier stages (Quattrini et al., 2007).

It may be possible to improve the sensitivity of skin biopsy assessment by making a distinction between peptidergic and non-peptidergic fibers. A recent study suggests that peptidergic innervation may be preferentially affected by diabetes (Johnson et al., 2007b). As was mentioned in chapter 4, it is possible that early reductions in the peptidergic population are subsumed by the total innervation. Although we did not detect a reduction in SP-immunoreactive IENF density after 2 weeks of STZ-induced diabetes, but rather observed signs of sprouting, the sprouting may have been an early response to fiber damage that is

soon followed by degeneration. Hence, peptidergic fibers would be the first to degenerate, and focusing on quantifying these fibers could potentially detect diabetic neuropathy sooner.

Our observed disconnect between structure and function also has implications for the use of epidermal nerve fiber assessment as a measure of efficacy for clinical trials. The ability of a potential therapeutic to prevent reductions in PGP9.5-immunoreactive IENF density does not necessarily mean that the therapeutic can preserve sensory function. If early biochemical changes, such as the reduction in sciatic nerve SP levels observed in our STZ-diabetic mice, are not targeted, patients may be left with structurally intact, yet non-functional, epidermal C-fibers. Although their IENF densities would be within normal range, they could still experience sensory loss and be susceptible to trauma and infection. However, there are several areas in which the assessment of skin biopsies is still advantageous over quantitative sensory testing.

Quantitative sensory testing relies on the subjective response of the patient, and can thus be complicated by patients who are either consciously or unconsciously biased toward demonstrating abnormality (Dyck et al., 1998). The size of the probe used can also affect results (Khalili et al., 2001), making it difficult to compare data collected at multiple sites. The evaluation of skin biopsies, on the other hand, is relatively unbiased, and with the publication of standardized guidelines for processing and quantification (Lauria et al., 2005b), comparisons can be drawn between skin biopsies obtained at various sites. An

ideally designed clinical trial would include both behavioral and structural assessments.

7.4 The Utility of Mouse Models in the Study of Epidermal Nerve Fiber Loss

Although one of the initial aims of this dissertation was to examine the pathogenesis of epidermal nerve fiber loss in rodent models of diabetes, in several of our later studies, we observed no change in epidermal nerve fiber density. From these studies, we were able to identify a dissociation between structural and functional changes, as was discussed in chapter 4. However, without a loss of epidermal innervation in our diabetic mice, we were unable to examine the mechanisms of fiber loss and assess the efficacy of various therapeutic agents. In order for STZ-diabetic Swiss Webster mice to be a suitable model for the evaluation of therapeutics, the ability to accurately predict the timing of epidermal nerve fiber degeneration is necessary. Without an accurate time frame, suitable endpoints for studies are difficult to identify. Therefore, we retrospectively examined several of our studies in hopes of identifying factors that would predict epidermal fiber loss.

Body weight can be considered an indicator of the severity of diabetes, and therefore, seemed to be a likely indicator of IENF loss. However, although the mean body weight of the diabetic mice from some of the studies where we did not observe fiber loss was higher than that of the diabetic mice from the studies where we did observe fiber loss, this was not true in every case. When we compared final body weight of the diabetic mice expressed as a percentage

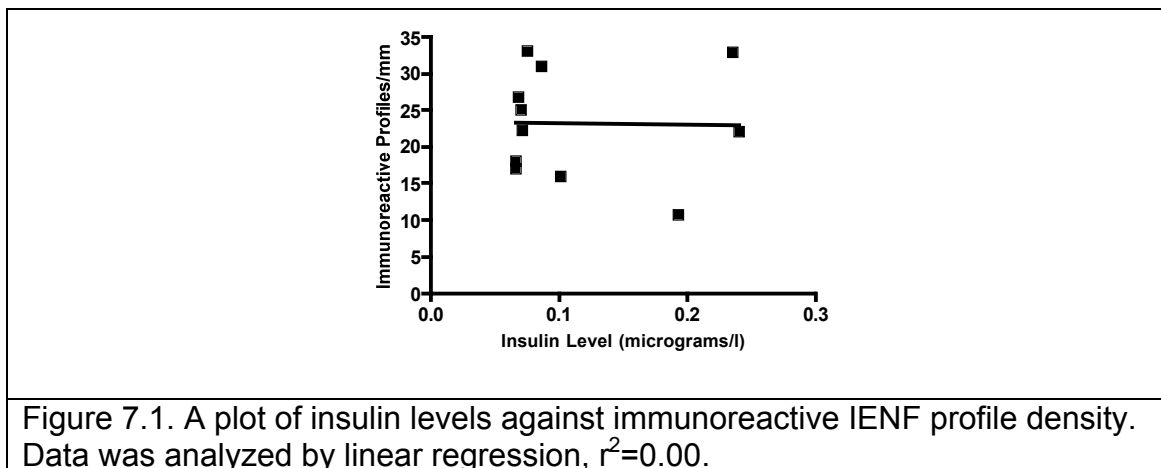
of the mean body weight of the control mice, again a clear pattern did not emerge. A comparison of the total amount of weight lost by the diabetic mice from each study also failed to predict which mice developed fiber loss (see Table 7.2). It appears as though change in body weight alone is not enough to predict the onset of epidermal C-fiber retraction.

Table 7.2. A comparison of final body weight and total change in body weight of untreated diabetic Swiss Webster mice from the experiments described in this thesis.				
N	Duration of Diabetes (weeks)	IENF Loss	Final Body Weight (g) (% of Control Body Weight)	Change in Body Weight (g)
8	4	Yes	23.2 (73.3%)	4.0
11	4	No	30.6 (84.6%)	4.2
11	4	No	22.9 (72.2%)	2.0
8	4	No	25.6 (78.8%)	6.8
10	8	No	27.0 (82.7%)	0.4

We hypothesized that the variability in severity of diabetes in our mice could be due to variation in the extent to which the STZ injection was able to eliminate insulin-producing beta cells. We considered the possibility that, due to incomplete destruction of beta cells, some injected mice may have continued to produce low levels of residual insulin. These levels may have been too low to affect blood glucose levels, yet may still have been high enough to provide a measure of protection against epidermal nerve fiber loss. Indeed, the epidermal

nerve fibers of STZ-diabetic rats are protected by insulin, delivered intrathecally, at doses too low to affect blood glucose levels (Toth et al., 2006).

To address this issue, we attempted to measure insulin levels in our mice using an ultrasensitive insulin ELISA kit (Merckodia, Winston Salem, NC) with a lower detection limit of 0.025 $\mu\text{g/l}$. The diabetic mice from a study where we observed significant fiber loss all had insulin levels below the limit of detection. However, 61% of the diabetic mice from a study in which we did not observe epidermal fiber loss had detectable levels of insulin, although the levels were still quite low and did not correlate with epidermal nerve fiber density (Figure 7.1). These results are far from conclusive, yet they do hint at the involvement of insulin in the preservation of epidermal innervation.



Although measuring insulin levels in STZ-diabetic mice could provide an explanation as to why certain mice are protected against fiber loss, the amount of blood required for the assay makes it impossible to complete without sacrificing the animal. Until more sensitive assays are developed, residual insulin levels cannot be routinely determined in live STZ-diabetic mice and therefore, this is not

a suitable means of determining whether or not mice will have developed fiber loss prior to the conclusion of a study. Given the difficulty of accurately predicting when fiber loss will develop in STZ-diabetic Swiss Webster mice, perhaps alternative models would be more appropriate for examining epidermal nerve fiber degeneration. An ideal model would allow for continuous assessment of IENF density, rather than a single endpoint measurement.

Because the removal of skin is relatively non-invasive, small biopsies could be taken from mice at multiple timepoints. However, due to the small surface area of the mouse footpad, removal of skin from this area would complicate behavioral testing. Instead, biopsies would have to be taken from the hairy skin on the back. This alternative is not ideal given the evidence presented in chapter 3 that epidermal nerves retract in a length dependent manner. Hence, biopsies from the most distal regions, such as the footpad, would be the first to show IENF loss. Also, footpad skin is necessary for an accurate correlation of changes in epidermal nerve fiber density and changes in paw thermal withdrawal latency.

Thy1-YFP mice, which express a fluorescent protein in their neurons that allows for noninvasive monitoring of cutaneous innervation, would appear to be a logical choice for continuous monitoring of diabetes-induced IENF loss (Chen et al., 2005). However, only the innervation of hairy skin can be quantified in these mice because the thickness of footpad skin blurs the fibers, making them difficult to count. Again, hairy skin on more proximal regions of the body would be slower

to develop reductions in epidermal innervation and the correlation of footpad IENF densities with paw withdrawal latencies would not be possible.

The use of a larger species could allow for repeated removal of skin biopsies. Although diabetic rats develop fiber loss and have a larger footpad, there is still insufficient surface area for repeated sampling. However, this issue may be overcome through the use of feline models. Indeed, recent evidence suggests that cats model many of the structural changes observed in humans with diabetic neuropathy (Mizisin et al., 2007). Although changes in epidermal innervation have not yet been reported in cats with diabetes, both thermal hypoalgesia and reductions in IENF density have been reported in feline models of HIV neuropathy (Kennedy et al., 2004). However, the onset of diabetes is difficult to control in spontaneously diabetic cats, and large treatment groups may be difficult to assemble. Although STZ-diabetic mice may not be ideal for the study of epidermal nerve fiber loss, alternative models have drawbacks as well. Future studies should focus on identifying factors that may be predictive of epidermal fiber loss in mice, so that the timing of C-fiber degeneration can be better understood.

7.5 Implications of epidermal thinning

Our observation of a thinning of the 3 bottommost layers of the epidermis in rodent models of diabetes is novel, and the role that skin thinning may play in sensory loss requires consideration. As noted in chapter 4, keratinocytes may play a role in heat sensation. Indeed, the skin has recently been described as the largest sensory organ in the body (Zhao et al., 2008). In addition to expressing

multiple heat-sensitive receptors (Denda et al., 2001; Peier et al., 2002; Chung et al., 2003), epidermal keratinocytes also release several substances involved in modulating sensation, including pro-nociceptive endothelin-1 (Gokin et al., 2001), anti-nociceptive β -endorphin (Khodorova et al., 2003) and ATP (Koizumi et al., 2004). Furthermore, keratinocytes express voltage-gated sodium channels (Zhao et al., 2008), which are thought to be involved in the pathogenesis of pain (Waxman et al., 1999). Given the ample evidence of the contribution of keratinocytes to pain sensation, a reduction in keratinocyte number and the consequent thinning of the epidermis may contribute to the development of thermal hypoalgesia. This hypothesis could seemingly be negated by our observation of thermal hypoalgesia, despite epidermal thickening, in the db/db mice. However, because the C-fibers of the db/db mice had already begun to retract, the connections between the nerve endings and the keratinocytes may have already been disrupted, rendering the fibers less sensitive to heat. To address this issue, future studies should focus on the contribution of keratinocytes to heat sensation. CD44 knockout mice show significant epidermal thinning (Bourguignon et al., 2006), and given that the CD44 protein is associated with rapidly dividing cells (Underhill, 1992), one would not expect the knockout to greatly affect nerve fibers. After first confirming that IENF density is unaffected, an analysis of thermal withdrawal latency in these knockout mice may help to clarify the role that epidermal thinning plays in the loss of heat sensitivity.

Another potential way that the apparent epidermal thinning observed in our mice could contribute to the loss of heat sensation involves changes in the stratum corneum. Because this outermost layer tends to separate during tissue processing, we were not able to examine the effects of diabetes on this layer. It is possible that the epidermal thinning we observed may not have actually been a thinning of the entire epidermis. Disruption of keratinocyte turnover could have resulted in both the thinning of the lower layers, which we were able to quantify, and a consequent thickening of the stratum corneum. Given that even the most distal nerve endings terminate in the stratum granulosum (Navarro et al., 1995), a thickening of the stratum corneum could create a barrier between the heat stimulus and the C-fiber terminal, resulting in a loss of heat sensitivity. Total epidermal thickness, including the stratum corneum, can be assessed in vivo using either confocal microscopy or ultrasound (Nouveau-Richard et al., 2004). Future studies should be focused on determining whether or not the thickness of the stratum corneum is altered by diabetes.

7.6 Mechanisms of Thermal Hypoalgesia and Epidermal Nerve Fiber Loss

While multiple pathogenic pathways have been implicated in the development of diabetic neuropathy, the specific mechanisms of loss of thermal sensation and epidermal innervation remain unclear. In this dissertation, we sought to increase our understanding of the mechanisms involved in these deficits by examining the effects of various therapeutics designed to target proposed pathogenic pathways. The inability of an aldose reductase inhibitor and an NGF-enhancing substance to prevent the development of thermal

hypoalgesia could be interpreted as evidence that increased flux through the polyol pathway and loss of neurotrophic support do not contribute to this deficit.

However, as was

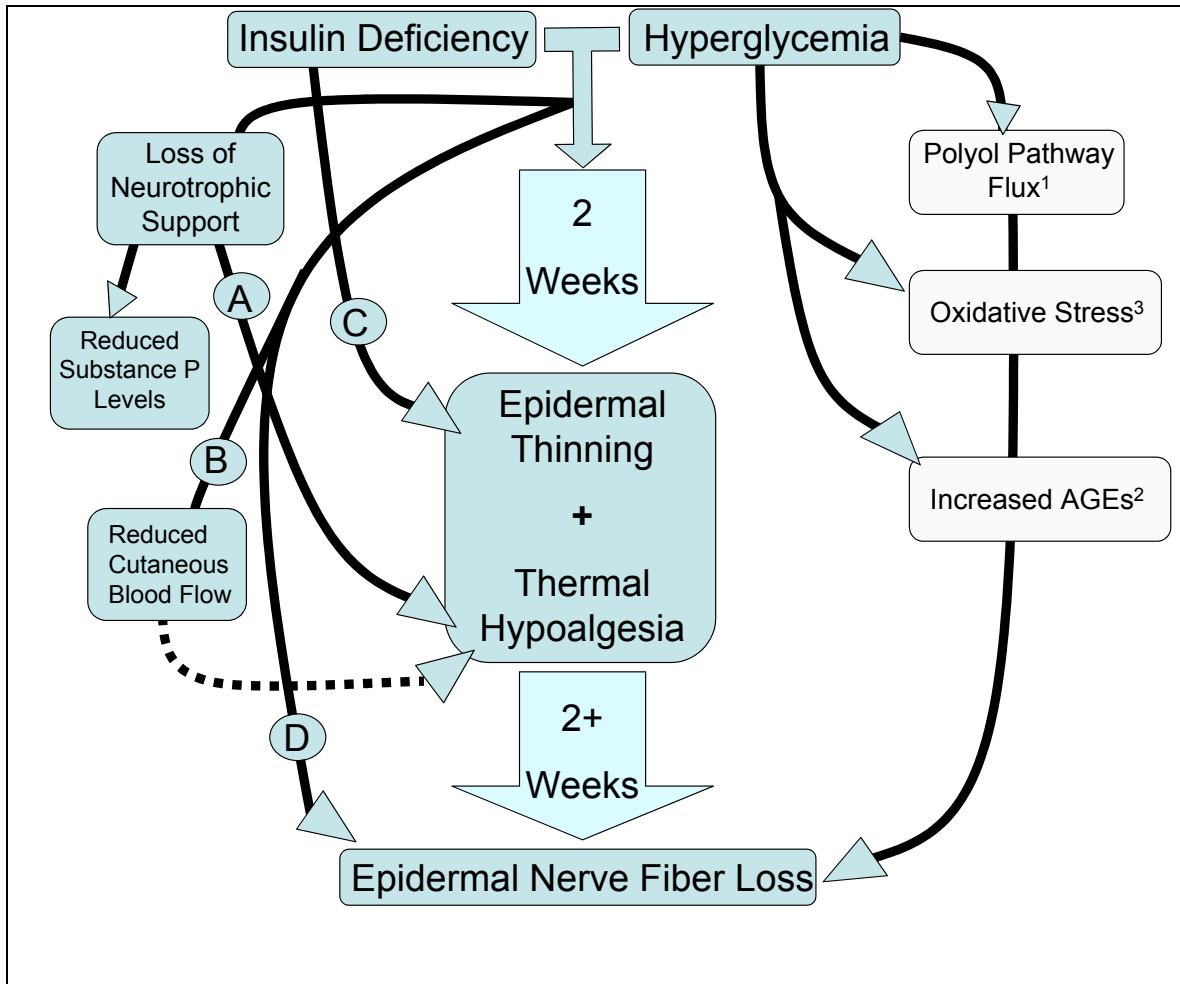


Figure 7.2. A schematic depicting the major findings of this dissertation. Dotted lines represent proposed hypotheses.

A- See experiments described in chapter 5

B- See experiments described in chapter 4

C,D- See experiments described in chapter 3

¹Drel et al., 2006

²Toth et al., 2008

³Drel et al., 2007; Vareniuk et al., 2007

discussed in chapter 5, dosing issues may be responsible for the lack of efficacy.

Aldose reductase inhibitors and both Neotrofin and NGF have shown efficacy in

other rodent models of diabetes (Apfel et al., 1994; Diemel et al. 1994; Calcutt et al., 2004; Calcutt et al., 2006; Drel et al., 2006). Our observation of the prevention of thermal hypoalgesia by treatment with CNTF and TX14(A) suggests that loss of neurotrophic support may indeed play a role in the loss of thermal sensation. This conclusion is further supported by the ability of insulin to prevent thermal hypoalgesia without normalizing blood glucose levels. Given the relationship between neurotrophic factors and neuropeptide levels (Diemel et al., 1994; Fernyhough et al., 1994) and the involvement of SP in pain transmission (Mantyh et al., 1997; Cao et al., 1998; Laneuville et al., 1998; Nichols et al., 1999; Vierck et al., 2003), loss of neurotrophic support may be contributing to the development of thermal hypoalgesia through downregulation of SP.

As was discussed previously, given that the untreated diabetic mice in many of our studies examining therapeutics did not develop epidermal nerve fiber loss, we were unable to draw conclusions about the potential pathogenic mechanisms. However, during the course of my research, studies have been published implicating polyol pathway flux (Drel et al., 2006), oxidative/nitrosative stress (Vareniuk et al., 2007; Drel et al., 2007) and non-enzymatic glycosylation (Toth et al., 2008) in the development of both thermal hypoalgesia and epidermal nerve fiber loss. Most likely, a combination of mechanisms contributes to these deficits and ideal treatments may need to target several pathways.

Our observation of a reduction in cutaneous blood flow in mice that had been diabetic for 2 weeks identifies another diabetes-induced physiological deficit that may contribute to loss of thermal sensation and C-fiber degeneration.

Although the epidermis may be able to meet some of its oxygen needs through diffusion from the atmosphere (Stucker et al., 2002), epidermal cells are still dependent on their dermal blood supply for removal of waste. Therefore, a shunting of blood away from the dermal capillaries may contribute to the degeneration of epidermal C-fibers. The observation of aldose reductase within the axons of the perivascular sympathetic nerves points to a potential mechanism of reduced cutaneous blood flow (Jiang et al., 2006). The accumulation of polyols could disrupt the function of these sympathetic nerves, resulting in reduced constriction of the arteriovenous shunt and subsequent diversion of blood from the dermal capillaries. Future studies should examine the effects of aldose reductase inhibition on dermal blood flow and explore how the potential correction of blood flow deficits may relate to thermal withdrawal latency and epidermal nerve fiber density.

The results of our studies examining the effects of various therapeutics also highlight the differences between small and large fiber neuropathy. In many of our studies, nerve conduction velocity, which is a reflection of large fiber function, was assessed as a measure of efficacy. The aldose reductase inhibitor IDD 676 partially ameliorated nerve conduction velocity slowing without affecting thermal withdrawal latency, suggesting that large fibers may be more vulnerable to the effects of polyol pathway flux. Furthermore, the results of our study examining the effects of varied doses of insulin found that high doses lessened nerve conduction velocity slowing after 4 weeks of diabetes. However, this therapeutic effect was lost after 8 weeks. These results suggest that at early

stages, insulin is able to counteract the effects of hyperglycemia on large fibers. However, eventually other hyperglycemia-related defects, such as the buildup of polyols or free radicals, may overcome the neurotrophic effects of insulin, resulting in nerve conduction velocity slowing. Given that thermal hypoalgesia was still prevented by insulin after 8 weeks of diabetes, our results indicate the small and large fibers may have different levels of vulnerability to various pathogenic mechanisms. Indeed, others have demonstrated that treatment with a peroxynitrite decomposition catalyst completely prevents motor nerve conduction velocity slowing, while only partially ameliorating thermal hypoalgesia (Drel et al., 2007).

7.7 Final Conclusions

The experiments described in this dissertation have characterized rats and mice as a model of diabetes-induced epidermal nerve fiber loss and identified the novel structural change of epidermal thinning. We have also identified a separation between loss of thermal nociception and reductions in epidermal nerve fiber density. These results confirm the importance of epidermal nerve fiber assessment in the study of diabetic neuropathy, but also caution against assuming that behavioral deficits are always accompanied by structural changes.

References

- Akinna SK, Patterson CL, Wright DE (2001) GDNF rescues nonpeptidergic unmyelinated primary afferents in streptozotocin-treated diabetic mice. *Exp Neurol* 167:173-182.
- Anand P, Terenghi G, Warner G, Kopelman P, Williams-Chestnut RE, Sinicropi DV (1996) The role of endogenous nerve growth factor in human diabetic neuropathy. *Nat Med* 2(6):703-7.
- Apfel SC, Arezzo JC, Brownlee M, Federoff H, and Kessler JA (1994) Nerve growth factor administration protects against experimental diabetic sensory neuropathy. *Brain Res* 634:7-12.
- Apfel SC, Schwartz S, Adornato BT, Freeman R, Biton V, Rendell M, Vinik A, Giuliani M, Stevens JC, Barbano R, Dyck PJ (2000) Efficacy and safety of recombinant human nerve growth factor in patients with diabetic polyneuropathy: A randomized controlled trial. rhNGF Clinical Investigator Group. *JAMA* 284(17):2215-21.
- Archer AG, Roberts VC, Watkins PJ (1984) Blood flow patterns in painful diabetic neuropathy. *Diabetologia* 27(6):563-7.
- Bianchi R, Buyukakilli B, Brines M, Savino C, Cavaletti G, Oggioni N, Lauria G, Borgna M, Lombardi R, Cimen B, Comelekoglu U, Kanik A, Tatarolgu C, Cerami A, and Ghezzi P. (2004) Erythropoietin both protects from and reverses experimental diabetic neuropathy. *PNAS* 101:823-828.
- Birder LA, Perl ER (1994) Cutaneous sensory receptors. *J Clin Neurophysiol* 11(6):534-52.
- Bjorklund H, Dalsgaard CJ, Jonsson CE, Hermansson A (1986) Sensory and autonomic innervation of non-hairy and hairy human skin. An immunohistochemical study. *Cell Tissue Res* 243:51-7.
- Boucek P, Havrdova T, Voska L, Lodererova A, Saudek F, Lipar K, Janousek L, Adamec M, Sommer C (2005) Severe depletion of intraepidermal nerve fibers in skin biopsies of pancreas transplant recipients. *Transplant Proc* 37:3574-5.
- Boulton AJ, Scarpello JH, Ward JD (1982) Venous oxygenation in the diabetic neuropathic foot: evidence of arteriovenous shunting? *Diabetologia* 22:6-8.
- Bourguignon LY, Ramez M, Gilad E, Singleton PA, Man MQ, Crumrine DA, Elias PM, Feingold KR (2006) Hyaluronan-CD44 interaction stimulates keratinocyte

differentiation, lamellar body formation/secretion, and permeability barrier homeostasis. *J Invest Dermatol* 126(6):1356-65.

Brownlee M. Biochemistry and molecular cell biology of diabetic complications (2001) *Nature* 414:813-820.

Brussee V, Cunningham A, Zochodne DW (2004) Direct insulin signaling of neurons reverses diabetic neuropathy. *Diabetes* 53:1824-30.

Butler R, Morris AD, Belch JJ, Hill A, Struthers AD (2000) Allopurinol normalized endothelial dysfunction in type 2 diabetics with mild hypertension. *Hypertension* 35:746-51.

Calcutt NA, Willars GB, Tomlinson DR (1988) Statil-sensitive polyol formation in nerve of galactose-fed mice. *Metabolism* 37(5):450-53.

Calcutt NA, Muir DF, Powell HC, and Mizisin AP (1992) Reduced ciliary neurotrophic factor-like activity in nerves from diabetic or galactose-fed rats. *Brain Res* 575:320-24.

Calcutt NA, Mizisin AP, Kalichman MW (1994) Aldose reductase inhibition, Doppler flux and conduction in diabetic rat nerve. *Eur J Pharmacol* 251(1):27-33.

Calcutt NA, Malmberg AB, Yamamoto T, Yaksh TL (1994b) Tolrestat treatment prevents modification of the formalin test model of prolonged pain in hyperglycemic rats. *Pain* 58(3):413-20.

Calcutt NA, Li L, Yaksh TL, Malmberg AB (1995) Different effects of two aldose reductase inhibitors on nociception and prostaglandin E. *Eur J Pharmacol* 285(2):189-97.

Calcutt NA, Jorge MC, Yaksh TL, Chaplan SR (1996) Tactile allodynia and formalin hyperalgesia in streptozotocin-diabetic rats: effects of insulin, aldose reductase inhibition and lidocaine.

Calcutt NA, Campana WM, Eskeland NL, Mohiuddin L, Dines KC, Mizisin AP, O'Brien JS (1999) Prosaposin gene expression and the efficacy of a prosaposin-derived peptide in preventing structural and functional disorders of peripheral nerve in diabetic rats. *J Neuropath Exp Neurol* 58:628-636.

Calcutt NA, Stiller C, Gustafsson H, Malmberg AB (2000a) Elevated substance-P-like immunoreactivity levels in spinal dialysates during the formalin test in normal and diabetic rats. *Brain Res* 856(1-2):20-7.

Calcutt NA, Freshwater JD, O'Brien JS (2000b) Protection of sensory function and antihyperalgesic properties of a prosaposin-derived peptide in diabetic rats. *Anesthesiology* 93(5):1271-8.

Calcutt NA, Freshwater JD, and Mizisin AP (2004) Prevention of sensory disorders in diabetic Sprague-Dawley rats by aldose reductase inhibition or treatment with ciliary neurotrophic factor. *Diabetologia* 47(4):71824.

Calcutt NA, Freshwater JD, Hauptmann N, Taylor EM, Mizisin AP (2006) Protection of sensory function in diabetic rats by Neotrofin. *Eur J Pharmacol* 534:197-193.

Cameron NE, Cotter MA, Maxfield EK (1993) Anti-oxidant treatment prevents the development of peripheral nerve dysfunction in streptozotocin-diabetic rats. *Diabetologia* 36(4):299-304.

Cameron NE, Cotter MA, Archibald V, Dines KC, and Maxfield EK (1994) Anti-oxidant and pro-oxidant effects on nerve conduction velocity, endoneurial blood flow and oxygen tension in non-diabetic and streptozotocin-diabetic rats. *Diabetologia* 37:449-459.

Cameron NE, Cotter MA (1996) Interaction between oxidative stress and gamma-linolenic acid in impaired neurovascular function in diabetic rats. *Am J Physiol* 271(3 Pt 1):E471-6.

Cameron NE, Tuck Z, McCabe L, Cotter MA (2001) Effect of the hydroxyl radical scavenger, dimethylthiourea, on peripheral nerve tissue perfusion, conduction velocity and nociception in experimental diabetes. *Diabetologia* 44(9):1161-9.

Cao YQ, Mantyh PW, Carlson EJ, Gillespie AM, Epstein CJ, Basbaum AI (1998) Primary afferent tachykinins are required to experience moderate to intense pain. *Nature* 392(6674):390-94.

Carr ME (2001) Diabetes mellitus: a hypercoagulable state. *J Diabetes Complications* 15(1):44-54.

Casselli A, Rich J, Hanane T, Uccioli L, Veves A (2003) Role of C-nociceptive fibers in the nerve axon reflex-related vasodilation in diabetes. *Neurology* 60:297-300.

Caterina MJ, Schumacher MA, Tominaga M, Rosen TA, Levine JD, Julius D (1997) The capsaicin receptor: a heat-activated ion channel in the pain pathway. *Nature* 389:816-24.

Chaplan SR, Bach FW, Pogrel JW, Chung JM, Yaksh TL. (1994) Quantitative assessment of tactile allodynia in the rat paw. *J Neurosci Meth* 53:55-63.

Chateau Y, Misery L (2004) Connections between nerve endings and epidermal cells: are they synapses? *Exp Dermatol* 13(1):2-4.

Chattopadhyay M, Krisky K, Wolfe D, Glorioso JC, Mata M, Fink DJ (2005) HSV-mediated gene transfer of vascular endothelial growth factor to dorsal root ganglia prevents diabetic neuropathy. *Gene Therapy* 12:1377-1384.

Chattopadhyay M, Mata M, Goss J, Wolfe D, Huang S, Glorioso JC, Fink DJ (2007) Prolonged preservation of nerve function in diabetic neuropathy in mice by herpes simplex virus-mediated gene transfer. *Diabetologia* 50:1550-8.

Cheatham B, Vlahos CJ, Cheatham L, Wang L, Blenis J, Kahn CR (1994) Phosphatidylinositol 3-kinase activation is required for insulin stimulation of pp70 S6 kinase, DNA synthesis, and glucose transporter translocation. *Mol Cell Biol* 14(7):4902-11.

Chen H, Charlat O, Tartaglia LA, Woolf EA, Weng X, Ellis SJ, Lakey ND, Culpepper J, Moore KJ, Breitbart RE, Duyk GM, Tepper RI, Morgenstern JP. (1996) Evidence that the diabetes gene encodes the leptin receptor: identification of a mutation in the leptin receptor gene in db/db mice. *Cell* 84(3):491-5.

Chen YS, Chung SSM, Chung SK (2005) Noninvasive monitoring of diabetes-induced cutaneous nerve fiber loss and hypoalgesia in *thy1-YFP* transgenic mice. *Diabetes* 54:3112-3118.

Chiang HY, Huang IT, Chen WP, Chien HF, Shun CT, Chang YC, Hsieh ST (1998) Regional difference in epidermal thinning after skin denervation. *Exp Neurol* 154(1):137-45.

Christianson JA, Riekhof JT, Wright DE (2003) Restorative effects of neurotrophin treatment on diabetes-induced cutaneous axon loss in mice. *Exp Neurol* 179:188-199.

Christianson JA, Ryals JM, McCarson KE, Wright DE (2003b) Beneficial actions of neurotrophin treatment on diabetes-induced hypoalgesia in mice. *J Pain* 4(9):493-504.

Christianson JA, Ryals JM, Johnson MS, Dobrowsky RT, Wright DE (2007) Neurotrophic modulation of myelinated cutaneous innervation and mechanical sensory loss in diabetic mice. *Neuroscience* 145(1):303-13.

Chung MK, Lee H, Caterina MJ (2003) Warm temperatures activate TRPV4 in mouse 308 keratinocytes. *J Biol Chem* 278(34):32037-32046.

Chung SSM, Ho ECM, Lam KSL, Chung SK (2003) Contribution of polyol pathway to diabetes-induced oxidative stress. *J Am Soc Nephrol* 14:S233-S236.

Conti AM, Fischer SJ, Windebank AJ (1997) Inhibition of axonal growth from sensory neurons by excess nerve growth factor. *Ann Neurol* 42(6):838-46.

Cotter MA, Cameron NE (1995) Neuroprotective effects of carvedilol in diabetic rats: prevention of defective peripheral nerve perfusion and conduction velocity. *Naunyn Schmiedebergs Arch Pharmacol* 351(6):630-5.

Cotter MA, Cameron NE, Hohman TC (1998) Correction of nerve conduction and endoneurial blood flow deficits by the aldose reductase inhibitor, tolrestat, in diabetic rats. *J Peripher Nerv Syst* 3(3):217-23.

Daalsgard CJ, Rydh M, Haegerstrand A (1989) Cutaneous innervation in man visualized with protein gene product 9.5 (PGP9.5) antibodies. *Histochemistry* 92:385-9.

Davar G, Waikar S, Eisenberg E, Hattori M, Thalhammer JG (1995) Behavioral evidence of thermal hyperalgesia in non-obese diabetic mice with and without insulin-dependent diabetes. *190(3):171-4.*

De Graan PNE, Van Hooff COM, Tilly BD, Oestreicher AB, Schotman P, Gispen WH (1985) Phosphoprotein B-50 in nerve growth cones from fetal rat brain. *Neurosci Lett* 61(3):235-41.

Denda M, Fuziwara S, Inoue K, Denda S, Akamatsu H, Tomitaka A, Matsunaga K (2001) Immunoreactivity of VR1 on epidermal keratinocyte of human skin. *Biochem and Biophys Res Comm* 285:1250-1252.

Diemel LT, Brewster WF, Fernyhough P, Tomlinson DR (1994) Expression of neuropeptides in experimental diabetes; effects of treatment with nerve growth factor or brain –derived neurotrophic factor. *Mol Brain Res* 21:171-5.

Drel VR, Mashtalir N, Ilnytska O, Shin J, Li F, Lyzogubov VV, Obrosova IG (2006) The leptin-deficient (*ob/ob*) mouse: A new animal model of peripheral neuropathy of type 2 diabetes and obesity. *Diabetes* 55:3335-43.

Drel VR, Pacher P, Vareniuk I, Pavlov I, Ilnytska O, Lyzogubov VV, Tibrewala J, Groves JT, Obrosova IG (2007) A peroxydinitrite decomposition catalyst counteracts sensory neuropathy in streptozotocin-diabetic mice. *Eur J Pharmacol* 569(1-2):48-58.

Dubuisson D, Dennis SG. (1977) The formalin test: a quantitative study of the analgesic effects of morphine, meperidine, and brain stem stimulation in rats and cats. *Pain* 4(2):161-74.

Dyck PJ, Dyck PJB, Kennedy WR, Kesserwani H, Melanson M, Ochoa J, Shy M, Stevens JC, Suarez GA, O'Brien PC (1998) Limitations of quantitative sensory testing when patients are biased toward a bad outcome. *Neurology* 50(5):P1213.

Dyck PJ, Dyck PJ, Larson TS, O'Brien PC, Velosa JA (2000) Patterns of quantitative sensation testing of hypoesthesia and hyperalgesia are predictive of diabetic polyneuropathy: a study of three cohorts. Nerve growth factor study group. *Diabetes Care* 23(4):510-7.

Edmonds ME, Roberts VC, Watkins PJ (1982) Blood flow in the diabetic neuropathic foot. *Diabetologia* 22:9-15.

Eliasson SG (1964) Nerve conduction changes in experimental diabetes. *J Clin Invest* 43:2353-8.

Facer P, Casula MA, Smith GD, Benham CD, Chessell IP, Bountra C, Sinisi M, Birch R, Anand P (2007) Differential expression of the capsaicin receptor TRPV1 and related novel receptors TRPV3, TRPV3 and TRPM8 in normal human tissues and changes in traumatic and diabetic neuropathy. *BMC Neurol* 7:11.

Fernyhough P, Mill JF, Roberts ML, Ishii DN (1989) Stabilization of tubulin mRNAs by insulin and insulin-like growth factor during neurite formation. *Brain Res Mol Brain Res* 6(2-3):109-20.

Fernyhough P, Willars GB, Lindsay RM, Tomlinson DR (1993) Insulin and insulin-like growth factor I enhance regeneration in cultured adult rat sensory neurons. *Brain Res* 607:117-124.

Fernyhough P, Diemel LT, Brewster WJ, Tomlinson DR (1994) Deficits in sciatic nerve neuropeptide content coincide with a reduction in target tissue nerve growth factor messenger RNA in streptozotocin-diabetic rats: effects of insulin treatment. *Neuroscience* 62(2):337-44.

Fernyhough P, Diemel LT, Brewster WJ, Tomlinson DR (1995) Altered neurotrophin mRNA levels in peripheral nerve and skeletal muscle of experimentally diabetic rats. *Diabetologia* 64:1231-1237.

Fernyhough P, Diemel LT, Tomlinson DR (1998) Target tissue production and axonal transport of neurotrophin-3 are reduced in streptozotocin-diabetic rats. *Diabetologia* 41:300-306.

- Forst T, Kann P, Pfutzner A, Lobmann R, Schafer H, Beyer J (1994) Association between "diabetic thick skin syndrome" and neurological disorders in diabetes mellitus. *Acta Diabetol* 31:73-77.
- Forst T, Caduff A, Talary M, Weder M, Brandle M, Kann P, Flacke F, Friedrich CH, Pfutzner A (2006) Impact of environmental temperature on skin thickness and microvascular blood flow in subjects with and without diabetes. *Diabetes Technol Ther* 8(1):94-101.
- Freeman R (1999) Human studies of recombinant human nerve growth factor and diabetic peripheral neuropathy. *Eur Neurol* 41(S1):20-6.
- Gabra BH, Sirois P (2002) Role of bradykinin B(1) receptors in diabetes-induced hyperalgesia in streptozotocin-treated mice. *Eur J Pharmacol* 457(2-3):115-24.
- Gabra BH, Sirois P (2003) Beneficial effect of chronic treatment with the selective bradykinin B1 receptor antagonists, R-715 and R-954, in attenuating streptozotocin-diabetic thermal hyperalgesia in mice. *Peptides* 24(8):1131-9.
- Gabra BH, Sirois P (2005) Hyperalgesia in non-obese diabetic (NOD) mice: a role for the inducible bradykinin B1 receptor. *Eur J Pharmacol* 514(1):61-7.
- Gai W, Schott-Ohly P, Schulte im Walde S, Gleichmann H. (2004) Differential target molecules for toxicity induced by streptozotocin and alloxan in pancreatic islets of mice in vitro. *Exp Clin Endocrinol Diabetes* 112(1):29-37.
- Georgieff IS, Liem RK, Couchie D, Mavilia C, Nunez J, Shelanski (1993) Expression of high molecular weight tau in the central and peripheral nervous systems. *J Cell Sci* 105:729-737.
- Gibran NS, Jang YC, Isik FF, Greenhalgh DG, Muffley LA, Underwood RA, Usui ML, Larsen J, Smith DG, Bunnett N, Ansel JC, and Olerud JE (2002) Diminished neuropeptide levels contribute to impaired cutaneous healing response associated with diabetes mellitus. *J Surg Res* 108:122-28.
- Gillon DR, Hawthorne JN, Tomlinson DR (1983) Myo-inositol and sorbitol metabolism in relation to peripheral nerve function in experimental diabetes in the rat: the effect of aldose reductase inhibition. *Diabetologia* 25(4):365-71.
- Glasky AJ, Glasky MS, Ritzmann RF, Rathbone MP (1997) AIT-082, a novel purine derivative with neuroregenerative properties. *Exp Opin Invest Drugs* 6:1413-1417.

Gokin AP, Fareed MU, Pan HL, Hans G, Strichartz GR, Davar G (2001) Local injection of endothelin-1 produces pain-like behavior and excitation of nociceptors in rats. *J Neurosci* 21(14):5358-66.

Gopinath P, Wan E, Holdcroft A, Facer P, Davis JB, Smith GD, Bountra C, Anand P (2005) Increased capsaicin receptor TRPV1 in skin nerve fibres and related vanilloid receptors TRPV3 and TRPV4 in keratinocytes in human breast pain. *BMC Womens Health* 5:2.

Greene DA, Lattimer SA (1983) Impaired rat sciatic nerve sodium-potassium adenosine triphosphatase in acute streptozotocin diabetes and its correction by dietary myo-inositol supplementation. *J Clin Invest* 72(3):1058-63.

Hamdy O, Abou-Elenin K, LoGerfo FW, Horton ES, Veves A (2001) Contribution of nerve-axon reflex-related vasodilation to the total skin vasodilation in diabetic patients with and without neuropathy. *Diabetes Care* 24:344-49.

Hammes HP, Du X, Edelstein D, Taguchi T, Matsumura T, Ju Q, Lin J, Bierhaus A, Nawroth P, Hannak D, Neumaier M, Bergfeld R, Giardino I, Brownlee M (2003) Benfotiamine blocks three major pathways of hyperglycemic damage and prevents experimental diabetic neuropathy. *Nat Med* 9(3):294-9.

Hargreaves K, Dubner R, Brown F, Flores C, Joris J (1998) A new and sensitive method for measuring thermal nociception in cutaneous hyperalgesia. *Pain* 32:77-88.

Haupt E, Ledermann H, Kopcke W (2005) Benfotiamine in the treatment of diabetic polyneuropathy—a three-week randomized, controlled pilot study (BEDIP study). *Int J Clin Pharmacol Ther* 43(2):71-7.

Hellweg R and Hartung HD (1990) Endogenous levels of nerve growth factor (NGF) are altered in experimental diabetes. *J Neurosci Res* 28:258-267.

Hellweg R, Raivich G, Hartung HD, Hock C, Kreutzberg GW (1994) Axonal transport of endogenous nerve growth factor (NGF) and NGF receptor in experimental diabetic neuropathy. *Exp Neurol* 130(1):24-30.

Henderson JT, Seniuk NA, Richardson PM, Gauldie J, Roder JC (1994) Systemic administration of ciliary neurotrophic factor induces cachexia in rodents. *J Clin Invest* 93(6):2632-8.

Hermenegildo C, Raya A, Roma J, Romero FJ (1993) Decreased glutathione peroxidase activity in sciatic nerve of alloxan-induced diabetic mice and its correlation with blood glucose levels. *Neurochem Res* 18:893-6.

Herrmann DN, Griffin JW, Hauer P, Cornblath DR, McArthur JC (1999) Epidermal nerve fiber density and sural nerve morphometry in peripheral neuropathies. *Neurology* 53:1634-1640.

Hirai A, Yasuda H, Joko M, Maeda T, Kikkawa R (2000) Evaluation of diabetic neuropathy through quantitation of cutaneous nerves. *J Neurol Sci* 172:55-62.

Hiraiwa M, Taylor EM, Campana WM, Darin SJ, O'Brien JS (1997) Cell death prevention, mitogen-activated protein kinase stimulation, and increased sulfatide concentrations in Schwann cells and oligodendrocytes by prosaposin and prosaptides. *Proc Natl Acad Sci USA* 94(9):4778-81.

Hong S, Wiley JW (2005) Early painful diabetic neuropathy is associated with differential changes in the expression and function of vanilloid receptor 1. *J Biol Chem* 280(1):618-27.

Holland NR, Stocks A, Hauer P, Cornblath DR, Griffin JW, McArthur JC. (1997) Intraepidermal nerve fiber density in patients with painful sensory neuropathy. *Neurology* 1997;48:708-11.

Holmes M, Maysinger D, Foerster A, Pertens E, Barlas C, Diamond J (2003) Neotrofin, a novel purine that induces NGF-dependant nociceptive nerve sprouting but not hyperalgesia in adult rat skin. *Mol Cell Neurosci* 24:568-580.

Huang TJ, Verkhratsky A, Fernyhough P (2005) Insulin enhances mitochondrial inner membrane potential and increases ATP levels through phosphoinositide 3-kinase in adult sensory neurons. *Mol Cell Neurosci* 28(1):42-54.

Hummel KP, Dickie MM, Coleman DL. (1966) Diabetes, a new mutation in the mouse. *Science* 153(740):1127-8.

Ihara C, Shimatsu A, Mizuta H, Murabe H, Nakamura Y, Nakao K (1996) Decreased neurotrophin-3 expression in skeletal muscle of streptozotocin-induced diabetic rats. *Neuropeptides* 30:309-312.

Inkster ME, Cotter MA, Cameron NE (2007) Treatment with the xanthine oxidase inhibitor, allopurinol, improves nerve and vascular function in diabetic rats. *Eur J Pharmacol* 561(1-3):63-71.

Ishii DN, Recio-Pinto E, Spinelli W, Mill JF, Sonnenfeld KH (1985) Neurite formation modulated by nerve growth factor, insulin, and tumor promoter receptors. *Int J Neurosci* 26(1-2):109-27.

Jakobsen J (1976) Axonal dwindling in early experimental diabetes. I. A study of cross sectioned nerves. *Diabetologia* 12(6):539-46.

Jennings PE, Chirico S, Lunec J, Barnett AH (1987) Vitamin C metabolites and microangiopathy in diabetes mellitus. *Diabetes Res* 6:151-4.

Jiang Y, Jakobsen J (2004) The role of the p75 neurotrophin receptor in the morphology of dorsal root ganglion cells in streptozotocin diabetic mice: effects of sciatic nerve crush. *Diabetologia* 47(9):1502-10.

Jiang Y, Calcutt NA, Ramos KM, Mizisin AP (2006) Novel sites of aldose reductase immunolocalization in normal and streptozotocin-diabetic rats. *J Periph Nerv Syst* 11(4):274-85.

Johnson MS, Ryals JM, Wright DE (2007) Diabetes-induced chemogenic hypoalgesia is paralleled by attenuated stimulus-induced fos expression in the spinal cord of diabetic mice. *J Pain* 8(8):637-49.

Johnson MS, Ryals JM, Wright DE (2007b) Differential vulnerabilities of nociceptive subpopulations in diabetic neuropathy. *J Periph Nerv Syst* 12:S41.

Jolivalt CG, Ramos KM, Herbertsson K, Esch FS, Calcutt NA (2006) Therapeutic efficacy of prosaposin-derived peptide on different models of allodynia. *Pain* 121(1-2):14-21.

Jorneskog G, Brismar K, Fagrell B (1995) Skin capillary circulation severely impaired in toes of patients with IDDM, with and without late diabetic complications. *Diabetologia* 38(4):474-80.

Kamiya H, Murakawa Y, Zhang W, Sima AA (2005) Unmyelinated fiber sensory neuropathy differs in type 1 and type 2 diabetes. *Diabetes Metab Res Rev* 21(5):448-58.

Kanbayashi H, Itoh H, Kashiwaya T, Atoh K, Makino I (2002) Spatial distribution of nociceptive neuropeptide and nerve growth factor depletion in experimental diabetic peripheral nervous system. *J Int Med Res* 30(5):512-9.

Kalichman MW, Powell HC, Calcutt NA, Mizisin AP. (1995) Mast cell degranulation and blood-nerve barrier permeability in rat sciatic nerve after 7 days of hyperglycemia. *Am J Physiol* 268(2 pt.2):H740-8.

Kalichman MW, Powell HC, Mizisin AP (1998) Reactive, degenerative, and proliferative Schwann cell responses in experimental galactose and human diabetic neuropathy. *Acta Neuropathol* 95(1):47-56.

Karanth SS, Springall DR, Francavilla S, Mirrlees DJ, and Polak JM (1990) Early increase in CGRP- and VIP-immunoreactive nerves in the skin of streptozotocin-induced diabetic rats. *Histochemistry* 94:659-66.

Kennedy JM, Hoke A, Zhu Y, Johnston JB, van Marle G, Silva C, Zochodne DW, Power C (2004) Peripheral neuropathy in lentivirus infection: evidence of inflammation and axonal injury. *AIDS* 18:1241-1250.

Kennedy WR, Wendelschafer-Crabb G (1993) The innervation of the human epidermis. *J Neurol Sci* 115:184-90.

Kennedy WR, Wendelschafer-Crabb G, Brelje, TC (1994) Innervation and vasculature of human sweat glands: an immunohistochemistry-laser scanning confocal fluorescence microscopy study. *J Neurosci* 14:6825-6833.

Kennedy WR, Wendelschafer-Crabb G, Johnson T (1996) Quantitation of epidermal nerves in diabetic neuropathy. *Neurology* 47:1042-48.

Kennedy WR, Nolano M, Wendelschafer-Crabb G, Johnson TL, Tamura E (1999) A skin blister method to study epidermal nerves in peripheral nerve disease. *Muscle Nerve* 22:360-71.

Kennedy WR (2004) Opportunities afforded by the study of unmyelinated nerves in skin and other organs. *Muscle Nerve* 29:756-767.

Kennedy JM, Zochodne DW (2005) Experimental diabetic neuropathy with spontaneous recovery: is there irreparable damage? *Diabetes* 54:830-837.

Khalili N, Wendelschafer-Crabb G, Kennedy WR, Simone DA (2001) Influence of thermode size for detecting heat pain dysfunction in a capsaicin model of epidermal nerve fiber loss. *Pain* 91(3):241-50.

Khodorova A, Navarro B, Jouaville LS, Murphy JE, Rice FL, Mazurkiewicz JE, Long-Woodward D, Stoffel M, Strichartz GR, Yukhananov R, Davar G (2003) Endothelin-B receptor activation triggers endogenous analgesic cascade at sites of peripheral injury. *Nat Med* 9(8):1055-61.

Konishi Y, Chui DH, Hirose H, Kunishita T, Tabira T (1993) Trophic effect of erythropoietin and other hematopoietic factors on central cholinergic neurons in vitro and in vivo. *Brain Res* 609:29-35.

Koskinen M, Hietaharju A, Kylaniemi M, Peltola J, Rantala I, Udd B, Haapasalo H. (2005) A quantitative method for the assessment of intraepidermal nerve fibers in small-fiber neuropathy. *J Neurol* 252:789-94.

Koizumi S, Fujishita K, Inoue K, Shigemoto-Mogami Y, Tsuda M, Inoue K (2004) Ca^{2+} waves in keratinocytes are transmitted to sensory neurons: the involvement of extracellular ATP and P2Y₂ receptor activation. *Biochem J* 380:329-38.

Kumar A, Kaundal RK, Iyer S, Sharma SS (2007) Effects of resveratrol on nerve functions, oxidative stress and DNA fragmentation in experimental diabetic neuropathy. *Life Sci* 80(13):1236-44.

Kunt T, Forst T, Schmidt S, Pfutzner A, Schneider S, Harzer O, Lobig M, Engelbach M, Goitom K, Pohlmann T, Beyer J (2000) Serum levels of substance P are decreased in patients with type 1 diabetes. *Exp Clin Endocrinol Diabetes* 108(3):164-7.

Laneuville O, Dorais J, Couture R (1988) Characterization of the effects produced by neurokinins and three agonists selective for neurokinin receptor subtypes in a spinal nociceptive reflex of the rat. *Life Sci* 42(13):1295-1305.

Lauria G, McArthur JC, Hauer PE, Griffin JW, Cornblath DR (1998) Neuropathological alterations in diabetic truncal neuropathy: evaluation by skin biopsy. *J Neurol Neurosurg Psychiatry* 65:762-66.

Lauria G, Borgna M, Morbin M, Lombardi R, Mazzoleni G, Sghirlanzoni A, Pareyson D (2004) Tubule and neurofilament immunoreactivity in human hairy skin: markers for intraepidermal nerve fibers. *Muscle Nerve* 30:310-6.

Lauria G, Lombardi R, Borgna M, Penza P, Bianchi R, Savino C, Canta A, Nicolini G, Marmiroli P, Cavaletti G (2005) Intraepidermal nerve fiber density in rat foot pad: Neuropathologic-neurophysiologic correlation. *J Periph Nerv Syst* 10:202-208.

Lauria G, Cornblath DR, Johansson O, McArthur JC, Mellgren SI, Nolano M, Rosenberg N, Sommer C (2005) EFNS guidelines on the use of skin biopsy in the diagnosis of peripheral neuropathy. *Eur J Neurol* 12:747-758.

Lauria G, Morbin M, Lombardi R, Capobianco R, Camozzi F, Pareyson D, Manconi M, Geppetti P (2006) Expression of capsaicin receptor immunoreactivity in human peripheral nervous system and in painful neuropathies. *J Peripher Nerv Syst* 11:262-71.

Lauria G, Devigili G (2007) Skin biopsy as a diagnostic tool in peripheral neuropathy. *Nat Clin Pract Neurol* 3(10):546-57.

Lee AY and Chung SS (1999) Contributions of the polyol pathway to oxidative stress in diabetic cataract. *FASEB J* 13:23-30.

Leonelli E, Bianchi R, Cavaletti G, Caruso D, Crippa D, Garcia-Segura LM, Lauria G, Magnaghi, Roglio I, Melcangi RC (2007) Progesterone and its derivatives are neuroprotective agents in experimental diabetic neuropathy: A multimodel analysis. *Neuroscience* 144:1293-1304.

Levine AS, Morley JE, Wilcox G, Brown DM, Handwerger BS (1982) Tail pinch behavior and analgesia in diabetic mice. *Physiol Behav* 28(1):39-43.

Levy DM, Karanth SS, Springall DR, Polak JM (1989) Depletion of cutaneous nerves and neuropeptides in diabetes mellitus: an immunocytochemical study. *Diabetologia* 32:427-433.

Levy DM, Terenghi G, Gu XH, Abraham RR, Springall DR, and Polak JM (1992) Immunohistochemical measurements of nerves and neuropeptides in diabetic skin: relationship to tests of neurological function. *Diabetologia* 35:889-97.

Li F, Obrosova IG, Abatan O, Tian D, Larkin D, Stuenkel EL, Stevens MJ (2005) Taurine replacement attenuates hyperalgesia and abnormal calcium signaling in sensory neurons of STZ-D rats. *Am J Physiol Endocrinol Metab* 288(1):E29-D36.

Lindberger M, Daa Schroder H, Schultzberg M, Kristensson K, Persson A, Ostman J, Link H (1989) Nerve fibre studies in skin biopsies in peripheral neuropathies. *J Neurol Sci* 93:289-96.

Low PA, Nickander KK (1991) Oxygen free radical effects in sciatic nerve in experimental diabetes. *Diabetes* 40:873-7.

Lubec B, Hayn M, Kitzmuller E, Vierhapper H, Lubec G (1997) L-Arginine reduces lipid peroxidation in patients with diabetes mellitus. *Free Radic Biol Med* 22:355-57.

Lubvigson MA, Sorenson RL (1980) Immunohistochemical localization of aldose reductase. I. Enzyme purification and antibody preparation—localization in peripheral nerve, artery, and testis. *Diabetes* 29(6):438-49.

Malmberg AB, Mizisin AP, Calcutt NA, von Stein T, Robbins WR, Bley KR (2004) Reduced heat sensitivity and epidermal nerve fiber immunostaining following single applications of a high-concentration capsaicin patch. *Pain* 111:360-7.

Mantyh PW, Rogers SD, Honore P, Allen BJ, Ghilardi JR, Li J, Daughters RS, Lappi DA, Wiley RG, Simone DA (1997) Inhibition of hyperalgesia by ablation of lamina I spinal neurons expressing the substance P receptor. *Science* 278(5336):275-79.

Mayer JH and Tomlinson DR (1983) Prevention of defects of axonal transport and nerve conduction velocity by oral administration of myo-inositol or an aldose reductase inhibitor in streptozotocin-diabetic rats. *Diabetologia* 25:433-38.

McArthur JC, Stocks EA, Hauer P, Cornblath DR, Griffin JW (1998) Epidermal nerve fiber density: Normative reference range and diagnostic efficiency. *Arch Neurol* 55:1513-1520.

Medina-Santillan R, Morales-Franco G, Espinoza-Raya J, Granados-Soto V, Reyes-Garcia G (2004) Treatment of diabetic neuropathic pain with gabapentin alone or combined with vitamin B complex. Preliminary results. *Proc West Pharmacol Soc* 47:109-12.

Mill JF, Chao MV, Ishii DN (1985) Insulin, insulin-like growth factor II, and nerve growth factor effects on tubulin mRNA levels and neurite formation. *Proc Natl Acad Sci USA* 82(20):7126-30.

Miwa I, Kanbara M, Okuda J (1989) Improvement of nerve conduction velocity in mutant diabetic mice by aldose reductase inhibitor without affecting myo-inositol content. *Chem Pharm Bull (Tokyo)* 37(6):1581-2.

Mizisin AP, Calcutt NA, DiStefano PS, Acheson A, Longo FM (1997) Aldose reductase inhibition increases CNTF-like bioactivity and protein in sciatic nerves from galactose-fed and normal rats. *Diabetes* 46:647-52.

Mizisin AP, Kalichman MW, Bache M, Dines KC, DiStefano PS (1998) NT-3 attenuates functional and structural disorders in sensory nerves of galactose-fed rats. *J Neuropathol Exp Neurol* 57:803-813.

Mizisin AP, DiStefano PS, Li X, Garret D, and Tonra JR (1999) Decreased accumulation of endogenous brain-derived neurotrophic factor against constricting sciatic nerve ligatures in streptozotocin-diabetic and galactose-fed rats. *Neurosci Lett* 263:1-4.

Mizisin AP, Steinhardt RC, O'Brien JS, Calcutt NA (2001) TX14(A), a prosaposin-derived peptide, reverses established nerve disorders in streptozotocin-diabetic rats and prevents them in galactose-fed rats. *J Neuropathol Exp Neurol* 60(10):953-60.

Mizisin AP, Vu Y, Shuff M, Calcutt NA (2004) Ciliary neurotrophic factor improves nerve conduction and ameliorates regeneration deficits in diabetic rats. *Diabetes* 53:1807-1812.

Mizisin AP, Nelson RW, Sturges BK, Vernau KM, LeCouteur RA, Williams DC, Burgers ML, Shelton GD (2007) Comparable myelinated nerve pathology in feline and human diabetes mellitus. *Acta Neuropathol* 113:431-442.

Myers MG, Grammer TC, Wang LM, Sun XJ, Pierce JH, Blenis J, White MF (1994) Insulin receptor substrate-1 mediates phosphatidylinositol 3'-kinase and p70S6k signaling during insulin, insulin-like growth factor-1, and interleukin-4 stimulation. *J Biol Chem* 269(46):28783-9.

Navarro X, Verdu E, Wendelschafer-Crabb G, Kennedy WR (1995) Innervation of cutaneous structures in the mouse hind paw: a confocal microscopy immunohistochemistry study. *J Neurosci Res* 41(1):111-20.

Nicholls DG, Budd SL (2000) Mitochondria and neuronal survival. *Physiol Rev* 80(1):315-60.

Nichols ML, Allen BJ, Rogers SD, Ghilardi JR, Honore P, Luger NM, Finke MP, Li J, Lappi DA, Simone DA, Mantyh PW (1999) Transmission of chronic nociception by spinal neurons expressing the substance P receptor. *Science* 286(5444):1558-61.

Nickander KK, Schmelzer JK, Rohwer DA, Low PA (1994) Effect of α -tocopherol deficiency on indices of oxidative stress in normal and diabetic peripheral nerve. *J Neurol Sci* 126-6-14.

Nolano M, Simone DA, Wendelschafer-Crabb G, Johnson T, Hazen E, Kennedy WR (1999) Topical capsaicin in humans: parallel loss of epidermal nerve fibers and pain sensation. *Pain* 81:135-45.

Nothias F, Boyne L, Murray M, Tessler A, Fischer I (1995) The expression and distribution of tau proteins and messenger RNA in rat dorsal root ganglion neurons during development and regeneration. *Neuroscience* 66(3):707-719.

Nouveau-Richard S, Monot M, Bastien P, de Lacharriere O (2004) In vivo epidermal thickness measurement: ultrasound vs. confocal imaging. *Skin Research and Technology* 10:136-40.

Oates PJ (2008) Aldose reductase, still a compelling target for diabetic neuropathy. *Curr Drug Targets* 9(1):14-36.

Obrosova IG, Fathallah L, and Stevens MJ (2001) Taurine counteracts oxidative stress and nerve growth factor deficit in early experimental diabetic neuropathy. *Exp Neurol* 172(1):211-9.

- Obrosova IG, Van Huysen C, Fathallah L, Cao XC, Greene DA, Stevens MJ (2002) An aldose reductase inhibitor reverses early diabetes-induced changes in peripheral nerve function, metabolism, and antioxidative defense. *FASEB J* 16(1):123-5.
- Obrosova IG, Mabley JG, Zsengeller Z, Charniauskaia T, Abatan OI, Groves JT, Szabo C (2005) Role for nitrosative stress in diabetic neuropathy: evidence from studies with a peroxynitrite decomposition catalyst. *FASEB J* 19(3):401-3.
- Obrosova IG, Ilnytska O, Lyzogubov VV, Pavlov IA, Mashtalir N, Nadler JL, Drel VR (2007) High-fat diet induced neuropathy of pre-diabetes and obesity: effects of "healthy" diet and aldose reductase inhibition. *Diabetes* 56(10):2598-608.
- Ohi T, Saita K, Furukawa S, Ohta M, Hayashi K, Matsukura S (1998) Therapeutic effects of aldose reductase on experimental diabetic neuropathy thought synthesis/secretion of nerve growth factor. *Exp Neurol* 151:215-220.
- Okada H, Moriwaki K, Kanno Y, Sugahara S, Nakamoto H, Yoshizawa M, Suzuki H (2000) Vitamin B6 supplementation can improve peripheral polyneuropathy in patients with chronic renal failure on high-flux haemodialysis and human recombinant erythropoietin. *Nephrol Dial Transplant* 15(9):1410-3.
- Ordonez G, Fernandez A, Perez R, Sotelo J (1994) Low contents of nerve growth factor in serum and submaxillary gland of diabetic mice. *J Neurol Sci* 121:163-166.
- Pabbidi RM, Yu SQ, Peng S, Khardori R, Pauza ME, Premkumar LS (2008) Influence of TRPV1 on diabetes-induced alterations in thermal pain sensitivity. *Mol Pain* 4:9.
- Pare M, Albrecht PJ, Noto CJ, Bodkin NL, Pittenger GL, Schreyer DJ, Tigno XT, Hansen BC, Rice FL (2007) Differential hypertrophy and atrophy among all types of cutaneous innervation in the glabrous skin of the monkey hand during aging and naturally occurring type 2 diabetes. *J Comp Neurol* 501:543-567.
- Parkhouse N, LeQuesne PM (1988) Impaired neurogenic vascular response in patients with diabetes and neuropathic foot lesions. *N Engl J Med* 318(20):1306-9.
- Peier AM, Reeve AJ, Andersson DA, Moqrich A, Earley TJ, Hergarden AC, Story GM, Colley S, Hogenesch JB, McIntyre P, Bevan S, Patapoutian A (2002) A heat-sensitive TRP channel expressed in keratinocytes. *Science* 296(5575):2046-9.

- Periquet MI, Novak V, Collins MP, Nagaraja HN, Erdem S, Nash SM, Freimer ML, Sahenk Z, Kissel JT, Mendell JR (1999) Painful sensory neuropathy: prospective evaluation by skin biopsy. *Neurology* 53:1641-47.
- Petruska JC, Streit WJ, Johnson RD (1997) Localization of unmyelinated axons in rat skin and mucocutaneous tissue utilizing the isolectin GS-I-IB4. *Somatosens Mot Res* 14:17-26.
- Pfeifer MA, Schumer MP, Gelber DA (1997) Aldose reductase inhibitors: the end of an era or the need for different trial designs? *Diabetes* 46(Suppl 2):S82-9.
- Pirart J, Lauvaux JP, Rey W (1978) Blood sugar and diabetic complications. *N Engl J Med* 298:1149.
- Pittenger GL, Ray M, Burcus NI, McNulty P, Basta B, and Vinik AI (2004) Intraepidermal nerve fibers are indicators of small-fiber neuropathy in both diabetic and nondiabetic patients. *Diabetes Care* 27:1974-9.
- Pittenger GL, Mehrabyan A, Simmons K, Rice A, Dublin C, Barlow P, Vinik AI (2005) Small fiber neuropathy is associated with metabolic syndrome. *Metab Syndr Relat Disord* 3:113-121.
- Polydefkis M, Hauer P, Sheth S, Sirdofsky M, Griffin JW, McArthur JC (2004) The time course of epidermal nerve fibre regeneration: studies in normal controls and in people with diabetes, with and without neuropathy. *Brain* 127:1606-1615.
- Pop-Busui R, Sullivan KA, Van Huysen C, Bayer L, Cao X, Towns R, Stevens MJ (2001) Depletion of taurine in experimental diabetic neuropathy: implications for nerve metabolic, vascular, and functional deficits. *Exp Neurol* 168(2):259-72.
- Powell HC, Garrett RS, Kador PF, Mizisin AP (1991) Fine-structural localization of aldose reductase and ouabain-sensitive, K(+)-dependent p-nitrophenylphosphatase in rat peripheral nerve. *Acta Neuropathol* 81(5):529-39.
- Properzi G, Francavilla S, Poccia G, Aloisi P, Gu X, Terenghi G, and Polak JM (1993) Early increase precedes a depletion of VIP and PGP9.5 in the skin of insulin-dependent diabetics – correlation between quantitative immunohistochemistry and clinical assessment of peripheral neuropathy. *J Pathol* 169:269-277.
- Quattrini C, Tavakoli M, Jeziorska M, Kallinikos P, Tesfaye S, Finnigan J, Marshall A, Boulton AJ, Efron N, Malik RA (2007) Surrogate markers of small fiber damage in human diabetic neuropathy. *Diabetes* 56(8):2148-54.

Ramasamy R, Oates PJ, Schaefer S (1997) Aldose reductase inhibition protects diabetic and nondiabetic rat hearts from ischemic injury. *Diabetes* 46(2):292-300.

Rendell MS, Bergman T, O'Donnell G, Drobny E, Borgos J, Bonner RF (1989) Microvascular blood flow, volume, and velocity measured by laser Doppler techniques in IDDM. *Diabetes* 38:819-24.

Robinson JP, Willars GB, Tomlinson DR, Keen P (1987) Axonal transport and tissue contents of substance P in rats with long-term streptozotocin-diabetes. Effects of the aldose reductase inhibitor 'statil'. *Brain Res* 426(2):339-48.

Rodriguez-Pena A, Botana M, Gonzalez M, Requejo F (1995) Expression of neurotrophins and their receptors in sciatic nerve of experimentally diabetic rats. *Neurosci Lett* 200:37-40.

Roglio I, Bianchi R, Giatti S, Cavaletti G, Caruso D, Scurati S, Crippa D, Garcia-Segura LM, Camozzi F, Lauria G, Melcangi R.C (2007) Testosterone derivatives are neuroprotective agents in experimental diabetic neuropathy. *Cell Mol Life Sci* 64:1158-1168.

Sadagurski M, Nofech-Mozes S, Weingarten G, White MF, Kodowaki T, Wertheimer E (2007) Insulin receptor substrate 1 (IRS-1) plays a unique role in normal epidermal physiology. *J Cell Physiol* 213:519-27.

Sagara M, Satoh J, Wada R, Yagihashi S, Takahashi K, Fukuzawa M, Muto G, Muto Y, and Toyota T (1996) Inhibition of development of peripheral neuropathy in streptozotocin-induced diabetic rats with N-acetylcysteine. *Diabetologia* 39:263-269.

Saini AK, Kumar HAS, Sharma SS (2007) Preventative and curative effect of edaravone on nerve functions and oxidative stress in experimental diabetic neuropathy. *Eur J Pharmacol* 568(1-3):164-72.

Schnedl WJ, Ferber S, Johnson JH, Newgard CB. (1994) STZ transport and cytotoxicity. Specific enhancement in GLUT2-expressing cells. *Diabetes* 43(11):1326-33.

Sharma K, McGowan TA (2000) TGF-beta in the diabetic kidney disease: role of novel signaling pathways. *Cytokine Growth Factor Rev* 11(1-2):115-23.

Sharma SS, Sayyed SG (2006) Effects of trolox on nerve dysfunction, thermal hyperalgesia and oxidative stress in experimental diabetic neuropathy. *Clin Exp Pharmacol Physiol* 33(11):1022-8.

Shun CT, Chang YC, Wu HP, Hsieh SC, Lin WM, Lin YH, Tai TY, and Hsieh ST (2004) Skin denervation in type 2 diabetes: correlations with diabetic duration and functional impairments. *Brain* 127:1593-1605.

Sima AA, Robertson DM (1979) Peripheral neuropathy in the diabetic mutant mouse: An ultrastructural study. *Lab Invest* 40(6):627-32.

Sima AA, Lattimer SA, Yagihashi S, Geene DA (1986) Axo-glial dysjunction. A novel structural lesion that accounts for poorly reversible slowing of nerve conduction in the spontaneously diabetic bio-breeding rat. *J Clin Invest* 77(2):474-84.

Simone DA, Nolano M, Johnson T, Wendelschafer-Crabb, Kennedy WR (1998) Intradermal injection of capsaicin in humans produces degeneration and subsequent reinnervation of epidermal nerve fibers: correlation with sensory function. *J Neurosci* 18(21):8947-59.

Smith AG, Ramachandran P, Tripp S, and Singleton JR (2001) Epidermal nerve innervation in impaired glucose tolerance and diabetes-associated neuropathy. *Neurology* 57:1701-1704.

Smith AG, Howard JR, Kroll R, Ramachandran P, Hauer P, Singleton JR, McArthur J (2005) The reliability of skin biopsy with measurement of intraepidermal nerve fiber density. *J Neurol Sci* 228:65-69.

Smith AG, Russell J, Feldman EL, Goldstein J, Peltier A, Smith S, Hamwi J, Pollari D, Bixby B, Howard J, Singleton JR (2006) Lifestyle intervention for pre-diabetic neuropathy. *Diabetes Care* 29:1294-1299.

Smith AG, Pollari D, Tovbias J, Sutton MA, Muhammad N, Babbar S, Chanda S, Bley KR (2007) The effect of counting criteria on intraepidermal nerve fiber density estimates. *J Peripher Nerv Syst* 12(S1):82.

Snider WD, McMahon SB (1998) Tackling pain at the source: new ideas about nociceptors. *Neuron* 20:629-32.

Sorensen L, Molyneaux L, Yue DK (2006) The relationship among pain, sensory loss, and small nerve fibers in diabetes. *Diabetes Care* 29:883-887.

Spravchikov N, Sizyakov G, Gartsbein M, Accili D, Tennenbaum T, Wertheimer E (2001) Glucose effects on skin keratinocytes: Implications for diabetes skin complications. *Diabetes* 50:1627-35.

Srinivasan S, Stevens M, Wiley JW (2000) Diabetic peripheral neuropathy: evidence for apoptosis and associated mitochondrial dysfunction. *Diabetes* 49(11):1932-8.

Stansberry KB, Shapiro SA, Hill MA, McNitt PM, Meyer MD, Vinik AI (1996) Impaired peripheral vasomotion in diabetes. *Diabetes Care* 19(7):715-21.

Stracke H, Lindemann A, Federlin K (1996) A benfotiamine-vitamin B combination in treatment of diabetic polyneuropathy. *Exp Clin Endocrinol Diabetes* 104(4):311-6.

Stucker M, Struk A, Altmeyer P, Herde M, Baumgartl H, Lubbers DW (2002) The cutaneous uptake of atmospheric oxygen contributes significantly to the oxygen supply of human dermis and epidermis. *J Physiol* 538(3):985-94.

Sullivan KA, Lentz SI, Roberts JL, Feldman EL (2008) Criteria for creating and assessing mouse models of diabetic neuropathy. *Curr Drug Targets* 9(1):3-13.

Sumner CJ, Sheth S, Griffin JW, Cornblath DR, Polydefkis M (2003) The spectrum of neuropathy in diabetes and impaired glucose tolerance. *Neurology* 60:108-11.

Thomas PK, Lascelles RG (1966) The pathology of diabetic neuropathy. *Q J Med* 140:489-509.

Thomas PK (1997) Classification, differential diagnosis, and staging of diabetic peripheral neuropathy - Current State and Perspectives of Diabetes Research: Chronic Complications. *Diabetes* 46(2):S54-57.

Tomlinson DR, Holmes PR, Mayer JH (1982) Reversal, by treatment with an aldose reductase inhibitor, of impaired axonal transport and motor nerve conduction velocity in experimental diabetes. *Neurosci Lett* 31:189-193.

Tomlinson DR, Robinson JP, Willars GB, Keen P (1988) Deficient axonal transport of substance P in streptozotocin-induced diabetic rats. Effects of sorbinil and insulin. *Diabetes* 37(4):488-93.

Toth C, Brussee V, Zochodne W (2006) Remote neurotrophic support of epidermal nerve fibres in experimental diabetes. *Diabetologia* 49:1081-88.

Toth C, Rong LL, Yang C, Martinez J, Song F, Ramji N, Brussee V, Liu W, Durand J, Nguyen MD, Schmidt AM, Zochodne DW (2008) Receptor for advanced glycation end products (RAGEs) and experimental diabetic neuropathy. *Diabetes* 57(4):1002-17.

Ueno Y, Kizaki M, Nakagiri R, Kamiya T, Sumi H, and Osawa T (2002) Dietary glutathione protects rats from diabetic nephropathy and neuropathy. *J Nutr* 132:897-900.

Umapathi T, Tan WL, Loke SC, Soon PC, Tavintharan S, Chan YH (2007) Intraepidermal nerve fiber density as a marker of early diabetic neuropathy. *Muscle Nerve* 35:591-98.

Underhill C (1992) CD44: the hyaluronan receptor. *J Cell Sci* 103:293-8.

Underwood RA, Gibran NS, Muffley LA, Usui ML, Olerud JE (2001) Color subtractive-computer-assisted image analysis for quantification of cutaneous nerves in a diabetic mouse model. *J Histochem Cytochem* 49:1285-1291.

Vareniuk I, Pavlov IA, Drel VR, Lyzogubov VV, Ilnytska O, Bell SR, Tibrewala J, Groves JT, Obrosova IG (2007) Nitrosative stress and peripheral diabetic neuropathy in leptin-deficient (*ob/ob*) mice. *Exp Neurol* 205:425-36.

Verze L, Paraninfo A, Ramieri G, Viglietti C, Panzica GC. (1999) Immunocytochemical evidence of plasticity in the nervous structures of the rat lower lip. *Cell Tissue Res* 297:203-11.

Verze L, Viglietti-Panzica C, Maurizo S, Sica M, Panzica G (2003) Distribution of GAP-43 nerve fibers in the skin of the adult human hand. *Anat Rec* 272A:467-73.

Vierck CJ, Kline RH, Wiley RG (2003) Intrathecal substance p-saporin attenuates operant escape from nociceptive thermal stimuli. *Neuroscience* 119(1):223-32.

Vincent AM, Russel JW, Low P, and Feldman E (2004) Oxidative stress in the pathogenesis of diabetic neuropathy. *Endocr Rev* 25(4):612-628.

Vlassara H, Brownlee M, Cerami A (1981) Nonenzymatic glycosylation of peripheral nerve protein in diabetes mellitus. *Proc Natl Acad Sci USA* 78(8):5190-2.

Vlassara H, Brownlee M, Cerami A (1985) Recognition and uptake of human diabetic peripheral nerve myelin by macrophages. *Diabetes* 34(6):553-7.

Wang L, Hilliges M, Jernberg T, Wiegleb-Edstrom D, and Johansson O (1990) Protein gene product 9.5-immunoreactive nerve fibres and cells in human skin. *Cell Tissue Res* 261:25-33.

Wang C, Li Y, Angelides KJ, Ishii DN (1992) Effects of insulin and insulin-like growth factors on neurofilament mRNA and tubulin mRNA content in human neuroblastoma SH-SY5Y cells. *Brain Res Mol Brain Res* 13(4):289-300.

Wang Z, Gleichmann H. (1998) GLUT2 in pancreatic islets: crucial target molecule in diabetes induced with multiple low doses of streptozotocin in mice. *Diabetes* 47(1):50-6.

Waxman SG, Dib-Hajj S, Cummins TR, Black JA (1999) Sodium channels and pain. *Proc Natl Acad Sci USA* 96(14):7635-9.

Wertheimer E, Trebicz M, Eldar T, Gartsbein M, Nofeh-Moses S, Tennenbaum T (2000) Differential roles of insulin receptor and insulin-like growth factor receptor in differentiation of murine skin keratinocytes. *J Invest Dermatol* 115(1):24-9.

Wertheimer E, Spravchikov M, Trebicz M, Gartsbein M, Accili D, Avinoah I, Nofeh-Moses S, Sizyakov G, Tennenbaum T (2001) The regulation of skin proliferation and differentiation in the IR null mouse: Implications for skin complications of diabetes. *Endocrinology* 142:1234-41.

Wilkinson KD, Lee KM, Deshpande S, Duerksen-Hughes P, Boss JM, Pohl J (1989) The neuron-specific protein PGP9.5 is a ubiquitin carboxyl-terminal hydrolase. *Science* 246:670-73.

Willars GB, Calcutt NA, Compton AM, Tomlinson DR, Keen P (1989) Substance P levels in peripheral nerve, skin, atrial myocardium and gastrointestinal tract of rats with long-term diabetes mellitus. Effects of aldose reductase inhibition. *J Neurol Sci* 91(1-2):153-64.

Wu S, Ren J (2006) Benfotiamine alleviates diabetes-induced cerebral oxidative damage independent of advanced glycation end-product, tissue factor and TNF- α . *Neurosci Lett* 394(2):158-62.

Wuarin L, Guertin DM, and Ishii DN (1994) Early reduction in insulin-like growth factor gene expression in diabetic nerve. *Exp Neurol* 130(1):106-14.

Xia P, Kramer RM, King GL (1995) Identification of the mechanism for the inhibition of Na, K-ATPase by hyperglycemia involving activation of protein kinase C and cytosolic phospholipase A2. *J Clin Invest* 96:733-740.

Xu QG, Li XQ, Kotecha SA, Cheng C, Sun HS, Zochodne DW (2004) Insulin as an in vivo growth factor. *Exp Neurol* 188:43-51.

Yeomans DC, Pirec V, Proudfit HK (1996) Nociceptive responses to high and low rates of noxious cutaneous heating are mediated by different nociceptors in the rat: behavioral evidence. *Pain* 68(1):133-40.

Yeomans DC, Proudfit HK (1996) Nociceptive responses to high and low rates of noxious cutaneous heating are mediated by different nociceptors in the rat: electrophysiological evidence. *Pain* 68(1):141-50.

Yue DK, Hanwell MA, Satchell PM, and Turtle JR (1982) The effect of aldose reductase inhibition on motor nerve conduction velocity in diabetic rats. *Diabetes* 31:789-794.

Zhao P, Barr TP, Hou Q, Dib-Hajj SD, Black JA, Albrecht PJ, Petersen K, Eisenberg E, Wymer JP, Rice FL, Waxman SG (2008) Voltage-gated sodium channel expression in rat and human epidermal keratinocytes: Evidence for a role in pain. *Pain*, In Press.

Ziegler D, Hanefeld M, Ruhnau KJ, Meissner HP, Lobisch M, Shutte K, Gries FA (1995) Treatment of symptomatic diabetic peripheral neuropathy with the antioxidant alpha-lipoic acid. A 3-week multicentre randomized controlled trial (ALADIN Study). *Diabetologia* 38(12):1425-33.

Zuang HX, Wuarin L, Fei ZJ, and Ishii DN (1997) Insulin-like growth factor (IGF) gene expression is reduced in neural tissues and liver from rats with non-insulin-dependent diabetes mellitus, and IGF treatment ameliorates diabetic neuropathy. *J Pharmacol Exp Ther* 283(1):366-74.